

THESIS

2
3004
55525721



This is to certify that the
thesis entitled

MODELING THERMAL AND MECHANICAL DEGRADATION
OF ANTHOCYANINS IN EXTRUSION PROCESSING

presented by

Kathy P.K. Lai

has been accepted towards fulfillment
of the requirements for the

 M.S. degree in Biosystems Engineering

A handwritten signature in cursive script, appearing to read "Keith Dolan".

Major Professor's Signature

A handwritten date "6/18/03" written in a simple, blocky style.

Date

PLACE IN RETURN BOX to remove this checkout from your record.
TO AVOID FINES return on or before date due.
MAY BE RECALLED with earlier due date if requested.

DATE DUE	DATE DUE	DATE DUE
10 19 07 APR 24 2007		

**MODELING THERMAL AND MECHANICAL DEGRADATION OF
ANTHOCYANINS IN EXTRUSION PROCESSING**

By

Kathy P.K. Lai

A THESIS

**Submitted to
Michigan State University
In partial fulfillment of the requirements
for the degree of**

MASTER OF SCIENCE

Department of Agricultural Engineering

2003

ABSTRACT

MODELING THERMAL AND MECHANICAL DEGRADATION OF ANTHOCYANINS IN EXTRUSION PROCESSING

By

Kathy P.K. Lai

In this study, the separate thermal and mechanical effects from extrusion cooking were quantified and used to develop a predictive model for anthocyanin degradation. Grape pomace (anthocyanin source) mixed with wheat pastry flour (1:3, w/w dry basis) was extruded at screw speeds of 50, 100, 200, and 400 rpm at dough moisture content of 30%, at both 95°C and 125°C die temperatures. Thermal effect was investigated separately (isothermal and nonisothermal experiments) by heating the same mixture in steel cells in an oil bath at 80, 105, and 145°C. Anthocyanin degradation followed a pseudo first-order reaction. The rate constant and activation energy were $k_{80^{\circ}\text{C}} = 2.81 \times 10^{-4} \text{ s}^{-1}$ and $\Delta E = 75,273 \text{ J/g-mol}$, respectively. Anthocyanin loss from extrusion ranged from 38 – 47% at 125°C die temperature, of which mechanical loss ranged from 1% and 63% at 50 rpm and 400 rpm, respectively. For extrusion at 95°C die temperature, total loss accounted for 29 – 35%, where mechanical loss accounted for 51% at 50 rpm to 66% at 400 rpm. An empirical equation was developed for mechanical loss versus shear history. The equation for mechanical loss was statistically different between the two extrusion temperatures.

DEDICATION

To my parents, Tak San Lai and Har Lin Tang-Lai, for their selfless sacrifice which allowed me to pursue my dreams, and to my younger sisters Patricia Pui-Hang Lai and Pauline Po-Tin Lai for their support. To the late Mrs.Sue Nevala for believing in me before I knew how.

ACKNOWLEDGEMENTS

I would like to express my utmost gratitude to my major professor, Dr. Kirk Dolan, for his untiring support throughout this research study. His patience, persistence, and understanding have helped me make this work possible. I would also like to express my appreciation to my committee, Dr. Perry Ng, Dr. Jerry Cash, and Dr. Bradley Marks for their time and helpful suggestions. I would especially like to thank Dr. Perry Ng for allowing me to use his extruder and spectrophotometer and Mr. Richard Wolthuis for his technical expertise.

Special thanks goes to Mavis Tan, Shelly Dorn, and Mitzi Ma for their technical help. My deepest appreciation goes to Gi chan Yoo for his advice and support during my extrusion work. In addition, thank you to Ari Gajraj, Akiko Kubota, Masahiro Otani, and Edmund Tanhehco for their scientific advice and friendship. Finally, many thanks to my "Room 110" mates Korada "P-Kay" Sunthanont, Maria "Super Mar" Suparno, and Monali "Supe" Yajnik for their love, encouragement, and support.

Table of Contents

LIST OF TABLES	viii
LIST OF FIGURES	x
KEY TO SYMBOLS OR ABBREVIATIONS	xiii
INTRODUCTION	1
1. LITERATURE REVIEW	3
1.1 Extrusion	3
1.1.1 Independent and dependent variables	5
1.1.2 Modeling	5
1.2 Anthocyanins	8
1.2.1 Stability	11
1.2.2 Importance to food industry	15
1.2.3 Analysis	17
1.3 Grape pomace	18
2. THEORETICAL MODEL DEVELOPMENT	21
2.1 Overall model	21
2.2 Primary model describing rate of anthocyanin degradation	24
2.3 Secondary model describing temperature and moisture effects	25
2.3.1 Case 1 – Temperature and moisture content changing with time	25
2.3.2 Case 2 – Isothermal heating at different constant moisture content to estimate b	27
2.3.2.1 Slope method to estimate b	27
2.3.2.2 Constant heating time method to estimate b	28
2.3.3 Moisture correction methods	30
2.3.3.1 Case 1 – Nonisothermal heating	30
2.3.3.2 Case 2 – Isothermal heating	32
2.4 Estimation of thermal kinetic parameters	32

2.5	Thermal effect on anthocyanin retention from extrusion	33
2.6	Mechanical effect on anthocyanin retention and final model equation	36
2.7	Model validation	38
2.8	Novelty of model development	39
3.	EXPERIMENTAL MATERIALS AND METHODS	40
3.1	Determination of anthocyanin content	40
3.1.1	Reagents	40
3.1.2	Extraction of anthocyanins	40
3.1.3	Analysis of anthocyanins	41
3.2	Thermal effects on anthocyanins in grape pomace-flour mixture	43
3.2.1	Sample preparation	43
3.2.2	Isothermal and nonisothermal heating of grape pomace-flour mixture: experimental design	45
3.2.3	Data analysis for thermal study	47
3.2.3.1	Time-temperature history	47
3.2.3.2	Moisture content correction	49
3.2.3.3	Estimation of parameters	49
3.2.3.4	Confidence intervals of parameters	52
3.3	Extrusion of grape pomace-flour mixture	54
3.3.1	Sample preparation	54
3.3.2	Extrusion experimental design	54
3.3.2.1	Mean residence time	58
3.3.2.2	Color-concentration calibration curve	58
3.3.2.3	Extruder degree of fill	59
3.3.3	Study of anthocyanin extraction from extrudates	60
3.3.4	Effects of dough moisture content on anthocyanins from extrusion	61
3.4	Thermal effects on anthocyanins from extrusion	61
3.5	Mechanical effects on anthocyanin from extrusion	62
3.6	Statistical analysis	62
4.	RESULTS AND DISCUSSION	64

4.1	Thermal effects on anthocyanins in grape pomace-flour mixture	64
4.1.1	Isothermal and nonisothermal heating of grape pomace-flour mixture	64
4.1.2	Estimating moisture content rate constant b	66
4.1.3	Moisture content correction	70
4.1.4	Estimation of parameters and confidence intervals	72
4.2	Extrusion of grape pomace-flour mixture	84
4.2.1	Mean residence time	84
4.2.2	Color versus concentration standard curve	87
4.2.3	Extruder degree of fill	88
4.2.4	Study of anthocyanin extraction from extrudates	90
4.2.5	Effects of dough moisture content on anthocyanins	91
4.2.6	Thermal and mechanical effects on anthocyanins in extruded wheat flour	92
4.3	Mechanical effects	96
4.3.1	High-temperature extrusion	96
4.3.2	Low-temperature extrusion	99
4.3.3	Combining mechanical loss from high and low-temperature extrusion	102
4.4	Model validation	106
5.	CONCLUSIONS AND RECOMMENDATIONS	107
5.1	Summary and conclusions	107
5.2	Recommendations for future research	109
Appendix 1	Anthocyanin analysis	110
Appendix 2	Sample approximate confidence intervals calculations	112
Appendix 3	Equations referenced in Results and Discussion section	114
Appendix 4	Lumped heat-capacity analysis	117
Appendix 5	Anthocyanin measurements from isothermal heating at 80°C and nonisothermal heating at 105°C and 145°C	119
Appendix 6	Moisture content correction factors	122
Appendix 7	Normal probability plot of residuals	125
Appendix 8	Anthocyanin measurements from extrusion	127
Appendix 9	Anthocyanin retention values from extrusion	130
Appendix 10	Extrusion data	132
References		135

List of Tables

Table

3.1.1	Specifications for Genesys 5 spectrophotometer	41
3.2.1	Experimental design for isothermal and nonisothermal heating of grape pomace-flour mixture	47
3.3.1	Screw configuration for high shear extrusion	55
3.3.2	Experimental plan for predicting extruder degree of fill	60
4.1.1	Nonlinear estimation results of parameters at reference temperature $T_r = 353.15$ K (80 °C) in Eq. (37) or (39)	74
4.1.2	Published kinetic parameters from thermal study of anthocyanin degradation using 1 st -order reaction.	77
4.2.1	Mean residence times from extrusion under high and low temperature profiles at screw speeds 50, 100, 200, and 400 rpm	87
4.2.2	Mass of dough from designated extruder sections taken from extrusion run at high temperature, screw speed 200 rpm	90
4.2.3	Total anthocyanin loss and % of total loss due to thermal & mechanical effects from extrusion at high-temperature at 50, 100, 200, and 400 rpm	95
4.2.4	Total anthocyanin loss and % of total loss due to thermal & mechanical effects from extrusion at high-temperature at 50, 100, 200, and 400 rpm	96
4.2.5	p-values for comparing the slope between high and low-temperature extrusion linear trendlines for mechanical loss versus screw speed, shear history, and <i>SME</i>	102
4.2.6	<i>PRESS</i> values for the model validation of mechanical loss in terms of shear history at various extrusion temperature conditions.	106
A.5.1	Absorbance values for 43% (db) samples heated isothermally at 80 °C and nonisothermally at 105 °C and 145 °C for various times	120
A.5.2	Absorbance values for 10% (db) and 20% (db) samples heated isothermally at 80 °C for various times	121

A.6.1	Correction factors for 43% moisture content (db) heated nonisothermally at 105 °C and 145 °C for 1 st -order ($n = 1$) and $n = 3.66$ reaction. $CF_{NI} = \beta/\beta_{T,MC}$, (Eq. (28))	123
A.6.2	Correction factors for 10, 20, 43% moisture content (db) heated isothermally at 80 °C for 1 st -order ($n = 1$) and $n = 3.66$ reaction. $CF_{NI} = \exp[-b (MC - MC_r)]$, (Eq. (35))	124
A.8.1	Averages and standard deviation for anthocyanin content (absorbance, dry weight basis) in raw material and extruded products at high-temperature and 400 rpm containing 5, 15, and 25% grape pomace (wb)	128
A.8.2	Averages and standard deviation for anthocyanin content (absorbance, dry weight basis) in raw material and extruded products at high-temperature and 400 rpm at 30, 35, and 40% dough moisture content (wb)	128
A.8.3	Averages and standard deviation for anthocyanin content (absorbance, dry weight basis) in raw material and extruded products	129
A.9.1	Values for total, thermal, and mechanical retention from samples extruded under high and low-temperature at 50, 100, 200, and 400 rpm	131
A.9.2	Values for total, thermal, and mechanical loss from samples extruded under high and low-temperature at 50, 100, 200, and 400 rpm	131
A.10.1	Processing data for extrusion under high and low-temperature	133
A.10.2	Data used to calculate <i>SME</i> and shear history	134

List of Figures

Figure	
1.2.1	Flavylium or 2-phenyl-benzopyrylium nucleus. 10
1.2.2	Six common anthocyanidins (aglycone). 10
1.2.3	Four forms of anthocyanins in equilibrium. 12
1.2.4	Equilibrium distribution of AH ⁺ , A, B, and C for malvidin-3-glucoside at different pH values at 25°C. (From Brouillard 1982). 12
2.3.1	Example of estimating <i>b</i> using slope method. 28
2.3.2	Graphical display of ln C ₀ and ln C'₀ for 1 st -order reaction. 29
2.6.1	An example of total retention, thermal retention and mechanical retention versus mechanical shear depicting graphical mechanical retention, <i>R_s</i> . <i>X_T</i> is total loss, <i>X_β</i> is thermal loss, and <i>X_s</i> is mechanical loss. 37
3.2.1	Grape pomace-flour mixture (1:3 w/w db). 44
3.2.2	Setup for thermal study 45
4.1.1	Absorbance versus time (43% (db) initial moisture content) of 1:3 (w/w) grape pomace-wheat flour mixture heated isothermally (80°C) and nonisothermally (105°C and 145°C) for different times. 65
4.1.2	Example curves of average sample temperatures versus time. 65
4.1.3	First-order log plot of absorbance versus time for 10, 20, and 43% moisture content (db) samples heated isothermally at 80 °C. 67
4.1.4	Constant heating time method to estimate the moisture rate constant <i>b</i> assuming first-order reaction (<i>n</i> = 1). The slope of each line is the estimate of <i>b</i> at each heating time. 67
4.1.5	<i>n</i> th -order plot of absorbance versus time for 10, 20, and 43% moisture content samples heating isothermally at 80°C for <i>n</i> = 3.66, the converged value. This plot is the <i>n</i> th -order analog to 4.1.3. 69
	Constant heating time method to estimate moisture constant rate <i>b</i> (<i>n</i> = 3.66). 69

4.1.7	Moisture content over time for samples heated isothermally at 80°C and nonisothermally at 105°C and 145°C.	71
4.1.8	a and b Absorbance of samples in Figure 4.1.1 versus time corrected to reference 43% moisture content for a) 1 st -order and b) n^{th} -order reaction.	72
4.1.9	a and b Best-fit nonlinear regression line for absorbance versus time-temperature history for 1 st -order reaction using a) least-squares and b) weighted least-squares regression.	75
4.1.10	Best-fit nonlinear regression line for absorbance versus time-temperature history for n^{th} -order reaction.	81
4.1.11	a, b, and c Residuals versus model values for a) 1 st -order, least-squares; b) 1 st -order, weighted least-squares; and c) n^{th} -order reaction.	84
4.2.1	RTD curves for low temperature extrusion at 50, 100, 200, and 400 rpm at 43% moisture.	86
4.2.2	RTD curves for high temperature extrusion at 50, 100, 200, and 400 rpm at 43% moisture.	86
4.2.3	Calibration curve for color concentration versus Hunter color values (a^*) extruded under high temperature profile at screw speeds of 50, 200, and 300 rpm.	88
4.2.4	Percent fill calculated from samples extruded under high temperature at 50, 200, and 400 rpm.	89
4.2.5	Pictorial view of extruder degree of fill opened after dead-stop at 200 rpm.	89
4.2.6	Absorbance versus % grape pomace in mixture from samples extruded under high temperature at screw speed of 400 rpm and 30% moisture.	91
4.2.7	Constant heating time method to estimate the moisture rate constant, b , from samples extruded under high temperature, screw speed 400 rpm, at 30, 35, and 40% moisture content (wb).	92
4.2.8	Product temperature versus thermocouple distance from feed inlet end of the extruder barrel (from high temperature profile, 50 rpm).	93

4.2.9	Measured, thermal, and mechanical loss of anthocyanins versus screw speed for samples extruded under high temperature. Data are from two replications, each on different days.	94
4.2.10	Total, thermal, and mechanical loss of anthocyanins versus screw speed for samples extruded under high temperature. Data are from two replications, each on different days.	94
4.3.1	a, b, and c % mechanical loss from high temperature extrusion versus a) screw speed, b) shear history, and c) <i>SME</i> .	98
4.3.2	a, b, and c % mechanical loss from low temperature extrusion versus a) screw speed, b) shear history, and c) <i>SME</i> .	101
4.3.3	a, b, and c % mechanical loss from high and low temperature extrusion versus a) screw speed, b) shear history, and c) <i>SME</i> .	104
A.1.1	Finding the maximum absorbance using extracts diluted at dilution factor = 3 with pH 1.0 buffer.	111
A.1.2	Linear range of absorbance versus anthocyanin concentrations using extracts diluted with pH 1.0 and 4.5 buffer.	111
A.4.1	The log of temperature ratio versus time used in lumped heat capacity analysis to calculate heat transfer coefficient.	118
A.7.1	Normal probability plot of residuals for WLS 1 st -order reaction.	126

Key to symbols and abbreviations

a	vector of parameter estimates
A	absorbance, AU
A_s	steel cell surface area, m ²
b	moisture content rate constant
c	color concentration
c_p	specific heat, J/kg °C
C	concentration or analogous to anthocyanin absorbance
C_o	initial concentration
C'_o	pseudo initial concentration
C_r	concentration at reference moisture content
CF_i	moisture content correction factor for isothermal heating
CF_{NI}	moisture content correction factor for nonisothermal heating
CF_{RT}	residence time correction factor
(C/C_o)_{element}	retention of an individual element, decimal
(\bar{C}/C_o)_{at exit}	mean retention of reactant (anthocyanins) in exit stream, decimal
d	mechanical shear constant
E_v	power, kJ/s
E(t)	normalized residence time distribution, s ⁻¹
f	a function
g	number of barrel sections
h	heat transfer coefficient, W/m ² °C
i	index

j	index
k	rate constant, $[\text{concentration}]^{1-n} [\text{time}]^{-1}$
k'	mixer viscometer constant
$k_{mixture}$	thermal conductivity, W/m °C
k_r	rate constant at reference temperature T_r , $[\text{concentration}]^{1-n} [\text{time}]^{-1}$
m	mass, kg or g; or number of data points in thermal study
m_i	mass of dough in section i , kg
\dot{m}	mass flow rate of grape pomace-flour mixture, kg/s
\dot{m}_T	mass flow rate of grape pomace-flour mixture and water, kg/s
MC	moisture content dry weight basis, decimal
MC_r	reference moisture content dry weight basis, decimal
$MC(t)$	moisture content dry weight basis with respect to time, decimal
MSE	mean square error
N	screw speed, rev/s
n	reaction order, dimensionless, or number of cases in Chapter 2.7
p	number of exit times
P_w	extruder power, calculated from manufacturer's equation, W
q	heat flow, W
Q	volumetric flow rate, ml/s
r	rate, $[\text{time}]^{-1}$
R	universal gas constant, 8.314 J/mol K
RTD	residence time distribution
R_T	total retention

R_{β}	thermal retention
R_{ϕ}	mechanical retention
SME	specific mechanical energy, kJ/kg
S	mechanical shear term
SS	screw speed, rpm
SS_E	sum of squares of errors
SS_T	total sum of squares
t	time or element exit age, s, min
\bar{t}	mean residence time, s
T	temperature, °C, K
T_c	sample center temperature, °C
T_o	initial sample temperature, °C
T_w	steel wall temperature, °C
T_{∞}	oil bath temperature, °C
T_r	reference temperature, °C, K
$T(t)$	time-temperature relationship, °C, K
$T(x_i)$	temperature at extruder barrel length x in section i , °C, K
V	extruder void volume, ml
W	weighting function
x_c	carbohydrate fraction in grape pomace-flour mixture
x_i	distance along extruder barrel length for section i ,
x_w	water fraction in grape pomace-flour mixture
X_T	total loss

X_β	loss due to thermal effects
X_S	loss due to mechanical effects
Y_i	observed responses
$\hat{Y}_{i(t)}$	predicted responses for the i th case

Greek

α	flow behavior index, dimensionless
β	time-temperature history, s
$\beta_{T,MC}$	time-temperature and moisture content history, s
$\beta(t)$	time-temperature history per exit time t , s
$\dot{\gamma}_a$	average shear rate, s^{-1}
ΔE	activation energy, J/g mol
ΔP	extruder die pressure, Pa
Δt	time increment, s
Δt_i	residence time of and element in barrel section i , s
$\bar{\Delta t}_i$	mean residence time of dough in barrel section i , s
Δx	steel cell inner thickness, m
Δx_i	length of barrel section i , m
ϕ	shear history, dimensionless
ρ	dough density, g/ml

Introduction

Extrusion technology is increasingly important in the food industry for transforming ingredients into intermediate or finished products. The wide range of moisture contents (12 – 40%), feed ingredients, cooking temperatures (~80 – 200°C), and controllable short residence times make the modern day extruder extremely versatile. An array of extrusion-cooked products include precooked and modified starches, puffed snacks, RTE cereals, pasta, sausage, confectionery products, pet foods, animal feed, protein supplements and meat analogs such as texturized vegetable proteins (Harper 1981).

Although food extrusion offers processing benefits such as reducing microbial load and denaturing enzymes, the thermal and mechanical energy used to cook the material may also degrade beneficial vitamins or minerals in the food ingredient (Camire and others 1990). Such health-promoting compounds include thiamin, beta-carotene, and anthocyanins. Anthocyanins, found mainly in fruits with red, blue, and purple hues, are important in the food industry as a source of natural color pigment (Francis 1989, Greaves 2002, Stout 2002). In addition, studies have shown these compounds possess potent health-promoting antioxidants. Due to the current consumer interest for diverse nutritional products, a potential exists for the addition of fruits containing anthocyanins to extruded products.

To predict the level of anthocyanins in the finished product, it is necessary to understand how the process may degrade the compound. A predictive model would save time and expense necessary to run experiments at every possible

condition. Although studies exist regarding the effects of extrusion on loss of various nutrients (Thompson and others 1976, Guzman-Tello and Cheftel 1987), little work has been done on anthocyanin loss during extrusion. Therefore, the research goal was to develop a model equation to predict thermal and mechanical shear effects from extrusion on the degradation of total anthocyanin using a grape pomace (anthocyanin source)-flour mixture. The specific objectives were

1. To estimate the thermal effects on anthocyanin loss in a grape pomace-flour mixture in a shearless environment;
2. To estimate the mechanical shear effects on anthocyanin loss in an extruded grape pomace-flour mixture.

1. Literature review

1.1 Extrusion

Extrusion was first utilized in the food industry in the mid 1930s when a single-screw extruder was used as a continuous pasta press. "Food extrusion is a process in which a food material is forced to flow, under one or more of a variety of conditions of mixing, heating, and shear, through a die which is designed to form and/or puff-dry the extrudate" (Rossen and Miller 1973). This continuous process combines the heating with the act of extrusion to create a cooked and shaped food product.

The basic extruder consists of screw elements held on a shaft, tightly fit inside a cylindrical barrel with a constricted opening (the die) at the end. Food ingredients are fed continuously into an inlet hopper and transported forward by one or two sets of screws. An extruder with one shaft and one set of screws is called a single-screw extruder, and those with two shafts and two sets of screws are called twin-screw extruders. Changing screw geometry consisting of feeding screws, single lead screws, and kneading paddles inside the barrel can offer different degrees of mixing and shear. As the raw material is fed, compressed, and metered down the extruder, thermal and mechanical energy can convert the food ingredients into a plasticized mass, reduce microbial load, denature enzymes, gelatinize starch, and create a texturized end product (Harper 1978). The major energy input comes from viscous dissipation from the rotating screws (Mohamed and others 1990) or additional heat can be added from an external source. The material is sheared throughout the entire barrel with the highest

shear rate inside the exit die hole. Upon exiting the die, changes in pressure cause the moisture inside the extrudate to flash off as steam, causing product expansion and rapid cooling (Harper 1981).

Viscous dissipation can be evaluated using shear rate. Mohamed and others (1990) modeled the average shear rate in a co-rotating twin-screw extruder using principles of mixer viscometry for three screw configurations by assuming the extruder is a mixer. A relationship between the impeller Power number (Po) and Reynolds number (Re) was established with Newtonian standards (Metzner and Otto 1957). The Power number was used to express the power consumption in mixing vessels and characterized as

$$Po = \frac{E_v}{\rho N^3 D_h^5}$$

where E_v is the viscous dissipation of mechanical energy, D_h is the hydraulic diameter of the extruder, N is the screw speed, and ρ is the Newtonian fluid density. The power consumed in mixing a Newtonian fluid in the laminar region is inversely proportional to the Reynolds number (Metzner and Otto 1957), and the Reynolds number for a Newtonian fluid in a twin-screw extruder was defined as

$$Re = \frac{D_h^2 N \rho}{\mu}$$

where μ is the Newtonian viscosity. Using the matching viscosity assumption (Metzner and Otto 1957, Mackey and others 1987) and non-Newtonian fluids,

Mohamed and others (1990) found constants to convert screw speed to an average shear rate. They reported the average shear rate is highest for kneading paddles, followed by that for feed screws and single lead screws.

1.1.1 Independent and dependent variables

Independent or *process* variables are factors that can be controlled during extrusion runs to influence product output. They include screw configuration, die size and shape, screw speed, feed rate, water and/or steam addition, and barrel temperature. The independent process variables have considerable effect on the dependent or *system* variables. They include the product temperature profile, die pressure, torque, and screw degree of fill. From these variables, extruder performance can be analyzed in terms of throughput, energy consumption (specific mechanical energy), flow behavior, and residence time distribution (Fichtali and van de Voort 1989). Nonetheless, the most important dependent variables are the product quality attributes such as texture, color, flavor, nutritional value, and other measurable properties. However, these product properties are measured or analyzed off-line, making it difficult to assess the effect of process variables on product quality. Having a model that predicts the effects of extrusion process variables on product characteristics would be extremely beneficial for the processor, because the model would save time and expense required during the experimental stages of product development.

1.1.2 Modeling

Despite the vast use of extrusion technology in the food and feed industry, theoretical models were not applied to food extrusion to the same extent as those

in the polymers industry (Harper 1978). Many of the improvements involving food extrusion attained in the past have been based more on empirical observations (trial-and-error). Foodstuffs (compared to polymers) are more complicated because 1) biological products are less homogeneous, 2) there is a lack of adequate information about their rheological and thermodynamic characteristics, and 3) there is more difficulty in predicting physicochemical changes that occur during the process (Fichtali and van de Voort 1989). Nonetheless, the theoretical concepts that have benefited the extrusion of polymers served as a useful basis for the study of the more complex field of food extrusion.

The key to developing a model is its application for scaling-up operations. Since most extrusion experimental studies are performed using lab scale extruders, the process variables must be independent of scale. They include shear rate, shear stress, energy input (*SME*), residence time, product temperature, and die pressure drop (Akdogan and McHugh 1999).

Although the majority of the models developed for food extrusion involve predicting dough rheological properties such as viscosity and fluid flow parameters, several key studies were published in regards to modeling nutrient loss from extrusion. Thompson and others (1976) developed a model equation to predict lysine loss as a function of glucose, moisture content, temperature, and pH from extrusion-line processing. Guzman-Tello and Cheftel (1987) modeled thiamin loss assuming the extruder was a continuous chemical reactor. Their final model equation was reported as

$$X_A = \int_0^{\infty} \left\{ 1 - \exp \left[-1225t \left[\exp \left(\left(-5672/T_p \right) - 0.0153M + 0.0151N \right) \right] \right] \right\} E(t) dt$$

Thiamin loss (X_A) was described using a first-order kinetic model and integrated over the residence time distribution ($E(t)$). The reaction rate constant in the model was a function of product temperature just before the die, moisture content (M), and screw speed (N) and was multiplied by the mean residence time (t). The effect of temperature was described using the Arrhenius relationship while both the effect of moisture content and screw speed was modeled using an exponential dependency. The activation energy from the Arrhenius relationship was found from near-isothermal product temperatures of 133, 142, and 152°C. This is a limitation to the study, because it is very difficult to maintain isothermal temperatures down the entire extruder barrel. Therefore assuming near-isothermal temperatures may cause ~30% underestimation of ΔE and a 3-orders-of-magnitude underestimation of the rate constant (Dolan 2003).

Davidson and others (1984) studied mechanical degradation of wheat starch in a single-screw extruder. Temperature and molecular weight affect loss due to mechanical effects by their contribution to viscosity, which is a critical factor in this type of degradation. Mechanical degradation decreases with temperature up to a maximum temperature. Their model was developed assuming mechanically induced degradation occurred primarily in the fully melted starch, therefore not the entire barrel length was used. Also, they recognized in some cases the degradation was due to a combination of mechanical and thermal factors, which are difficult to separate.

Cha and others (2001) modeled both thermal and mechanical effects on thiamin retention from extruded wheat flour with 0.30% (w/w) thiamin hydrochloride. Thermal effects were isolated by heating small samples of the thiamin/flour mixture to estimate the activation energy. The samples were then extruded at the temperature profile 80/100/115/130/145°C from feed point and die, where total thiamin retention was measured. The entire product temperature profile (not solely product temperature at the die) was used to calculate retention due to thermal effects only from extrusion. Mechanical retention was calculated by mathematically removing thermal effects from the total measure thiamin retention.

1.2 Anthocyanins

Anthocyanins are natural and non-volatile water-soluble pigments belonging to the flavonoids compound group characterized by the flavylium or 2-phenyl-benzopyrylium nucleus (Figure 1.2.1). Their color is due to the presence of the extensive conjugated double bond system (chromophore) in the molecule. They are particularly associated with fruits, but also occur in vegetables, roots, tubers, bulbs, legumes and cereals (Bridle and Timberlake 1997) where they provide many of the orange, purple, red, and blue colors.

Several hundred anthocyanins are known (Clifford 2000) where the molecule consists of two or three parts; the aglycone (anthocyanidin) base on the flavylium nucleus, a group of sugars, and often a group of acyl acids (Francis 1989). The six commonly occurring aglycones include pelargonidin, cyanidin, peonidin, delphinidin, petunidin and malvidin (Figure 1.2.2). Differences among

individual anthocyanins are: the number of hydroxyl groups, degree of methylation of these hydroxyl groups, the nature and number of sugars attached to the molecule and attachment position, and the nature and number of acids attached to the sugars in the molecule (Mazza and Brouillard 1987). As the number of hydroxyls increase, the color changes from pink to blue. Methoxyl groups replacing hydroxyl groups reverse the trend (Mazza and Brouillard 1987).

Sugars substituted on the aglycone are, in order of occurrence in nature: glucose, rhamnose, xylose, galactose, arabinose, and fructose as monoglycosides, diglycosides, or triglycosides (Francis 1989). The sugars are attached at the 3, 5, 7, 3', 4', and 5' positions, and if only one sugar is present, it is usually on the 3 position (Francis 1989). The main acyl acids are *p*-coumaric, caffeic and ferulic acids (Timberlake 1980).

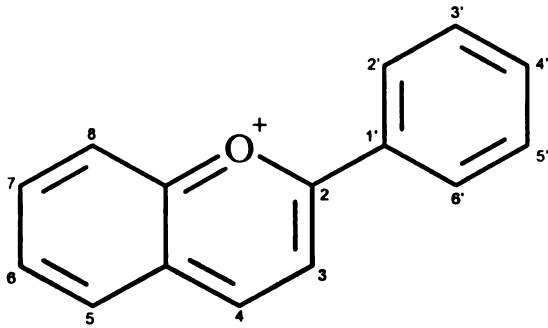
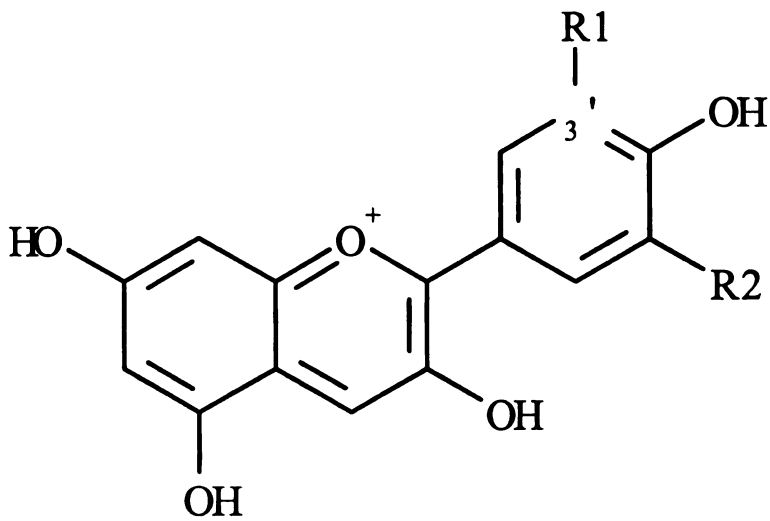


Figure 1.2.1 – Flavylium or 2-phenyl-benzopyrylium nucleus.



	R₁	R₂
Pelargonidin	H	H
Cyanidin	OH	H
Peonidin	OCH ₃	H
Delphinidin	OH	OH
Petunidin	OCH ₃	OH
Malvidin	OCH ₃	OCH ₃

Figure 1.2.2 – Six common anthocyanidins (aglycone).

1.2.1 Stability

pH

Due to the economic significance of anthocyanins as a potential food colorant, their stability has been studied extensively. The pH is the most important factor affecting color stabilization (Mazza and Brouillard 1987). Being electron deficient, the flavylum nucleus of anthocyanins would be expected to be highly reactive and can readily undergo undesirable structural and color changes from a variety of conditions. Brouillard and Delaporte (1977) studied the mechanism of the structural transformations of anthocyanins in acidic aqueous media using malvidin 3-glucoside at 25°C. They found it exists in four forms in equilibrium: the blue quinoidal base A, the red flavylum cation AH⁺, the colorless carbinol pseudobase (hemiketal) B, and colorless chalcone C (Figure 1.2.3).

Through the loss of a proton, the cation AH⁺ yields the quinoidal base A. The nucleophilic addition of water to the cation AH⁺ yields the pseudobase B. The carbinol pseudobase exists in tautomeric equilibrium with chalcone (C). Quinoidal and hemiketal forms are less stable and more sensitive to degradative reactions. Figure 1.2.4 shows the equilibrium distribution of AH⁺, A, B, and C for malvidin 3-glucoside at different pH values at 25°C (Brouillard 1982). The cation AH⁺, being the most important form in terms of visual color, exists in pH values below 4. Thus, very acidic media are required to stabilize colored anthocyanins.

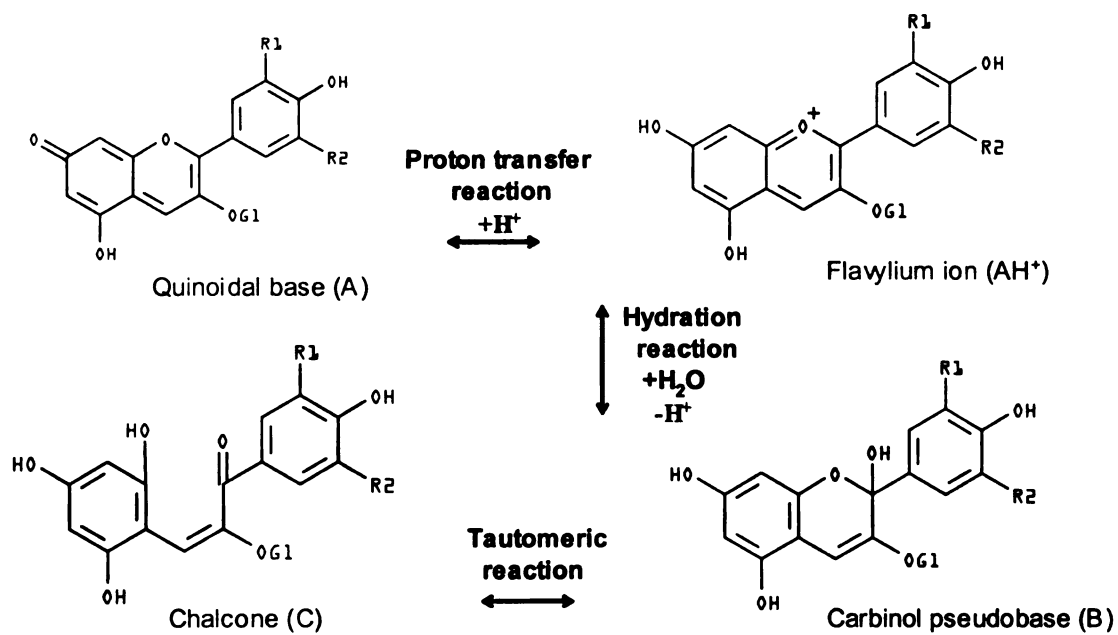


Figure 1.2.3 – Four forms of anthocyanins in equilibrium.

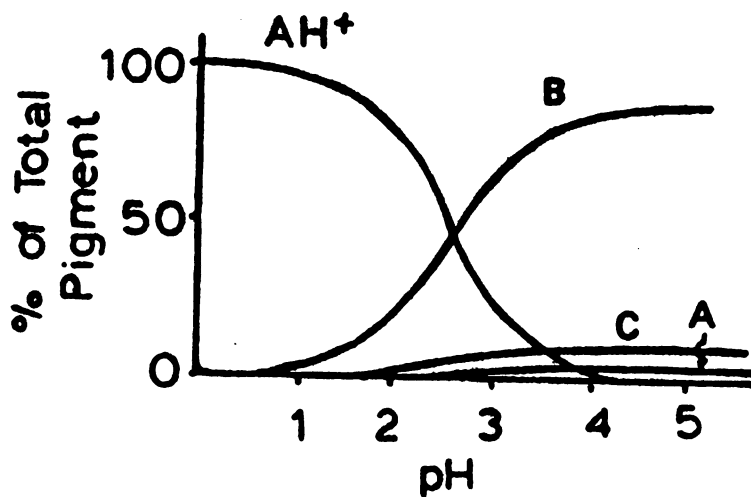


Figure 1.2.4 - Equilibrium distribution of AH⁺, A, B, and C for malvidin-3-glucoside at different pH values at 25°C. (From Brouillard 1982).

Temperature

Anthocyanins are also extremely sensitive to temperature, although the mechanism of their thermal degradation is not completely understood. Adams (1973) did a study of cyanidin-3-glycosides in acidified aqueous solution heated at 100°C and found the rate of sugar formation to be similar to the rate of red color loss. He suggests glycosidic hydrolysis may be the principal reaction leading to anthocyanin loss. On the other hand, Brouillard (1982) reported the opening of the pyrylium ring at elevated temperatures, to yield the colorless chalcone form that result in anthocyanin loss. After cooling and acidification, the quinoidal base (A) and carbinol base (B) are readily converted back to the cationic form (AH⁺) while conversion from chalcone may take up to 12 hours. The slow rate of chalcone conversion to the flavylum ion may have implications for the analysis on short- time-high-temperature degradation studies. If the samples are not allowed up to ~12 hours time to reestablish equilibria, the analysis results may be inaccurate.

Most thermal degradation studies were performed using liquid systems (Sastry and Tischer 1952, Markakis and others 1957, Tanchev and Yoncheva 1974, Calvi and Francis 1978, Cemeroglu and others 1994). Sastry and Tischer (1952) processed anthocyanin pigment concentrations obtained from Concord grape juice at 77, 99, and 121°C for process times varying from 5 to 100 min, respectively. The percent of pigment loss was analyzed using spectrophotometry and was found to be 32% at 77°C, 53% at 99°C, and 87% at 121°C. Markakis and others (1957) dissolved crystalline pelargonidin

3-monoglucoside (a main anthocyanin in strawberries) in citrate-HCl buffer at pH 2.0 and 3.4 sealed with nitrogen and heated the samples at the temperature ranges 45 – 110°C. pH 3.4 samples heated for 3 hours at 80°C degraded ~35% anthocyanins while samples pH 2.0 samples heated for 3 hours at 100°C degraded ~40%.

Tanchev and Yoncheva (1974) isolated two anthocyanins, delphinidin-3-rutinoside from eggplant and malvidin-3-glucoside from grape, to investigate their thermal stability. The anthocyanin extracts were brought to pH 2.5, 3.5 and 4.5 with 0.05 M citrate buffers and plum juice, and heated at 78, 88, 98 and 108°C for 15, 15, 5, and 3 minutes respectively. For delphinidin, the reaction rate constant was highest at pH 3.5 but did not differ between pH 2.5 and 4.5. Conversely, reaction rate was lowest at pH 3.5 for malvidin and also did not differ between pH 2.5 and 4.5. The solvent system had no effect on the thermal stability of malvidin; however, degradation of delphinidin was accelerated when juice was used as the medium.

Calvi and Francis (1978) heated an acidified methanol model system (pH 3.2) from Concord grapes under aerobic conditions at 85, 90, and 95°C at selected times. Although the data indicate zero-order kinetic degradation, the authors interpreted them as first order. Cemeroglu and others (1994) studied total anthocyanin content in sour cherry juice concentrate after heating it at 50, 60, 70 and 80°C at time intervals ranging from 1 to 48 hours. The concentrates were diluted to three different concentrations of 15°, 45° and 71 °Brix. Anthocyanin degradation increased with solids content, which is mostly glucose,

fructose, and malic acid in sour cherry juice. Sugar and sugar degradation products contribute to accelerating anthocyanin breakdown (Markakis and others 1957, Dravingas and Cain 1968). Activation energy and rate constant values from several of these studies are listed in Table 4.2.2, found in the Results and Discussion section.

Acylation

Acylation, or esterification of sugar hydroxyls in anthocyanins, has little effect on color but it can have a remarkable effect on pigment stability in neutral or weakly acidic aqueous solutions. The stability is attributed to the presence of two acyl groups, one attached above and the other below the pyrylium ring (Mazza and Brouillard 1987). Simply described, the stacking effect of acylation increases the color stability of anthocyanins in neutral solutions. This phenomenon is especially appealing as it expands the possible applications of colored anthocyanins in the food industry.

1.2.2 Importance to food industry

Due to their color properties, many researchers have been studying anthocyanins as a potential natural food colorant for the food industry. Clydesdale and others (1978) spray-dried concentrates of extracted anthocyanins from Concord grape juice sludge for use as colorants for beverages and gelatin desserts. Results were compared to samples colored with FD&C Red No. 2. The mean color quality score for samples colored with anthocyanins was lower than that with FD&C Red No. 2, but still reasonably acceptable, with the lowest score in the gelatin product. This may be due to the

high pH of the gelatin system that produced a more purple hue instead of red. McLellan and Cash (1979) extracted anthocyanins from dark, tart cherries for use as a colorant in the manufacture of maraschino-type cherries. They found the color to be relatively stable for an estimated period of 6 – 9 months depending on storage temperatures of 1.6, 18.3, and 37.2°C.

Since anthocyanins are stable at low pH, they are best suited for acidic systems. In baking, they are primarily used in sauces and fruit fillings. In extruded products, a brownish red shade is produced. A brighter red color may be achieved using acidic medium to gelatinize the dough during extrusion (Stout 2002). Also, a new generation of acylated anthocyanins has been developed which exhibits increase stability at higher pH levels which can be used in low water activity applications to produce purple, blue, green, and red shades in many snack food and cereal products (Greaves 2002).

In addition to their color properties, anthocyanins have received renewed attention as a health food constituent due to some positive therapeutic effects. Some include the treatment of diabetic retinopathy (Scharrer and Ober 1981), vision (Timberlake and Henry 1988), and various microcirculation diseases resulting from capillary fragility (Timberlake and Henry 1988). Anthocyanin content has also been directly correlated to antioxidant capacity (Wang and others 1997, Prior and others 1998, Wang and others 1999), which may reduce oxidative stress (Joseph and others 1999). Wang and others (1999) reported the antioxidant activities of anthocyanins from tart cherries to be comparable to that

of *tert*-butylhydroquinone and butylated hydroxytoluene and superior to vitamin E at 2 mM concentrations.

1.2.3 Analysis

One of the most utilized methods to measure total anthocyanins is the pH differential method. Sondheimer and Kertesz (1948b) first introduced this method, based on the structural transformation of the anthocyanin chromophore as a function of pH producing strikingly different absorbance spectra (measured using optical spectroscopy). Anthocyanins have absorption maximum in the 510 – 550 nm region (Fuleki and Francis 1968a). Sondheimer and Kertesz (1948b) used differential measurements between solutions of pH 2.0 and 3.4, where absorbance was read at the maximum absorption wavelength, to determine the concentration of anthocyanin in strawberry products. Fuleki and Francis (1968b) modified this procedure by using pH values of 1.0 and 4.5, where they found the greatest difference in absorbance. This ensures higher sensitivity and accuracy of the pH differential method because at pH 1.0 and 4.5, small variations in pH should cause only slight changes in absorbance. The colored flavylum form predominates at pH 1.0 and the colorless hemiketal form at pH 4.5.

Total anthocyanins can be expressed in absolute quantities by using molar extinction coefficient, the absorption of a 1% solution measure through a 1-cm cell path at a specified wavelength. The absorbancy of the anthocyanin molecule depends on the pH and the nature of the media (Fuleki and Francis 1968a) so the coefficient should be obtained in the same solvent system used for extraction. One issue with this approach is that anthocyanin mixtures may be

very complicated and not all absorption coefficients may be known. In addition, one would have to estimate the amount of each pigment present to get a value for total anthocyanin content. Niketic and Hrazdina (1972) suggested that with the grape varieties *V. labrusca*, *riparia*, *rupestris*, and *rotundifolis*, the pigment can be expressed as malvidin 3,5-diglucoside using molar extinction coefficient of 37,700 at 520 nm in 0.1 N HCl assuming a molecular weight of 691. Another option is to express it as malvidin 3-glucoside using the coefficient value of 28,000 in 0.1 N HCl at 520 nm assuming a molecular weight of 529.

1.3 Grape pomace

Grapes are the largest fruit crop worldwide, with annual production of approximately 65 million metric tons (Mazza 1995). Over 7,687,000 tons of fresh grapes were utilized in the United States in 2000 (USDA-NASS 2000). Michigan is the fourth leading state in grape production. One of the main varieties is the Concord grape. There are two major types of grapes: North American and European. European grapes, which belong to the species *Vitis vinifera* L., are grown principally in Italy, France, and Spain. In North America, there are two main species: *Vitis labrusca* and *Vitis rotundifolia*. *Vitis labrusca* grapes are grown mainly in the Great Lakes region of the U.S. and in Canada. *Vitis rotundifolia* are grown throughout the southeastern U.S., from North Carolina to eastern Texas.

In the U.S., roughly 12% of the grape crop is consumed fresh, with the remainder processed, dried, or canned in addition to pressed for wine and juice production (USDA-NASS 2000). In 1998, Michigan utilized 53,800 tons of

grapes for production of juice and wine (Concord Grape Association 1998). Grape processing generates large amounts of grape pomace or “marc” as industrial waste. It consists mainly of processed skins, seeds, and stems.

Historically, grape pomace has been used to feed livestock and fertilize soil, with considerable quantities remaining as waste. Disposing large amounts of grape pomace can be costly for processors and also create environmental concerns. Therefore, many researchers have found ways to find value in the grape by-product. The major anthocyanidins of Concord grapes were reported to be cyanidin and delphinidin (Ingalsbe and others 1963, Robinson and others 1966, Shewfelt and Ahmed 1966, Hrazdina 1975) and malvidin (Sastry and Tischer 1952, Van Buren 1970, Mazza 1995).

Grape skins as a by-product of the wine industry, have been used in the production of “enocianina” or “enocyanin”, a commercial food colorant, as early as 1879. Its primary use is to augment the color of wines, but has found extensive application in fruit juices and other food products. Grape skin extract is limited for beverage use in the United States, but grape color extract from Concord grapes can be used in nonbeverage applications (Stout 2002). Other possible uses of grape by-products such as grape pomace include ethanol, tartrates, citric acid (Hang and Woodams 1985) and grape seed oil, hydrocolloids, dietary fiber (Valiente and others 1995).

In the literature reviewed, no work was reported where grape pomace was used in extrusion processing. In fact, very few studies were published where fruit was used for extrusion. Akdogan and McHugh (1999) investigated the extrusion

of peach puree to explore possible ways to use imperfect peach pieces as value-added products. Camire and others (2002) extruded white corn meal with blueberry and Concord grape-juice concentrate (~3:1 w/w) at 300 rpm with barrel temperature profile 38/49/116/138/113 °C. For the grape juice-corn meal mixture, extrusion processing reduced anthocyanin by ~73%. Despite losses during extrusion, sufficient amounts of the colorants remain to produce a purple color.

2. Theoretical model development

2.1 Overall model

The purpose of this chapter is to introduce the theoretical model employed in this study. An extruder can be considered a continuous chemical reactor. Due to axial mixing, there is a distribution of residence times ($E(t)$) in the exit stream and the fundamental equation for mean retention of anthocyanins (the reactant) in that stream is (Levenspiel 1999):

$$\left(\bar{C}/C_o\right)_{\text{at exit}} = \int_0^{\infty} (C/C_o)_{\text{element}} E(t) dt \quad (1)$$

Complex systems such as food often result in different orders of reactions where the order changes with concentration or time. Nonetheless, useful estimates of parameters may be obtained by assuming an overall or 'apparent order' of reaction. In this study, "order" of reaction refers to the "apparent order". For ease of explanation, $(C/C_o)_{\text{element}}$ is assumed to follow a 1st-order reaction:

$$(C/C_o)_{\text{element}} = \exp(-kt) \quad (2)$$

Substituting Eqn. (2) into Eqn. (1) yields

$$\left(\bar{C}/C_o\right)_{\text{at exit}} = \int_0^{\infty} \exp(-kt) E(t) dt \quad (3)$$

The effects of temperature, moisture content, and mechanical shear on reaction rate constant k can be written as:

$$k = k_r \exp \left[\frac{-\Delta E}{R} \left(\frac{1}{T} - \frac{1}{T_r} \right) + b(MC - MC_r) + d(S) \right] \quad (4)$$

y

d

c

m

sh

where temperature term = $\frac{-\Delta E}{R} \left(\frac{1}{T} - \frac{1}{T_r} \right)$, moisture term = $b(MC - MC_r)$, and shear term = $d(S)$. Guzman-Tello and Cheftel (1987) estimated the parameters (k_r , ΔE , b , d) in Eqn. (4) by changing one variable at a time in extrusion experiments. However, there are limitations to this method. First, it is virtually impossible to maintain isothermal conditions in high-temperature extrusion processing. Second, only small ranges of screw speed can be studied, because varying screw speed (shear term in Eq. (4)) changes the residence time, so the time-temperature profile (temperature term) between runs is not constant.

Therefore, the approach of this study was to solve for thermal kinetic parameters (k_r and ΔE) separately in a shearless environment, (Section 2.1 – 2.3) and use that result to remove the effects of temperature from extrusion (Section 2.4) to yield the effects of shear on anthocyanin degradation (Section 2.5). Moisture content is constant within the extruder barrel. Setting the moisture content term $MC = MC_r$ and separating the temperature (T) and shear term (S) in Eq. (4) yields

$$k = k_r \exp \left[\frac{-\Delta E}{R} \left(\frac{1}{T} - \frac{1}{T_r} \right) \right] \exp [d(S)] \quad (5)$$

Since product is sheared throughout the barrel and die, it is reasonable to describe shear effects (S) using shear history. Since shear history already contains a time term, it cannot be incorporated into k in Eq. (5) because k will be multiplied with time to solve for retention (Eq. (2)). Therefore, we separated the shear term ($d(S)$) from the element rate constant expression (Eq.(5)) and

assumed an empirical function, $f(S)$, to describe the shear effects. Substituting Eq. (5) into Eq. (3) yields

$$\left(\bar{C}/C_o\right)_{\text{at exit}} = \left\{ \int_0^{\infty} \exp \left\{ -k_r \exp \left[\frac{-\Delta E}{R} \left(\frac{1}{T} - \frac{1}{T_r} \right) \right] \right\} t E(t) dt \right\} f(S) \quad (6)$$

where we described shear effects, S , in terms of screw speed, specific mechanical energy (SME), and shear history (explained further in Section 2.6). For shear history, an average shear rate was used, because present knowledge and experimental methodology do not allow accurate prediction of local shear rates in extruded dough. Since it is impossible to maintain isothermal conditions in high-temperature extrusion, temperature is a function of time, $T(t)$. Therefore,

the term $\exp \left(\frac{-\Delta E}{R} \left(\frac{1}{T} - \frac{1}{T_r} \right) \right) t$ becomes an integrated time-temperature history

term, which will be denoted $\beta(t)$ (explained further in Section 2.4). Substituting $\beta(t)$ into Eq. (6) yields

$$\left(\bar{C}/C_o\right)_{\text{at exit}} = \left[\int_0^{\infty} \left[\exp(-k_r \beta(t)) \right] E(t) dt \right] f(S) \quad (7)$$

In shorthand,

$$R_T = R_{\beta} R_S \quad (8)$$

where the total retention is $R_T = \left(\bar{C}/C_o\right)_{\text{at exit}}$;

and the retention due to thermal effect is

$$R_{\beta} = \int_0^{\infty} \exp(-k_r \beta(t)) E(t) dt \quad (9)$$

Thermal (R_β) and mechanical (R_S) effects are discussed in Sections 2.2 – 2.5 and 2.6, respectively..

2.2 Primary model describing rate of anthocyanin degradation

The rate of degradation, $-r$, of anthocyanins in solution has commonly been modeled using Eq. (10)

$$-r = -\frac{dC}{dt} = kC^n \quad (10)$$

Combining variables and integrating the left side from initial concentration C_0 to C yields

- for a first-order reaction ($n=1$),

$$\ln\left(\frac{C}{C_0}\right) = -\int_0^t k dt \quad (11)$$

- for an n^{th} -order reaction ($n \neq 1$),

$$\frac{C^{1-n}}{1-n} - \frac{C_0^{1-n}}{1-n} = -\int_0^t k dt \quad (12)$$

Several authors have found the rate to follow a first-order reaction (Sastry and Tischer 1952, Markakis and others 1956, Daravingas and Cain 1968, Tanchev and Yoncheva 1974, Cemeroglu and others 1994). Fresh fruits such as grapes may possess more than 15 different types of anthocyanins in varying proportions (Mazza 1995). Since an anthocyanin solution is not a single species sample, but rather a 'mixture' of anthocyanins, a 'pseudo' first-order reaction was modeled. Therefore, in this study, "first-order reaction rate" was used to refer to a "pseudo first-order reaction".

The rate is not only a function of anthocyanin concentration, C (Eq.(10)), but can also vary with temperature, moisture content, pH, pressure, properties of reactant(s), and other experimental conditions. The following sections will address how the rate was modeled as a function of different experimental conditions. We will refer to Eq. (11) and (12) as the “primary” models for 1st-order and n^{th} -order reactions, respectively. “Primary” refers to models describing concentration with time. An equation describing the rate constant, k , as a function of any variable will be called the “secondary” model.

2.3 Secondary model describing temperature and moisture effects

2.3.1 Case 1 – Temperature and moisture content changing with time

In the case where temperature and moisture content change with time, such as intermediate-moisture samples heated at high temperatures (>100°C), the rate may be dependent on temperature and moisture content. The reaction rate constant, k , typically follows the Arrhenius relationship with temperature (Tanchev and Yoncheva 1974, Labuza and Riboh 1982, Cemeroglu and others 1994). Assuming an exponential relationship with moisture content (Akdogan and McHugh 1999, Cha and others 2001), the secondary model for k can be written as

$$k = k_r \exp \left[\frac{-\Delta E}{R} \left(\frac{1}{T(t)} - \frac{1}{T_r} \right) + b(MC(t) - MC_r) \right] \quad (13)$$

Because both T and MC are functions of time, their terms must remain within the integral in Eq. (11) or (12). Substituting Eq. (13) into Eq. (11) or (12) for 1st-order and n^{th} -order reactions, respectively, yields

- for $n = 1$
$$\ln\left(\frac{C}{C_o}\right) = -k_r \beta_{T,MC} \quad (14)$$

- for n^{th} -order
$$\left(\frac{C^{1-n} - C_o^{1-n}}{1-n}\right) = -k_r \beta_{T,MC} \quad (15)$$

where

$$\beta_{T,MC} = \int_0^t \exp\left[\frac{-\Delta E}{R}\left(\frac{1}{T(t)} - \frac{1}{T_r}\right) + b(MC(t) - MC_r)\right] dt \quad (16)$$

To use the model in Eq. (14) - (15), three parameters must be estimated: temperature parameter ΔE , moisture parameter b , and reference rate constant k_r . Typically, ΔE is estimated by conducting isothermal experiments using at least 3 constant temperatures at $MC = MC_r$. The negative slopes of $\ln C$ ($n=1$, Eq. (11)) or $C^{1-n}/(1-n)$ ($n \neq 1$, Eq. (12)) versus t are the rate constants k . Finally, $-\Delta E/R$ is the slope of $\ln(k)$ versus $(1/T - 1/T_r)$ (Eq. (13)). The parameter, b , is found similarly: at least 3 constant moistures at one constant temperature $T=T_r$; and b is the slope of $\ln(k)$ versus $(MC - MC_r)$ (Eq. (13)). The third parameter, k_r , is the k at reference temperature T_r and reference moisture MC_r (Eq. (13)).

In this study, these standard procedures to obtain estimate ΔE could not be used because a) at $T > 100$ °C, constant temperature could not be attained before a significant amount of anthocyanins had already degraded; and b) moisture could not be held constant at $T > 100$ °C. Therefore, a nonisothermal method was used, as described in Section 3.2.2.

Theoretically, ΔE , b , and k_r could be estimated simultaneously by nonlinear regression of Eq. (14) or (15). However, increased number of

parameters increases the probability of convergence difficulties (multiple combinations of ΔE and b that give the same minimum sum of squares of residuals) and reduces degrees of freedom (larger confidence intervals). Furthermore, I was hesitant to use a nonlinear estimate of b at changing moisture and temperature without a linear comparison of b at constant moisture contents, because there were no reported values of b in the literature. Therefore, the fact that I could conduct lower-temperature (<100 °C) experiments at different constant moisture contents gave me the option of linear regression to estimate b at constant temperature. So, rather than take a fully nonlinear approach, I chose to take a two-step approach, which I found conceptually more satisfying: 1) hold temperature constant at 80 °C (chosen for minimal moisture loss) and use linear regression to estimate b ; 2) correct all data to MC_r so that the moisture term in Eq. (16) drops out; then use nonlinear regression to estimate ΔE , k_r , and C_o for 1st-order or n^{th} -order models.

The moisture content parameter, b , was estimated as described previously at $T_r = 80$ °C. We assumed that b would be nearly constant over the entire temperature range up to 145 °C. The following two sections describe the theory a) to estimate b (Section 2.2.2) and b) to correct C at any moisture content MC to C_r at reference moisture content MC_r (Section 2.2.3).

2.3.2 Case 2 – Isothermal heating at different constant moisture contents to estimate b

2.3.2.1 Slope method to estimate b

When a sample is heated isothermally at one temperature (<100 °C) where different constant moisture contents are used, Eq. (13) can be simplified

by setting the one temperature $T = T_r$ (reference temperature) and removing the time dependency of T and MC :

$$k = k_r \exp[b(MC - MC_r)] \quad (17)$$

Taking log of both sides allows linear regression to estimate b (Figure 2.2.1)

$$\ln(k) = \ln(k_r) + b(MC - MC_r) \quad (18)$$

A positive value of b would indicate the rate of degradation is faster at higher MC 's, and a negative b would indicate the reverse.

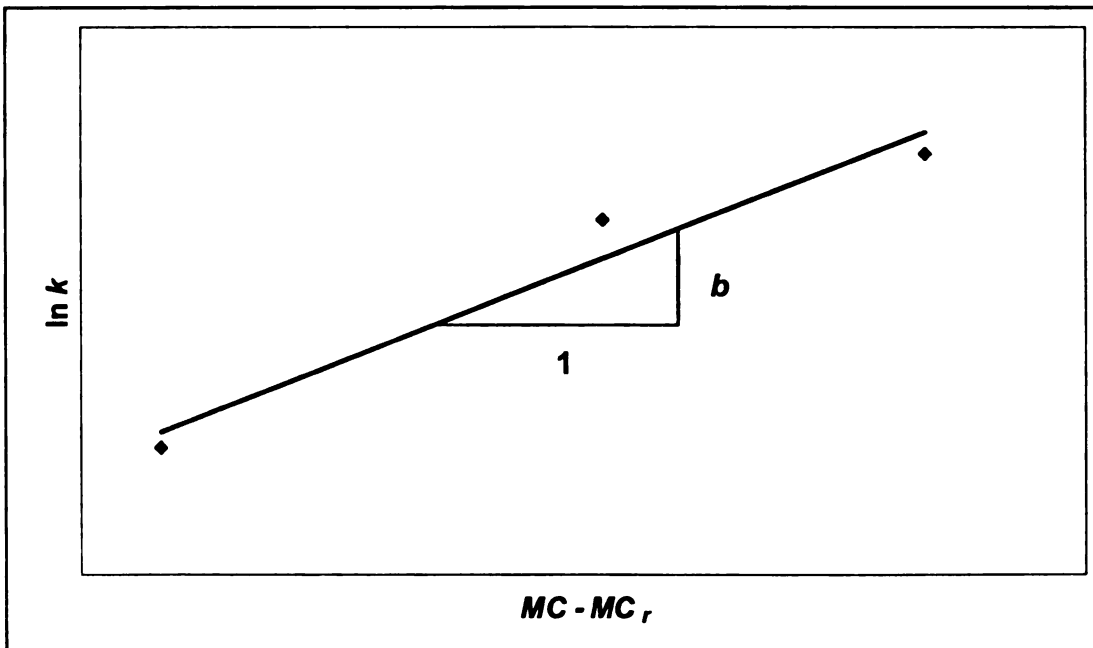


Figure 2.3.1 – Example of estimating b using slope method.

2.3.2.2 Constant heating time method to estimate b

An alternate approach to estimate b is to hold time constant. This method is especially useful when one of the slopes ($-k$) is poorly defined. Combining Eq. (13) with Eq. (11) and (12), respectively, where $T = T_r$ and moisture is not changing with time yields the follow primary-model equations after integrating:

- for $n = 1$:
$$\ln\left(\frac{C}{C_o}\right) = -k_r t \exp[b(MC - MC_r)] \quad (19)$$

- for n^{th} -order:
$$\left(\frac{C^{1-n} - C_o^{1-n}}{1-n}\right) = -k_r t \exp[b(MC - MC_r)] \quad (20)$$

If there is a lag time (time for temperature to reach nearly constant T), the lines described by Eq. (19) or (20) will not necessarily be straight during that lag time. To simplify the procedure to correct all C data to reference moisture MC_r , we assumed all lines described by Eq. (19) or (20) are straight with slope $-k_r \exp(b(MC - MC_r))$ that intersect at one point, $f(C'_o)$. Then Eq. (19) or (20) can be used by simply replacing C_o with C'_o , where $\ln C'_o$ or $(C'_o)^{1-n}/(1-n)$ is the average of the zero-time intercepts extrapolated from all $\ln C$ versus t (first-order reaction, Figure 2.2.2) or $C^{1-n}/(1-n)$ versus t (n^{th} -order reaction) lines.

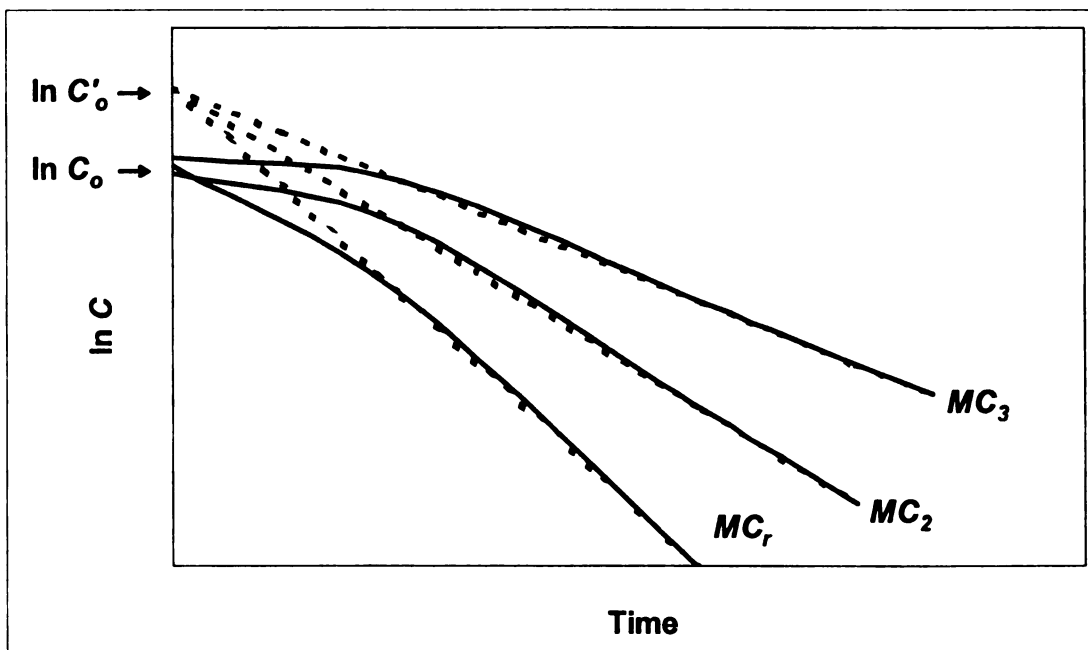


Figure 2.3.2 - Graphical display of $\ln C_o$ and $\ln C'_o$ for 1st-order reaction.

To estimate b at constant heating time, multiply Eq. (19) and (20) by -1 , and take the natural logarithm of both sides to yield

- for $n=1$:
$$\ln\left[-\ln\left(\frac{C}{C'_o}\right)\right] = \ln(k_r t) + b(MC - MC_r) \quad (21)$$

- for n^{th} -order:
$$\ln\left(-\frac{C^{1-n} - C'_o{}^{1-n}}{1-n}\right) = \ln(k_r t) + b(MC - MC_r) \quad (22)$$

The parameter b is the slope of $\ln\left[-\ln\left(\frac{C}{C'_o}\right)\right]$ versus $(MC - MC_r)$ (Eq. (21)) and

$\ln\left(-\frac{C^{1-n} - (C'_o)^{1-n}}{1-n}\right)$ versus $(MC - MC_r)$ (Eq. (22)). Because each heating time

may give slightly different estimates of b , we used the average of all b values at each constant time.

2.3.3 Moisture correction methods

Using the moisture constant, b , retention taken from samples at any moisture content can be corrected to a reference moisture content. The following sections provide the correction factor for each case.

2.3.3.1 Case 1 – Nonisothermal heating

The reference equation for temperature changing with time at a constant reference moisture content MC_r can be written by substituting MC_r into Eq. (16) and rewriting Eq. (14) and (15)

- for $n=1$:
$$\ln\left(\frac{C_r}{C_o}\right) = -k_r \beta \quad (23)$$

- for n^{th} -order:
$$\left(\frac{C_r^{1-n} - C_o^{1-n}}{1-n}\right) = -k_r \beta \quad (24)$$

where time-temperature history, β , equals

$$\beta = \int_0^t \exp\left[\frac{-\Delta E}{R}\left(\frac{1}{T(t)} - \frac{1}{T_r}\right)\right] dt \quad (25)$$

By dividing Eq. (23) at MC_r by Eq. (14) at MC for a first-order reaction;

$$\frac{\ln\left(\frac{C_r}{C_o}\right) = -k_r \beta}{\ln\left(\frac{C}{C_o}\right) = -k_r \beta_{T,MC}} \quad (26)$$

we obtained a relationship to correct any observed concentration (C) at MC to concentration (C_r) at MC_r using

- for $n=1$:
$$\ln\left(\frac{C_r}{C_o}\right) = \ln\left(\frac{C}{C_o}\right) \frac{\beta}{\beta_{T,MC}} \quad (27)$$

where the nonisothermal (NI) correction factor CF equals

$$CF_{NI} = \frac{\beta}{\beta_{T,MC}} \quad (28)$$

The same correction factor applies for n^{th} -order reaction, so Eq. (24) divided by Eq. (15) and solved for reference condition yields

- for n^{th} -order:
$$\left(\frac{C_r^{1-n} - C_o^{1-n}}{1-n}\right) = \left(\frac{C^{1-n} - C_o^{1-n}}{1-n}\right) \frac{\beta}{\beta_{T,MC}} \quad (29)$$

Assuming reaction order n is not a function of moisture content, Eq. (29) can be simplified by multiplying both sides by $1-n$ to yield

$$(C_r^{1-n} - C_o^{1-n}) = (C^{1-n} - C_o^{1-n}) \frac{\beta}{\beta_{T,MC}} \quad (30)$$

the analog to the 1st-order case, Eq. (27).

2.3.3.2 Case 2 – Isothermal heating

For isothermal heating at different constant moisture contents, the equation for constant temperature at reference moisture content is simplified from Eq. (19) and (20) for 1st-order and n^{th} -order reaction to

- for $n=1$:
$$\ln\left(\frac{C_r}{C'_o}\right) = -k_r t \quad (31)$$

- for n^{th} -order:
$$\left(\frac{C_r^{1-n} - (C'_o)^{1-n}}{1-n}\right) = -k_r t \quad (32)$$

Dividing Eq. (31) by Eq. (19) for 1st-order and Eq. (32) by Eq. (20) for n^{th} -order reactions and solving for reference condition yields

- for $n=1$:
$$\ln\left(\frac{C_r}{C'_o}\right) = \ln\left(\frac{C}{C'_o}\right) \exp[-b(MC - MC_r)] \quad (33)$$

- for n^{th} -order:
$$\left(C_r^{1-n} - (C'_o)^{1-n}\right) = \left(C^{1-n} - (C'_o)^{1-n}\right) \exp[-b(MC - MC_r)] \quad (34)$$

where n is not a function of MC and the isothermal (I) correction factor in this case is

$$CF_I = \exp[-b(MC - MC_r)] \quad (35)$$

For isothermal heating, we must use the pseudo-initial concentration, C'_o , to be consistent with the straight-line assumption of Eq. (19) and (20).

2.4 Estimation of thermal kinetic parameters

Once all data points are adjusted to reference moisture content, nonlinear regression can be used to fit corrected data to a selected model. A logarithmic form of the first-order reaction model was represented in Equation (23).

Exponential forms of Eq. (23) can be written as

- in terms of retention:
$$\frac{C_r}{C_o} = \exp(-k_r \beta) \quad (36)$$

- in terms of concentration:
$$C_r = C_o \exp(-k_r \beta) \quad (37)$$

The n^{th} -order reaction model (Eq. (24)) expressed in terms of retention and C_r , respectively are

- in terms of retention:
$$\frac{C_r}{C_o} = [1 + (n-1)k_r \beta C_o^{n-1}]^{\frac{1}{1-n}} \quad (38)$$

- in terms of concentration:
$$C_r = [(n-1)k_r \beta + C_o^{1-n}]^{\frac{1}{1-n}} \quad (39)$$

From Eq. (36)- (39), the corrected data (left-hand sides) were set equal to the selected model (right-hand sides) and the kinetic parameters k_r , ΔE , C_o , and n were estimated (where necessary) by minimizing the sum of squares of the residuals (observed data minus model results) using nonlinear regression.

2.5 Thermal effect on anthocyanin retention during extrusion

The kinetic parameters were used to calculate the thermal effect on anthocyanins during extrusion using Eq. (25) except a residence time distribution was included in the computation. In extrusion, an extrudate element undergoes a changing temperature profile along the barrel. Each element also travels at a different speed described by a residence time distribution, $E(t)$, due to axial mixing within the barrel. Quantifying the thermal effects from extrusion requires 2 integrals – first, integration over the length of the extruder barrel to determine the time-temperature history, $\beta(t)$, at each element exit time, t , and second, integrating the element retention over the residence time distribution (RTD) curve, $E(t)$. Therefore, Eq. (25) for extrusion becomes

$$\beta(t) = \int_0^t \exp\left[\frac{-\Delta E}{R} \left(\frac{1}{T(t)} - \frac{1}{T_r}\right)\right] dt \quad (40)$$

where $\beta(t)$ is the time-temperature history for an element with exit age, t . One must determine how to express $T(t)$ and dt for an element moving through the extruder. The extruder can be separated into sections i with length x to analyze the changing temperatures along the barrel. Then, temperature with respect to time ($T(t)$) can be converted to temperature with respect to extruder length ($T(x)$). If the weight of product can be measured (after a dead-stop) in each identified section Δx_i , the mean residence time of the dough in section Δx_i is $\Delta \bar{t}_i = \frac{m}{\dot{m}}$ (Cai and Diosady 1993, Dolan 2003) and the element residence time is estimated as

$\Delta t_i \approx \Delta \bar{t}_i \left(\frac{t}{\bar{t}}\right) = \frac{m_i}{\dot{m}} \frac{t}{\bar{t}}$. Theoretically, by conservation of mass, the sum of the

sectional mean residence times must equal the total mean residence time:

$$\sum_i \Delta \bar{t}_i = \bar{t} \quad (41)$$

Practically, the left side of Eq. (41) (from weighing after dead stop) was not exactly equal to the right side (from RTD curve), due to the two different measurement methods, loss of moisture after opening the barrel, and other experimental error. Therefore, we assumed the error in each section was proportional to the overall error and defined a correction factor for residence time based on Eq. (41):

$$CF_{RT} = \frac{\bar{t}}{\sum_i \Delta \bar{t}_i} = \frac{\bar{t}}{\sum_i m_i / \dot{m}}$$

Consequently, the final approximation of the element residence time Δt_i

$$\Delta t_i = \left(\frac{m_i}{\dot{m}} \right) \left(\frac{t}{\bar{t}} \right) \left(\frac{\bar{t}}{\sum_i m_i / \dot{m}} \right) = \frac{m_i}{\sum_i m_i} t \quad (42)$$

Equation (42) states that the element residence time in section i is equal to the element residence time in the entire extruder multiplied by the ratio of the dough mass in section i divided by the total dough mass in the extruder.

Substituting Δt_i for dt and $T(x_i)$ into Eq. (40) provides an equation for summing the time-temperature history of each section i over the total number of barrel sections g :

$$\beta(t) = \sum_{i=1}^g \exp \left[\frac{-\Delta E}{R} \left(\frac{1}{T(x_i)} - \frac{1}{T_r} \right) \right] \left(\frac{m_i}{\sum_j m_j} \right) t \quad (43)$$

For plug flow (when there is no residence time distribution), no integral is needed, and the element retention (C/C_o) can be measured. However, when there is a residence time distribution, it is only possible to measure the mean retention \bar{C}/C_o . The mean retention, previously defined as R_β , at constant dough moisture content was calculated by integrating the element over the RTD curve and solving the integral numerically using the trapezoidal rule to yield

$$R_\beta = \sum_i (C/C_o)_{\text{element}} E(t_i) \Delta t_i \quad (44)$$

where

- for 1st-order reaction (Eq. (36)): $R_\beta = \exp[-k_r \beta(t_i)]$ (45)

- for n^{th} -order reaction (Eq. (38)): $R_{\beta} = \left[1 + (n-1)k_r\beta(t_i)C_o^{n-1}\right]^{\frac{1}{1-n}}$ (46)

2.6 Mechanical effect on anthocyanin retention and final model equation

Equation (8) can be used to solve for mechanical retention, R_S . Then, total, thermal, and mechanical retention values can be converted to total loss (X_T), thermal loss (X_{β}), and mechanical loss (X_S). Rewriting Eq. (8) in terms of loss:

$$X_T = 1 - R_T = 1 - R_{\beta}R_S \quad (47)$$

If there were no shear effects during extrusion, the total loss, X_T , would equal the thermal loss ($R_S = 1$), or $X_T = X_{\beta}$. From Levenspiel (1999),

$X_T = \int_0^{\infty} \{1 - \exp[-k_r\beta(t)]\} E(t) dt$. Separating the integral yields

$$X_{\beta} = \int_0^{\infty} E(t) dt - \int_0^{\infty} \exp[-k_r\beta(t)] E(t) dt \quad (48)$$

By definition, $E(t) dt$ equals unity (Levenspiel 1999) so Eq. (48) becomes

$$X_{\beta} = 1 - \int_0^{\infty} \exp(-k_r\beta(t)) E(t) dt = 1 - R_{\beta} \quad (49)$$

Figure 2.6.1 shows graphically R_T , R_{β} , and R_S from which it can be seen that

$$X_T = X_{\beta} + X_S \quad (50)$$

where $X_T = 1 - (\bar{C}/C_o)_{\text{at exit}}$;

the loss due to thermal effect is $X_{\beta} = 1 - \int_0^{\infty} \exp[-k_r\beta(t)] E(t) dt$, and

the loss due to mechanical effect is $X_S = f(S)$. Thus, substituting X_T from Eq.

(47) and X_{β} from Eq. (49) into Eq. (50), mechanical loss can be calculated as:

$$X_s = R_\beta(1 - R_s) \quad (51)$$

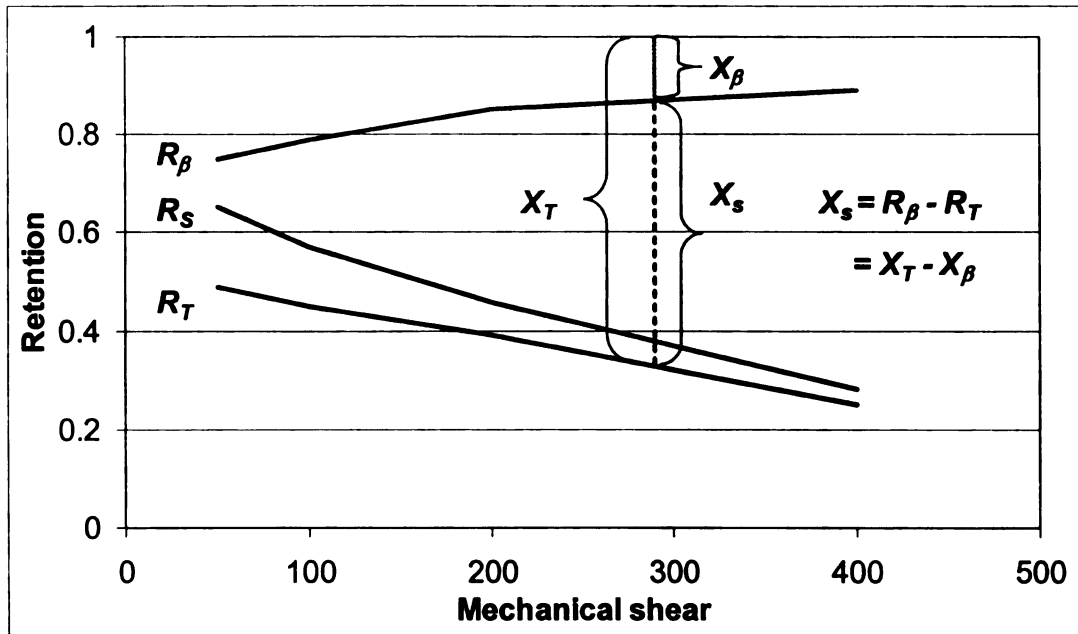


Figure 2.6.1 – An example of total retention, thermal retention and mechanical retention versus mechanical shear depicting graphically mechanical retention, R_s . X_T is total loss, X_β is thermal loss, and X_s is mechanical loss.

It is expected that the remaining effects on anthocyanin degradation (after thermal effects have been removed) may contain other factors in addition to mechanical effects. However, we assume the majority of it will be due to mechanical shear. Therefore, 'mechanical' effects in this study will refer to mechanical plus other effects.

In this study, mechanical loss was fit with an empirical equation:

$$X_s = f(S) \quad (52)$$

where S was expressed in terms of screw speed, SME , or shear history (Komolprasert and Ofoli 1990). The shear rate of the extruder constitutes the major source of heat energy for cooking extruders and is critical for evaluating

viscous dissipation (Mohamed and others 1990). Shear history is based on the average shear rate, $\dot{\gamma}_a$, and mean residence time, \bar{t} :

$$\phi = \dot{\gamma}_a \bar{t} \quad (53)$$

where average shear rate can be estimated using mixer viscometry techniques (Suparno and others 2002) as

$$\dot{\gamma}_a = k'N^\alpha \quad (54)$$

The specific mechanical energy is the mechanical energy input required to extrude 1 kg of product or feed (Bhattacharya and Choudhury 1994). It can be calculated as

$$SME = \frac{E_v}{\dot{m}} \quad (55)$$

where $E_v = P_w - \Delta PQ$

$P_w = 2.64N(\% \text{torque} - \% \text{base torque})$ from manufacturer

$$Q = \frac{\dot{m}}{\rho}$$

2.7 Model validation

The $PRESS_p$ (prediction of sum of squares) criterion, a measure of how well the use of the fitted parameter values for a subset model can predict observed responses (Y_i), was employed as a form of data splitting to assess the precision of the model predictions for X_β and X_S (Neter and others 1996). The $PRESS$ criterion was measured by deleting the i th case from the data set, estimating the regression function parameters for the subset model from the remaining $n - 1$ cases, and then using the fitted regression function parameters to

obtain the predicted value $\hat{Y}_{i(i)}$ for the i th case. The *PRESS* prediction error for the i th case is:

$$Y_i - \hat{Y}_{i(i)}$$

and the $PRESS_p$ criterion is the sum of the prediction error:

$$PRESS_p = \sum_{i=1}^n (Y_i - \hat{Y}_{i(i)})^2 \quad (56)$$

Models with small $PRESS_p$ values are considered good predictive models and $PRESS$ value close to SSE supports the validity of the fitted regression model (Neter and others 1996).

2.8 Novelty of model development

This study contained three novel elements in the model development:

- 1) The use of the retention model to predict anthocyanin retention during extrusion, and expression of the retention model to a loss model,
- 2) The moisture correction factors that were developed to convert all anthocyanin absorbance to reference moisture content because the thermal experiments (isothermal and nonisothermal heating) involved simultaneously changing temperature and moisture content.
- 3) The calculation of element residence time in the extruder, and the correction factor for residence time

3. Experimental Materials and Methods

“Images in this thesis are presented in color.”

3.1 Determination of anthocyanin content

3.1.1 Reagents

Extraction solvent –

95% ethanol in 1.5 N hydrochloric acid (85:15 v/v). pH = 0.85 ± 0.05 .

Potassium chloride –

0.2 N. Dissolve 3.725 g KCl in fresh water (Millipore, Bedford, MA, USA) to 250 ml.

Hydrochloric acid – 0.2 N. Dilute 4.15 ml of HCl up to 250 ml with fresh water.

Sodium acetate – 1 N. Dissolve 20.5 g CH₃COONa in fresh water to 250 ml.

Hydrochloric acid – 1 N. Dilute 20.75 ml of HCl up to 250 ml with fresh water.

pH 1.0 buffer – Started with 20 ml of 0.2 N KCl and 50 ml of 0.2 N HCl stirred together. pH was measured and KCl or HCl added as needed until pH = 1.0 ± 0.05 . The pH was checked each analysis day. Buffer stocks were made fresh monthly.

pH 4.5 buffer – Started with 20 ml 1N CH₃COONa and 10 ml HCl stirred together. pH was measured and CH₃COONa or HCl added as needed until pH = 4.5 ± 0.05 . The pH was checked each analysis day. Buffer stocks were made fresh monthly.

3.1.2 Extraction of anthocyanins

The methods of Fuleki & Francis (1968) and Giusti & Wrolstad (2001) were adapted for the extraction of anthocyanins using extraction solvent (E.S.) with pH 0.85 ± 0.05 . A 10.00 g sample was used for all extraction and its moisture content measured per AACC Method 44 -19 (AACC 1999). The total volume of E.S. used was experimentally determined as 100 ml E.S. per 2.60 g dry weight of grape pomace in the mixture. First, 40% of the total E.S. solvent was added to the sample held in small bottles and shaken using Maxi-Mix III shaker at speed

setting 600 (Type 65800, Thermolyne, Dubuque, IA, USA) for 1 hr at room temperature. Residue and extract were filtered through Whatman No. 4 filter paper and washed repeatedly with the remaining 60% E.S. solvent. Collected extracts were made up to final volume based on the ratio:

$$\text{Final volume} = 0.87 \times \text{Total volume of E.S.}$$

The ratio was determined from preliminary experiments that showed the overall recovery after filtration was ~87%. The extract (pH ~ 0.90) was left at room temperature until analysis.

3.1.3 Analysis of anthocyanins

The total monomeric anthocyanins content was evaluated based on the pH-differential method (Giusti and Wrolstad 2001) using spectrophotometry. Absorbance was read on a Genesys 5 spectrophotometer (Spectronic Instruments, Rochester, NY, USA) with specifications listed in Table 3.1.1.

Table 3.1.1 - Specifications for Genesys 5 spectrophotometer

Spectral slitwidth	5 nm
Optical system	Split-beam, dual detectors
Wavelength:	
Range	200 to 1100 nm
Accuracy	± 1 nm
Photometric (absorbance):	
Range	-0.1 to 3.000 A
Accuracy	±1% of reading from 0.3 to 2 A ±2% of reading from 2 A to 3 A

Two milliliters of each anthocyanin extract were diluted to 6 ml (dilution factor = 3 where dilution factor = final volume/volume of extract) with pH 1.0 and pH 4.5 buffers. Dilution factor was selected within the linear range of absorbance against concentration. Buffered samples were left to equilibrate to the buffer pH for 1 hr at room temperature (~25°C) then centrifuged using a Beckman centrifuge (Fullerton, CA, USA) at 12,000 rpm (16,000 g) for 10 min at ~25°C.

The spectrophotometer was turned on to warm up for at least 30 min. Extracts were pipetted into a 3 ml near-UV glass cell (Fisher Scientific, Pittsburgh, PA, USA). The absorbance (A), in arbitrary units (AU), of all samples was read at maximum absorbance wavelength, UV_{nm} (Appendix 1, Figure A.1.1) and 700 nm (to correct for light scattering) using distilled water as blanks. Since both distilled water and solvents had zero absorbance, distilled water was used as blanks for ease of analysis. Total monomeric anthocyanin content was expressed as the difference in absorbance (corrected for light-scattering):

$$A = (A_{UV_{max}} - A_{700})_{pH1.0} - (A_{UV_{max}} - A_{700})_{pH4.5} \quad (57)$$

The absorbance was divided by the dry weight of grape pomace in the mixture to yield absorbance per gram of grape pomace (dry basis). In most studies, absorbance is converted to concentration by using an extinction coefficient from the standard of a single predominant anthocyanin in the extract (Calvi and Francis 1978, Cemeroglu and others 1994, Camire and others 2002). However, it is not known whether individual anthocyanins or a mixture of anthocyanins confer health benefits. Also, since grape pomace contains a number of

anthocyanins, this study is focused on the degradation of “total anthocyanins” and thus analysis was based on total anthocyanins.

A standard curve was established to determine the linear range of absorbance against concentration (Appendix 1, Figure A.1.2). Sample extract was diluted to six concentrations: 0.0167, 0.1, 0.133, 0.167, 0.2, and 0.333 ml extract per ml total volume using pH 1.0 buffer and read at UV_{max} and 700 nm using spectrophotometer.

3.2 Thermal effects on anthocyanins in grape pomace-flour mixture

3.2.1 Sample preparation

Fresh grape pomace (*Vitis labrusca*, Concord variety) from the 2001 crop year was supplied courtesy of a local processor (Welch's, Lawton, MI, USA) and used as an anthocyanin source. The grape pomace, containing skins, seeds, twigs, and cellulose as a pressing aid, was stored at -20°C upon arrival. The pomace was first air dried for 1-2 days ($\sim 22^{\circ}\text{C}$, $\sim 40\%$ relative humidity) to remove excess moisture (for ease of grinding), and then ground repeatedly to pass through a 12.7 mm (0.5 in) screen. Grape pomace (moisture content $\sim 30\%$ wb) and pastry flour (Mennel Milling Company; Fostoria, OH, USA; moisture content $\sim 16\%$ wb) were mixed together on a 1:3 (w/w) ratio dry weight basis (25% grape pomace) in small batches using a Hobart A-200 mixer (The Hobart Mfg., Troy, OH, USA) at setting 1 for 20 min and air-dried overnight ($\sim 22^{\circ}\text{C}$, $\sim 40\%$ relative humidity). The mixture was passed through a Model 4E grinding mill (The Strauss Co., Hatboro, Pa, USA) to reduce particle size, rupture seeds, and improve sample homogeneity (Figure 3.2.1). The sample was mixed again

in batches for 10 min, and analyzed for moisture content. This final mixture (~14% moisture content (wb)) composition was established based on results from preliminary experimental extrusion runs.



Figure 3.2.1 – Grape pomace-flour mixture (1:3 w/w db).

Samples at 10, 20, and 43% moisture content dry basis (9, 17, and 30% wb) were used for the thermal study. The original mixture was oven-dried at 30°C to 10% moisture (db) while 20% and 43% moisture content (db) samples were prepared by spraying the appropriate amount of water onto the mixture, mixing for 20 minutes in batches, and allowing the moisture to equilibrate in a sealed container overnight. Moisture content analysis for all samples was determined in duplicate the next day and only mixture within $\pm 2\%$ of the target moisture content was used for the study.

Moisture content analysis for all samples in this study was determined in duplicate using AACC Method 44 -19 (AACC, 1999).

3.2.2 Isothermal and nonisothermal heating of grape pomace-flour mixture: experimental design

Fifteen-gram samples of the mixture at 43% moisture content (reference moisture content) were filled in a cylindrical stainless steel cell with inner thickness of 4.5 ± 0.5 mm, 100 mm diameter, and ~1mm steel wall thickness. Duplicate samples were heated at 80, 105, or 145°C using silicon oil (Fisher Scientific, Pittsburgh, PA, USA) in an Isotemp 10 BP heater bath (Fisher Scientific, Pittsburgh, PA, USA) and removed at 4 selected times such that anthocyanin retention would be in the 20 – 75% range (Figure 3.2.2). Each sample was replicated on another day.



Figure 3.2.2 – Setup for thermal study.

Heating at 80°C was isothermal, meaning that all samples were removed at times greater than lag time. Heating at 105°C and 145°C was nonisothermal. The cells were submerged in the oil bath using a basket so that the oil level was above the fill line of the sample. Cells were immediately cooled in an ice-water bath after heating. The center temperature of the samples was measured by a 30-gauge Cu-Cn thermocouple (Cole Parmer Instrument Co., Barrington, IL, USA) and recorded every 4 or 10 s using a Digi-Sense Model 92000-00 Scanning Thermometer data logger (Cole Parmer Instrument Co., Barrington, IL, USA) with the supplementary software Scanlink2. All thermocouples were calibrated prior to running the tests.

Because lag time at 105°C and 145°C was ~23 min and anthocyanin loss within that time frame was significant, all samples at these temperatures were necessarily heated nonisothermally. Given that a minimum grape pomace-flour sample size of ~12-g was needed for adequate anthocyanin measurement, thermal lag and resulting temperature gradient across the sample were unavoidable. These two problems were minimized by using a nonisothermal analysis and certain heat transfer assumptions, respectively, described in Section 3.2.3.1.

To address the expected moisture loss due to oil bath temperatures above 100°C, a separate study was done to investigate the effects of moisture content on thermal degradation by estimating moisture content rate constant b . Samples weighing 13-g at 10% moisture content (db) and 15-g at 20% and 43% moisture content (db) were heated isothermally at 80°C for 15, 45, and 75 minutes (lag

time ~ 12 min). For samples at 10% moisture content, 13-g was used to keep sample fill line below oil bath level.

Table 3.2.1 summarizes the experimental design for thermal study. All samples from thermal study were kept at -10°C prior to extraction and analysis the following day. The raw material was extracted in triplicate at each heating temperature.

Table 3.2.1 - Experimental design for isothermal and nonisothermal heating of grape pomace-flour mixture

Oil bath temperatures ($^{\circ}\text{C}$)	Heating time ranges (min)	%Moisture content (dry basis)
80 (Isothermal)	~15, 45, 75	10, 20, 43%
80 (Isothermal)	~16 – 105	43%
105 (Nonisothermal)	~9 – 70	43%
145 (Nonisothermal)	~6 – 50	43%

3.2.3 Data analysis for thermal study

3.2.3.1 Time-temperature history

For the steel cells in the oil bath, the heat flux to the cell wall via convection was set equal to the heat conducted to the product center at any time (neglecting temperature gradient across the 1 mm steel wall):

$$q = \frac{k_{\text{mixture}} A_s (T_w^i - T_c^i)}{\Delta x/2} = h A_s (T_{\infty} - T_w^i) \quad (58)$$

where superscript i is a time index. Because the half-width of the cell was small (~2.25 mm), an approximation of linear temperature profile across the cell's half-width was used to calculate the mass-average sample temperature for each heating time as:

$$T^i_{\text{average}} = \left(\frac{T_c^i + T_w^i}{2} \right) \quad (59)$$

where center temperature at time i , T_c^i , was measured by the thermocouple, and wall temperature, T_w^i , was calculated using Eq. (58). The temperatures T_c^i and T_∞ were measured every 4 or 10 s. The thermal conductivity of the mixture at its moisture content (wb) was estimated, assuming primarily water and carbohydrates (Hang 1988), using the empirical formula (Rao and Rizvi 1986):

$$k_{\text{mixture}} = 0.61x_w + 0.205x_c \quad (60)$$

The heat transfer coefficient of the oil on the vertical steel cell at each oil bath temperature was calculated using lumped heat-capacity analysis. A brass plate (5mm thick) at ambient temperature with a thermocouple sealed in its center was immersed in the oil bath at constant temperatures of 80, 105, or 145°C, and the time-temperature data were plotted using Eq. (61) to solve for the heat transfer coefficient from the slope (Holman 1976).

$$\ln\left(\frac{T - T_\infty}{T_o - T_\infty}\right) = -\left(\frac{hA_s}{c_p m}\right)t \quad (61)$$

All experiments were conducted in duplicate. The properties of the brass plate were: mass = 236.9 g, surface area = 0.0127 m², and specific heat = 385 J/kg-°C. Equation (58) was used to solve for product wall temperature at each time and substituted into Eq. (59) to calculate mass-average sample temperature. The mass-average temperature was set equal to T in Eq. (25) and integrated over the heating time to calculate β .

3.2.3.2 Moisture content correction

For samples heated nonisothermally at 105°C and 145°C, concentration was mathematically corrected to 30% moisture content using Eq. (27) or (30) for 1st-order or n^{th} -order reaction, respectively. For samples heated isothermally at 80 °C, concentration was mathematically corrected to 30% moisture content using Eq. (33) or (34) for 1st-order or n^{th} -order reaction, respectively. This correction was necessary for data analysis purposes.

3.2.3.3 Estimation of parameters

Observed values from experiment were fitted to a model using a one-step, nonlinear, least-squares regression routine in Excel[®] Solver. A model is linear (in a parameter) if the first partial derivative of the model with respect to the parameter is independent of the parameter (Van Boekel 1996). In this study, only the 1st-order partial derivative of the model with respect to C_0 was independent (Eq. (68)), while the other derivatives were not independent (Eq. (66) - (67), (69) - (72)). Therefore, nonlinear regression was used.

When the model is nonlinear in the parameters, no explicit analytical solutions are available for the parameters or the confidence intervals. The solution was found using weighted least-squares (WLS) regression by first supplying Solver with starting parameter values and through iteration, minimizing the sum of squares of residuals (SS_E):

$$SS_E = \sum W (C_{r,\text{observed}} - C_{\text{model}})^2 \quad (62)$$

where $W = C_{r,observed}^2$ was a weighting function. Higher $C_{r,observed}$ values from short heating times were emphasized in the weighting function, because extrusion heating times are usually short (<5 min). This weight also improves the fit for C_o , which is a way to test the robustness of the model (Van Boekel 1996). In addition, least-squares (LS) regression (using Eq. (62) without the weighting function, W) was also used to solve for the parameters and compared to results from weighted least-squares. For n^{th} -order reaction, LS regression was used.

For a 1st-order reaction, the proposed model was Eq. (37). The retention model (C/C_o) was not selected for several reasons. First, initial concentration C_o is treated as a fixed, initial value though it may also be subject to error and experimental uncertainties. Second, when results are reported in retention, the values of C and C_o are hidden in the fraction. Therefore, C_o was set as a parameter in the regression and used Eq. (37) where the 3 unknown parameters are k_r , ΔE , and C_o .

For n^{th} -order reactions, the proposed model was Eq. (39), where the 4 unknown parameters were k_r , ΔE , C_o , and n . The following command was used in Excel to prevent negative values for C_r :

IF $n < 1$ AND $k_r\beta > C_o^{1-n}$

$$C_r = 0$$

ELSE

$$C_r = \left[(n-1)k_r\beta + C_o^{1-n} \right]^{\frac{1}{1-n}}$$

Corrected values of C_r changed with both b and n (Eq. (30) and (34)) where b was a function of n (Eq. (22)). Because of these interactions, Solver was run

multiple times holding b constant during each run. The four parameters were estimated as with the 1st-order case, with the exception that Solver was run multiple times until both b and n converged. The parameter b was held constant for each Solver run, after which b and all C values were updated with each new n . A starting value of n was obtained by using b from a 1st-order reaction to correct all observed data to 43% reference moisture content, and by minimizing the SS_E of Eq. (39).

The square of the correlation (between observed data and the model), R^2 , was calculated as

$$R^2 = 1 - \frac{SS_E}{SS_T}$$

where and $SS_T = \sum W (C_{r,observed} - \overline{C_{r,observed}})^2$. Since the standard R^2 does not necessarily compare well between linear and nonlinear models, R^2 was re-calculated per corrected formula of Kvålseth (1985) as $R_a^2 = 1 - u(1 - R^2)$ where $u = (m-1)/(m-p-1)$. The values for R_a^2 in this study will be denoted as R^2 .

Residuals (individual deviations of the observed values from the fitted line) were plotted against model values to determine the merits of the model. If any systemic pattern exists, the model may be inadequate for the data set. The residuals are (Bates 1988):

- LS regression: Residuals = $C_r - C_{r,model}$
- WLS regression: Residuals = $\sqrt{W} (C_r - C_{r,model})$

But to compare residuals between all models (both LS and WLS regression), all residuals were calculated using $C_r - C_{r,model}$.

3.2.3.4 Confidence intervals of parameters

For linear models, confidence intervals for the parameters are exactly defined and symmetric, making its calculation straightforward. However, for nonlinear models, the confidence intervals are not symmetric. Approximate confidence intervals for each parameter were found by obtaining asymptotic standard errors (used in nonlinear regression) and deriving confidence intervals for individual parameters using the t test statistic at confidence level $1-0.5\alpha$ (Van Boekel 1996):

$$a_i \pm \sigma_i t_{(1-0.5\alpha),v} \quad (63)$$

where σ_i represents the asymptotic standard error calculated as the square root of the corresponding diagonal of the symmetric parameter variance-covariance matrix:

- For $n=1$:

$$\text{cov}(\mathbf{a}) = (\mathbf{X}^T \mathbf{X})^{-1} (\text{MSE}) = \begin{pmatrix} \sigma_{k_r}^2 & \sigma_{k_r, \Delta E} & \sigma_{k_r, C_o} \\ \sigma_{k_r, \Delta E} & \sigma_{\Delta E}^2 & \sigma_{\Delta E, C_o} \\ \sigma_{k_r, C_o} & \sigma_{\Delta E, C_o} & \sigma_{C_o}^2 \end{pmatrix} \quad (64)$$

- For n^{th} -order reaction:

$$\text{cov}(\mathbf{a}) = (\mathbf{X}^T \mathbf{X})^{-1} (\text{MSE}) = \begin{pmatrix} \sigma_{k_r}^2 & \sigma_{k_r, \Delta E} & \sigma_{k_r, C_o} & \sigma_{k_r, n} \\ \sigma_{k_r, \Delta E} & \sigma_{\Delta E}^2 & \sigma_{\Delta E, C_o} & \sigma_{\Delta E, n} \\ \sigma_{k_r, C_o} & \sigma_{\Delta E, C_o} & \sigma_{C_o}^2 & \sigma_{C_o, n} \\ \sigma_{k_r, n} & \sigma_{\Delta E, n} & \sigma_{C_o, n} & \sigma_n^2 \end{pmatrix} \quad (65)$$

where $MSE = \frac{SS_E}{m-p}$. The matrix was calculated using the sensitivity coefficients

X for each parameter as

- For first-order reaction ($n=1$), $Y = C_o \exp(-k_r \beta)$:

$$X_1 = \frac{\partial Y}{\partial k_r} = -\beta [C_o \exp(-k_r \beta)] \quad (66)$$

$$X_2 = \frac{\partial Y}{\partial \Delta E} = [-k_r C_o \exp(-k_r \beta)] \beta' \quad (67)$$

$$X_3 = \frac{\partial Y}{\partial C_o} = \exp(-k_r \beta) \quad (68)$$

- For n^{th} -order reaction, $Y = [(n-1)k_r \beta + C_o^{1-n}]^{\frac{1}{1-n}}$:

$$X_4 = \frac{\partial Y}{\partial k_r} = -\xi^{\frac{n}{1-n}} \beta \quad (69)$$

$$X_5 = \frac{\partial Y}{\partial \Delta E} = \left(\frac{k_r}{R}\right) \xi^{\frac{n}{1-n}} \beta' \quad (70)$$

$$X_6 = \frac{\partial Y}{\partial C_o} = \xi^{\frac{n}{1-n}} C_o^{-n} \quad (71)$$

$$X_7 = \frac{\partial Y}{\partial n} = \frac{\xi^{\frac{1}{1-n}}}{(1-n)^2} \ln \xi + \frac{\xi^{\frac{n}{1-n}}}{(1-n)} [k_r \beta - C_o^{1-n} \ln C_o] \quad (72)$$

where

$$\xi = (n-1)k_r \beta + C_o^{1-n} \quad (73)$$

$$\beta' = \int_0^t \left(\frac{1}{T(t)} - \frac{1}{T_r} \right) \exp \left[\frac{-\Delta E}{R} \left(\frac{1}{T(t)} - \frac{1}{T_r} \right) \right] dt \quad (74)$$

A detailed example of calculating the confidence interval from WLS 1st-order reaction can be found in Appendix 2. When parameters are simultaneously

determined by least-squares regression, their covariances may be significant (Van Boekel 1996). The correlation coefficient for i^{th} and j^{th} parameters was calculated as

$$\rho_{ij} = \frac{\sigma_{ij}}{(\sigma_i \sigma_j)} \quad (75)$$

For example, the correlation coefficient for k_r and ΔE is

$$\rho_{k_r, \Delta E} = \frac{\sigma_{k_r, \Delta E}}{(\sigma_{k_r} \sigma_{\Delta E})}$$

Correlation coefficient varies from -1 to $+1$, where $\rho = 0$ when the parameters are not correlated. Critical values are $|\rho_{ij}| > 0.99$ (Bates and Watts 1988).

3.3 Extrusion of grape pomace-flour mixture

3.3.1 Sample preparation

A grape-pomace-flour mixture was prepared according to the method in Section 3.2.1 (~14% moisture content (wb)).

3.3.2 Extrusion experimental design

An APV Baker MP19TC-25 co-rotating and intermeshing twin-screw extruder (APV Baker, Grand Rapids, MI, USA) with barrel diameter of 19 mm and length-to-diameter (L/D) ratio of 25:1 was used for extrusion processing. A high-shear screw configuration (Table 3.3.1) was selected to enhance mechanical effects during extrusion. The extruder barrel is divided into 5 zones (including the die) with temperature controlled by electrical heating elements and thermocouples. The barrel was cooled when necessary using cooling water lines. The dough temperatures from the feed end to the die were measured

using 5 thermocouples flush-mounted on the bottom of the barrel and die plate immediately before the die. A die with a tapered conical opening and exit diameter of 4 mm was used in all experiments. The product temperature inside the die was measured manually using a T-type needle thermocouple (Cole Parmer, Vernon Hills, IL, USA). The distances from the feed end to each flush-mounted thermocouple were 10.95, 25.56, 32.54, 40.32 and 45.88 cm (Figure 3.3.1). Percent torque was recorded. Discharge melt pressure prior to entering the exit die was monitored with a transducer (Dynisco, Model # EPR3-3M-6, Franklin, MA, USA) located 7 mm before the die entrance.

Table 3.3.1 – Screw configuration for high shear extrusion

8D ^a Twin Lead (TL)
7x30° Forward mixing paddles (FMP)
4D Twin lead (TL)
4x60° Forward mixing paddles (FMP)
4x30° Reverse mixing paddles (RMP)
2D Twin lead (TL)
6x60° Forward mixing paddles (FMP)
4x30° Reverse mixing paddles (RMP)
1D Single lead (SL)
7x90° Mixing paddles
2D Single lead (SL)

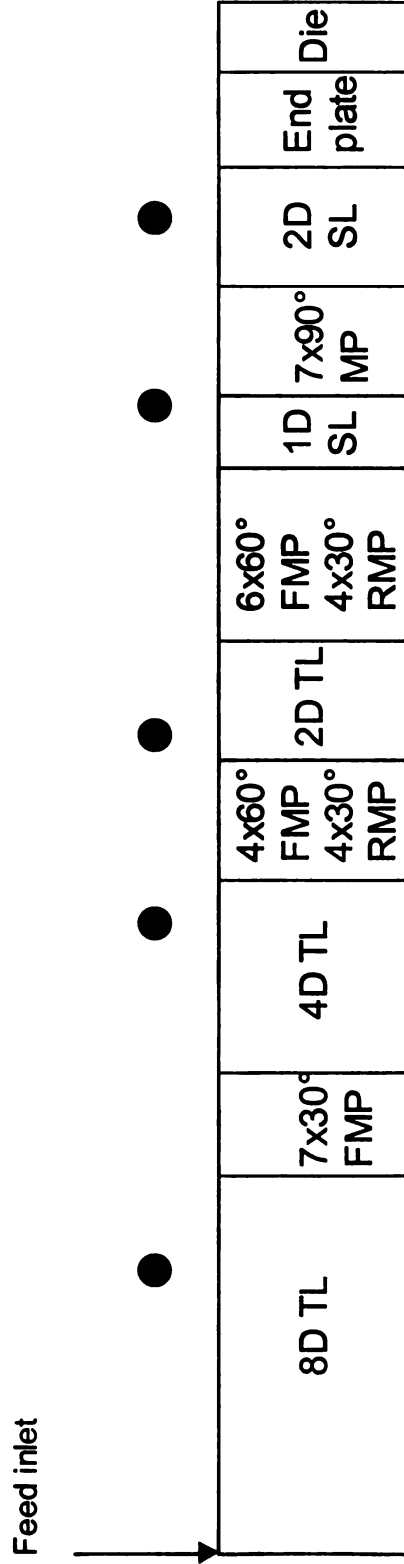
^aD = 19 mm

Grape pomace-flour mixture at ~14% moisture content (wb) was fed into the extruder with a K-Tron K2M twin-screw volumetric feeder (K-Tron Corp., Pitman, NJ, USA) equipped with a variable speed drive and digital control. The feed rates were 0.633, 0.679, 1.14, and 1.60 kg/hr for 50, 100, 200, and 400 rpm, respectively. Deionized water was injected at 0.143, 0.159, 0.277, and 0.386 kg/hr for 50, 100, 200, and 400 rpm, respectively, with an E2 Metripump positive

displacement metering pump (Bran & Luebbe, Northampton, U.K.) to maintain a dough moisture content of 30% wet basis (43% db) in all runs.

Samples were extruded in duplicate on different days at screw speeds of 50, 100, 200, and 400 rpm at 3 barrel temperature profiles (from feed end to die): 1) 40, 55, 70, 85, 95°C (low temperature), 2) 50, 70, 90, 110, 125°C (high temperature) and 3) ambient temperature. Extrusion at ambient temperature was selected in an attempt to investigate exclusively mechanical effects. Fifty rpm was the lowest speed achievable to maintain steady state at the operating conditions. Extrusion runs were brought to steady state (constant torque and die pressure readings) at each screw speed before extrudates were collected (~250 g) and air-dried for 2 days (22°C, 40% relative humidity).

Dough density was measured by opening the extruder after a dead stop and taking a product sample from inside the die cone, wrapping it tightly in a pre-weighed piece of plastic wrap, and weighing it. The volume of the sample was measured by water volume displacement. Samples were ground in an Udy Cyclone Sample Mill (Udy Corp., Fort Collins, CO, USA) through a 1.0 mm screen. Feed material and ground extrudates were stored in plastic freezer bags at ~-10°C prior to anthocyanin analysis. Raw material and samples from each extrusion condition were analyzed in triplicate to obtain the "total retention" of anthocyanins from extrusion.



- Flush-mounted thermocouples, D = 19 mm, TL = twin lead, SL, = single lead, FMP = forward mixing paddles, RMP = reverse mixing paddles, MP = mixing paddles

Figure not drawn to scale

Figure 3.3.1 – Schematic of high-shear screw configuration.

3.3.2.1 Mean residence time

The mean residence time and residence time distribution of the material was determined using the dye-tracer technique (Peng and others 1994) at every extrusion condition. Color marker was made by dyeing grape pomace with pink water-based dye (#1070-0500, craftstore.com, Cordova, TN, USA) mixed with flour on a 1:3 (w/w) ratio dry weight basis. A 3.0-g sample was instantaneously fed into the feed port. The time when the pink color first appeared was recorded and extrudates were collected every 5 or 10 s until no apparent pink color was left. Residence time samples were air-dried for at least two days and then ground with a Krups coffee grinder (Peoria, IL, USA). A HunterLab D25 colorimeter (Hunter Associates Laboratories, Inc., Reston, VA, USA) was used to read color values (a^*) from 1.2-g ground samples and control samples (ground samples with no color). Results were reported as color minus the control color. A white tile (Standard No. C2-30954) was used to standardize the colorimeter.

3.3.2.2 Color-concentration calibration curve

At high dye concentration, color values do not increase linearly with concentration because of a saturation effect; therefore a calibration curve converting color values to color concentration was established by a separate experiment (Peng and others 1994). Grape pomace, dyed pink in increasing concentration, was mixed with flour (1:3 w/w dry basis) in a KitchenAid Model K5-A mixer (The Hobart Mfg., Troy, OH) to obtain 5 batches with different red dye concentration: 0.003, 0.014, 0.066, 0.110, and 0.230 g dye per g mixture. Each batch was extruded at a feed rate of 1.1 kg/hr, 30% (wb) dough moisture, and

200 rpm at the high temperature profile. Extrudate samples were taken after reaching steady state.

In addition, two concentrations (0.014 and 0.110 g dye per g mixture) were extruded at 50 and 300 rpm with feed rate of 0.8 and 1.1 kg/hr, respectively, under the high temperature profile to study if screw speed had an effect on color formation. All extrudates were air-dried and ground. A 1.5-g sample was used to measure the extrudate color value of each batch. An equation was fit empirically to concentration versus color values to yield a calibration curve.

The calibration curve was used to convert all extrudate color values to color concentration, c . Normalized concentration $E(t)$ was calculated as (Levenspiel 1999)

$$E(t) = \frac{c(t)}{\int_0^{\infty} c(t) dt} \cong \frac{c_i}{\sum_i c_i \Delta t_i} \quad (76)$$

The normalized concentration, $E(t)$, was used to calculate mean residence time, \bar{t}

$$\bar{t} = \int_0^{\infty} t E(t) dt \cong \frac{\sum_i t_i c_i \Delta t_i}{\sum_i c_i \Delta t_i} \quad (77)$$

3.3.2.3 Extruder degree of fill

Extruding at different screw speeds changes degree of fill and shear effect on anthocyanin retention. Therefore, we attempted to maintain constant fill at all screw speeds by increasing feed rate. To estimate the relationship between feed rate and screw speed, the following experiments were conducted. Grape pomace-flour mixture was extruded using different feed rates at 3 screw speeds

and at 30% dough moisture content using the high temperature profile. Table 3.3.2 shows the experimental plan. The dough density and mean residence time were found per Section 3.2.3. Degree of fill (decimal) was estimated to be

$$\text{fill} = \frac{\dot{m}_r \bar{t}}{V\rho} \quad (78)$$

Table 3.3.2 - Experimental plan for predicting extruder degree of fill

Screw speed (rpm)	Feed rate (kg hr⁻¹)
50	0.6
50	0.7
50	0.8
200	0.8
200	1.1
400	0.8
400	1.1

The actual degree of fill was measured in duplicate by dead-stopping the extruder at 200 rpm and weighing the screws and product in designated sections displayed in Figure 3.3.1 (Fichtali and van de Voort 1989). The weight of the screws was subtracted from the total weight to obtain the mass of the product from the specific section. Due to the impracticality of opening the extruder numerous times, the product mass in each section was measured at only 200 rpm.

3.3.3 Study of anthocyanin extraction from extrudates

In extrusion, extrudates are typically compared against each other to ascertain the effects of different operating variables on specific properties.

However, this study compares anthocyanin content in raw material and extrudates. To verify the extractability of anthocyanin from extrudates, two additional feed materials with different percent grape pomace were mixed and extruded under identical condition. Grape pomace-flour mixture at 5% and 15% grape pomace (dry basis) was prepared as described in Section 3.3.1. Mixtures at 5%, and 15% grape pomace were extruded at 1.6 kg/hr, 400 rpm, 30% dough moisture content, and at the high-temperature profile per procedures described in Section 3.2.2. Results from anthocyanin extraction were compared to a similar run at 25% grape pomace-flour mixture.

3.3.4 Effects of dough moisture content on anthocyanins from extrusion

To investigate how dough moisture content affects the retention of anthocyanins and compare to thermal study results, duplicate extrusion runs were performed at the high-temperature profile with a feed rate of 1.1 kg/hr at 400 rpm with 43, 54, and 67% dry basis (30, 35, and 40% (wb)) dough moisture content. Constant heating time method was employed to estimate moisture constant b using Eq. (21) or (22), where $MC_r = 43\%$ reference moisture content.

3.4 Thermal effects on anthocyanins from extrusion

The extruder was conceptually divided into 11 (Figure 3.3.1) sections and product temperature at any location throughout the extruder, $T(x)$, was estimated by recording the product temperature at extruder length x and generating a best-fit line. The line was used to predict $T(x)$, which was used to calculate $\beta(t)$ in Eq. (43). Thermal retention from extrusion was calculated using Eq. (44) - (46) and this value was used to calculate loss due to thermal effects only (Eq. (49)).

3.5 Mechanical effects on anthocyanins from extrusion

Equation (8) was used to solve for mechanical retention, R_S , and then converted to loss using Eq. (51). Average shear rate was calculated at each screw speed using Eq. (54) where k' and α were found via empirical formulas developed from extrusion runs with a 3 mm circular die (Suparno and others 2002). Although a 4 mm circular die was used in this study, the shear rate difference was assumed to be negligible since the die diameter difference was small (1mm). Equation (79) and (80) were used to calculate k' , and the average was used.

- Flow behavior index = 0.30 $k' = 0.121(\% \text{ fill})^{1.306}$ (79)

- Flow behavior index = 0.70 $k' = 0.849(\% \text{ fill})^{0.785}$ (80)

Equation (81) was used to calculate α

$$\alpha = -0.0022(\% \text{ fill}) + 1.575 \quad (81)$$

Shear history was calculated using average shear rate and mean residence time in Eq. (53). Equation (55) was used to calculate *SME*. The function $f(S)$ was empirically fit using screw speed, shear history, and *SME*.

3.6 Statistical analysis

To investigate the effects of extrusion temperature profile (high and low-temperature) on mechanical loss, the Statistical Analysis Software (SAS) was used. The slope of the trendlines for mechanical loss versus screw speed, shear history, and *SME* from extrusion at high and low temperature were tested at 95% confidence interval using both the 'proc reg' and 'proc nlin' procedure. If the

slopes were significantly different (p -values < 0.05), then there was an interaction between barrel temperature and mechanical loss.

4. Results and Discussion

All equations referenced in this section are summarized in Appendix 3.

4.1 Thermal effects on anthocyanins in grape pomace-flour mixture

4.1.1 Isothermal and nonisothermal heating of grape pomace-flour mixture

Figure 4.1.1 shows the anthocyanin absorbance (AU) for all samples heated under isothermal (80°C) and nonisothermal (105°C and 145°C) conditions. A standard curve (Appendix 1, Figure A.1.2) showed absorbance was linearly proportional to the concentration range tested. Therefore absorbance units were used in place of concentration when describing anthocyanin content in this study. The heating time was calculated as the time from when the sample entered the oil bath until it was removed and cooled to a center temperature of ~26°C. The heat transfer coefficients at 80, 105, and 145°C were calculated as 122.8, 162.3, and 238.8 W/m²-°C (Appendix 4, Figure A.4.1). Sample temperature at each time (T_c^i in Eqn. (59)) ranged from 37 – 140°C from the three oil bath temperatures. Initial absorbance was calculated as the average of 9 samples to yield $C_o = 0.122 \pm 0.004$ AU (Appendix 5, Table A.5.1 and A.5.2). Figure 4.1.2 displays several sample temperature profiles.

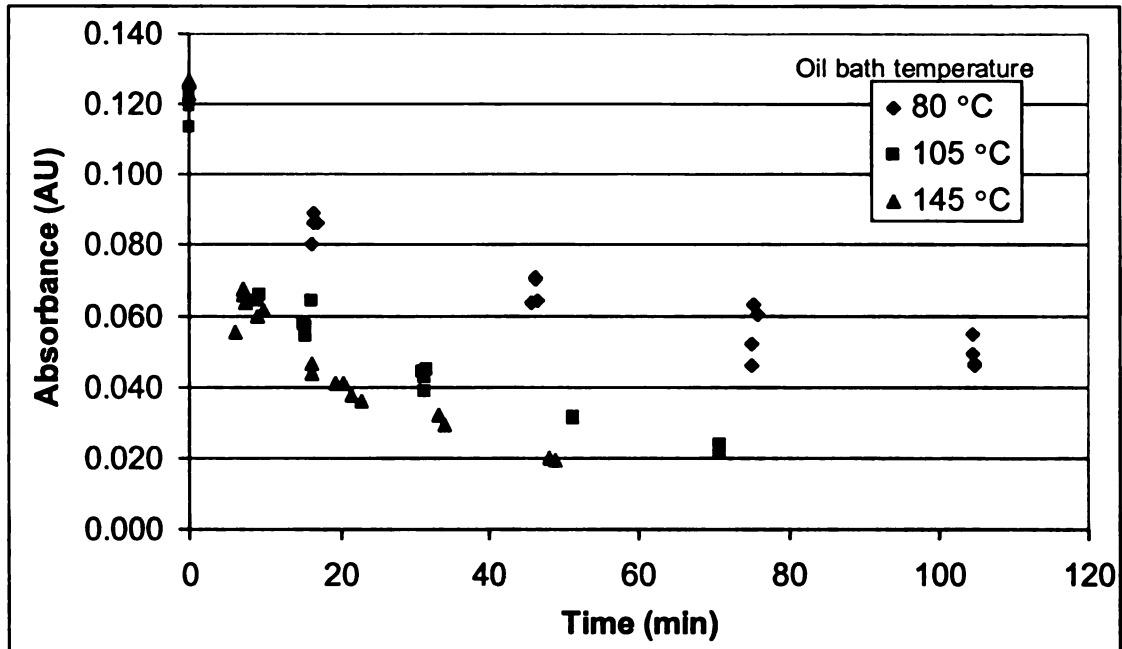


Figure 4.1.1 – Absorbance versus time (43% (db) initial moisture content) of 1:3 (w/w) grape pomace-wheat flour mixture heated isothermally (80°C) and nonisothermally (105°C and 145°C) for different times.

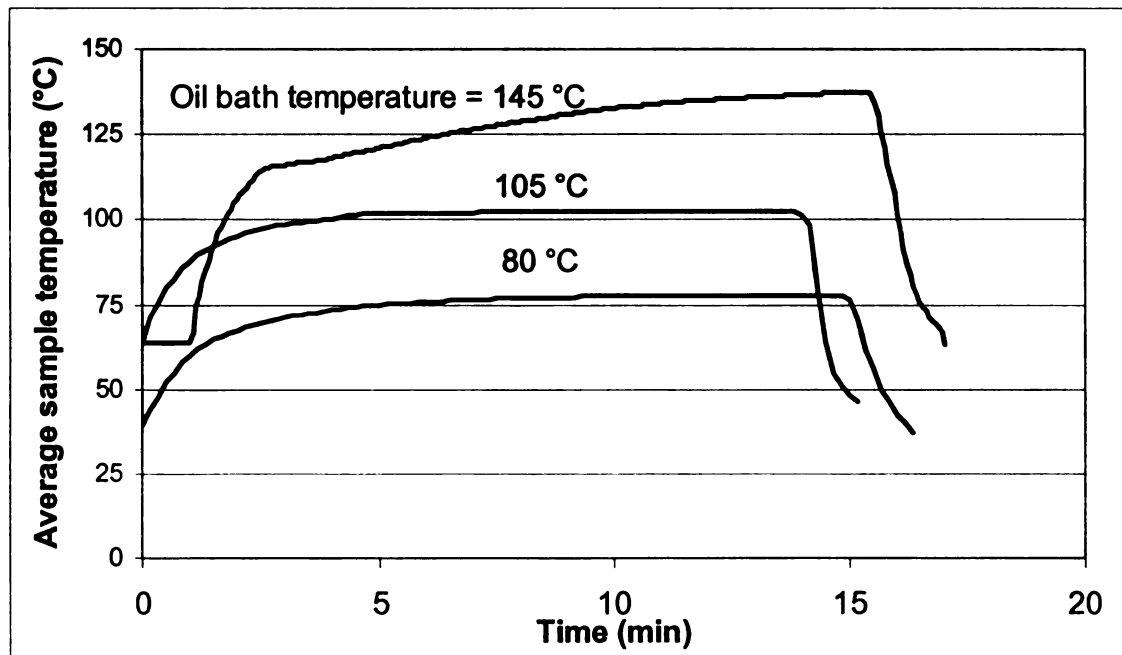


Figure 4.1.2 – Example curves of average sample temperatures versus time.

4.1.2 Estimating moisture content rate constant b

First-order reaction

Figure 4.1.3 shows the absorbance for 10, 20, and 43% (db) moisture content samples heated isothermally at 80°C for 15, 45, and 75 min. The 43% samples are the same as those in Figure 4.1.1. Anthocyanin loss and the rate constant at 10% moisture content were too low (slope ≈ 0) for accurate calculation; therefore, the constant heating-time method (Section 2.2.2.2) was used to estimate moisture constant b . Anthocyanin degradation increased with moisture content. This may be due to hydrolysis of the glycosidic bond, liberating the unstable aglycone, which decolorizes faster than the glycoside form (Markakis and others 1957). The pseudo-initial absorbance, C'_0 , was calculated by extrapolating $\ln C$ data to zero time (Figure 4.1.3) and taking the average from 20% and 43% moisture content samples. The value of C'_0 was found to be 0.094 AU and was used in Eq. (21) to estimate moisture constant b . At 15 minutes, moisture content effect was not evident since experimental variability appeared greater than the heating effect; therefore data at this time were not used to estimate b . Moisture constant b was estimated (Eq. (21)) as the average of the two slopes of $\ln[-\ln(C/C'_0)]$ versus $MC-MC_r$ at 45 and 75 min to obtain $\bar{b} = 4.28$ (Figure 4.1.4).

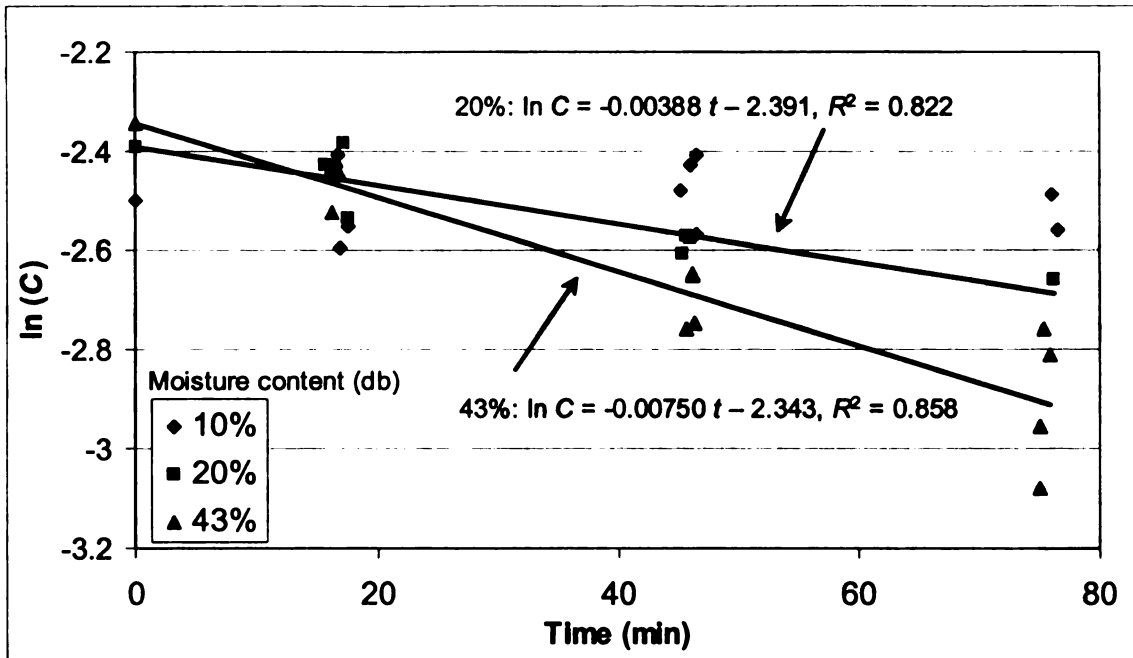


Figure 4.1.3 – First-order log plot of absorbance versus time for 10, 20, and 43% moisture content (db) samples heated isothermally at 80°C.

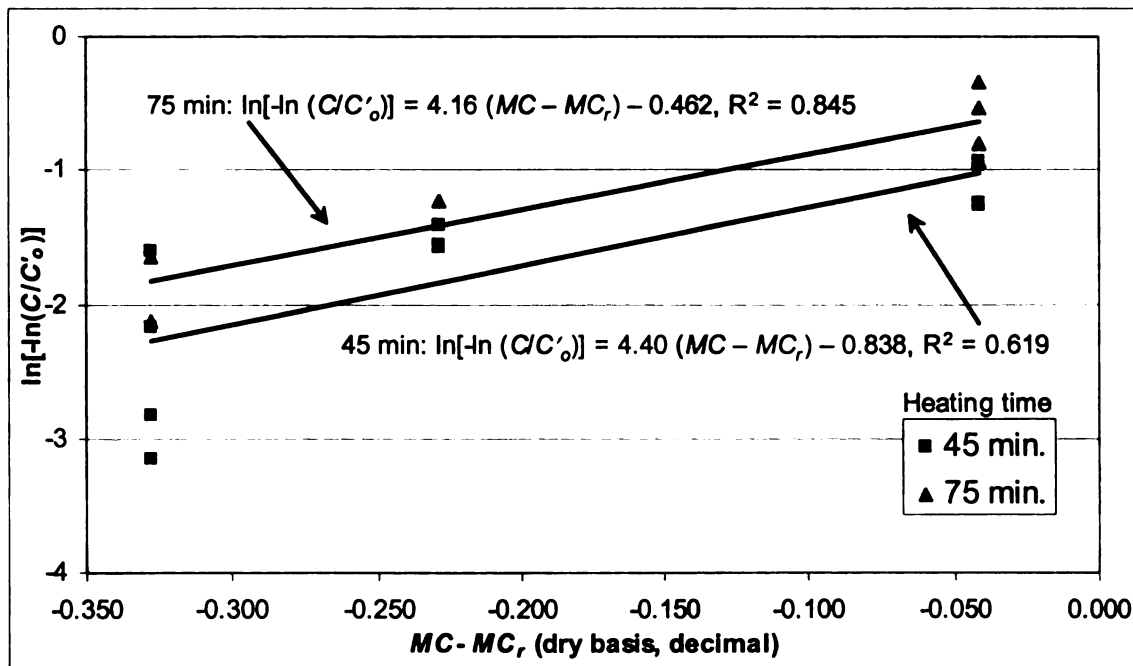


Figure 4.1.4 – Constant heating time method to estimate the moisture rate constant b assuming first-order reaction ($n=1$). The slope of each line is the estimate of b at each heating time.

n^{th} -order reaction

Using $\bar{b} = 4.28$ from 1st-order results to correct all absorbance values to 43% moisture content, a starting value of $n = 3.22$ was obtained from Solver. After ≈ 9 cycles using Solver, n converged to 3.66 and was used to plot Figure 4.1.5 and yield $C'_o = 0.108$ AU. Equation (22) was employed to estimate b from data at 45 and 75 min (Figure 4.1.6) and averaged to yield $\bar{b} = 4.25$. The moisture rate constants b are very comparable for both 1st-order ($\bar{b} = 4.28$) and n^{th} -order reaction ($\bar{b} = 4.25$).

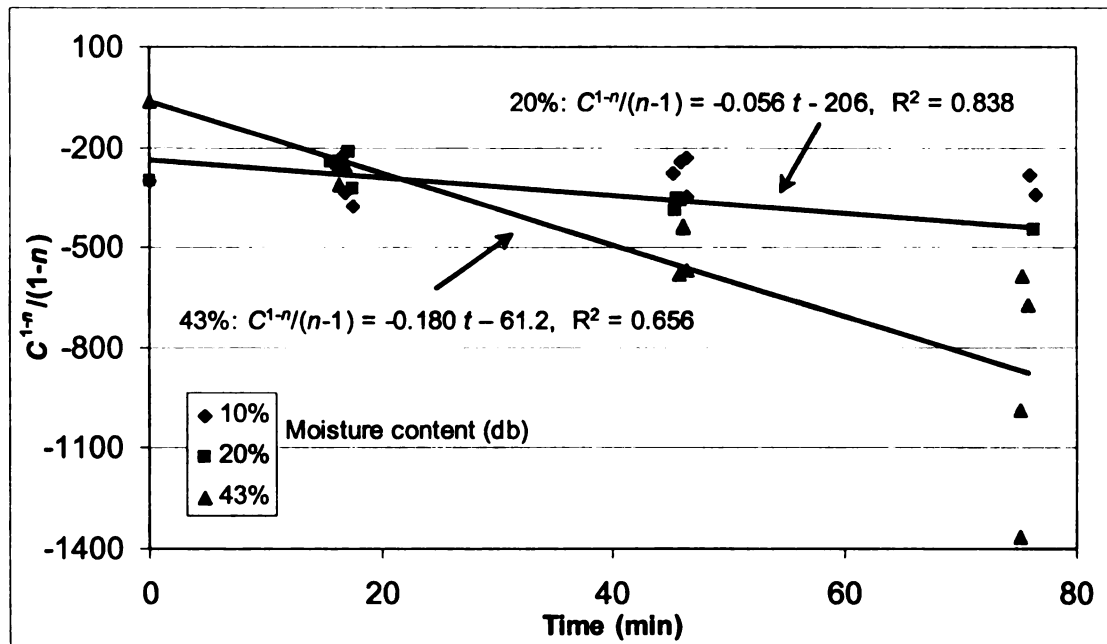


Figure 4.1.5 – n^{th} -order plot of absorbance versus time for 10, 20, and 43% moisture content samples heated isothermally at 80°C for $n = 3.66$, the converged value. This plot is the n^{th} -order analog to Figure 4.1.3.

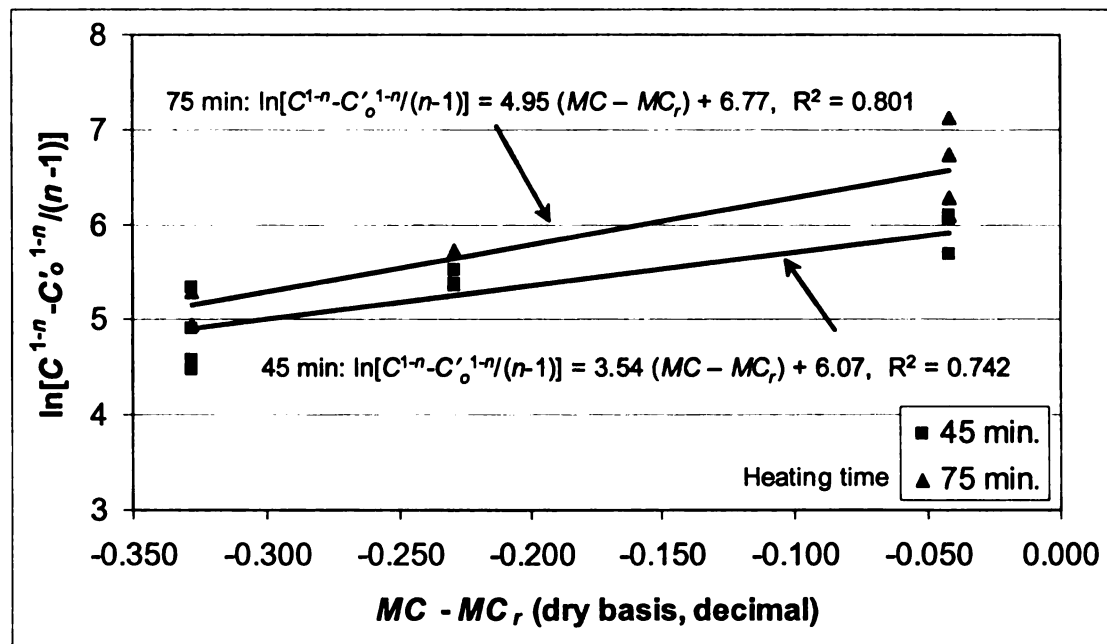


Figure 4.1.6 - Constant heating time method to estimate moisture constant rate b ($n = 3.66$).

4.1.3 Moisture content correction

Figure 4.1.7 shows the moisture change over time for 43% moisture samples heated at 80, 105, and 145°C. At 80°C, moisture content remained constant as expected, but at 105°C and 145 °C, there was significant moisture loss (up to ~80% loss). For heating at 105°C, moisture content change against time was fitted with an exponential equation: $MC = 0.424 e^{-0.0001t}$, $R^2 = 0.953$. At 145°C, 2 equations were used to ensure a reasonable fit: linear equation for time < 440 s ($MC = -0.0006t + 0.43$, $R^2 = <0.99$) and power equation for time > 440 s ($MC = 61.0t^{0.966}$, $R^2 = 0.878$).

There was almost no difference between the correction factors (Eq. (28) and (35), Appendix 6, Table A.6.1 and A.6.2) for 1st-order and n^{th} -order reactions because the moisture constant b was almost the same in both cases. These values were used to correct absorbance (from all samples except for 10 and 20% moisture content samples heated at 80°C for 15 min) to 43% reference moisture content (these samples were excluded because moisture content b was estimated from data at 45 and 75 min).

Figures 4.1.8a and b show anthocyanin concentration corrected to 43% reference moisture content and its degradation over time at 80, 105, and 145°C assuming both 1st-order and n^{th} -order reaction. Prior to moisture content correction, results showed anthocyanin loss of ~60 – 84% (Figure 4.1.1). Since there was a significant moisture loss, these absorbance values underestimated anthocyanin loss if MC remained constant at 43%. After correcting all

absorbance values to 43% moisture content, the actual loss ranged from ~67 – 100% (Figure 4.1.8a and b).

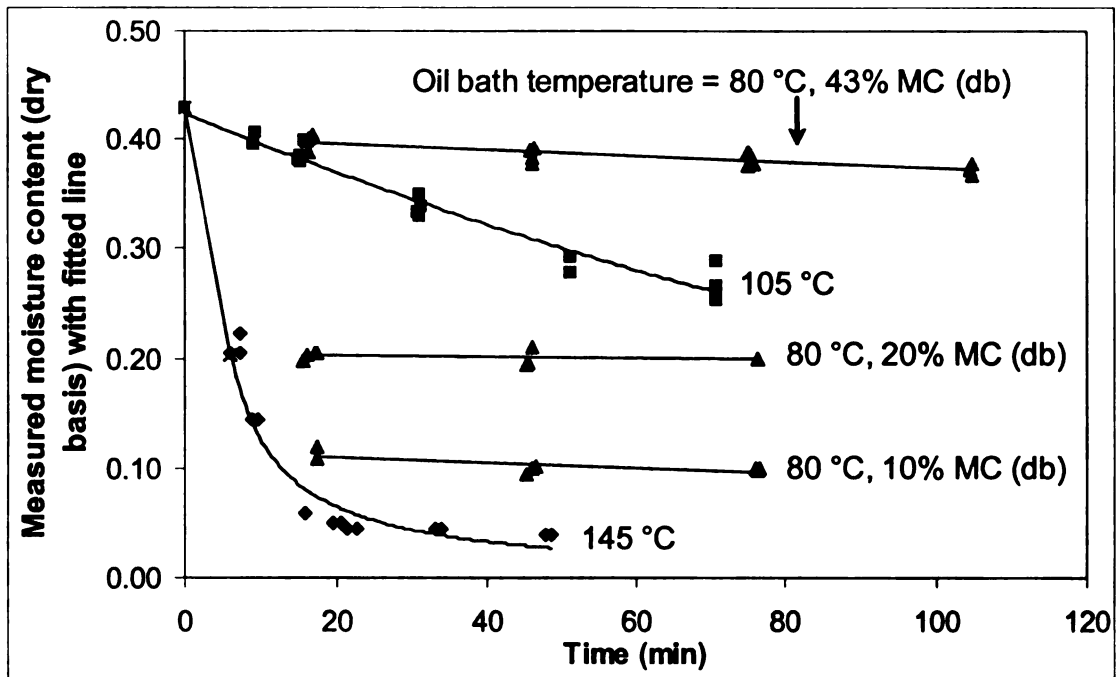
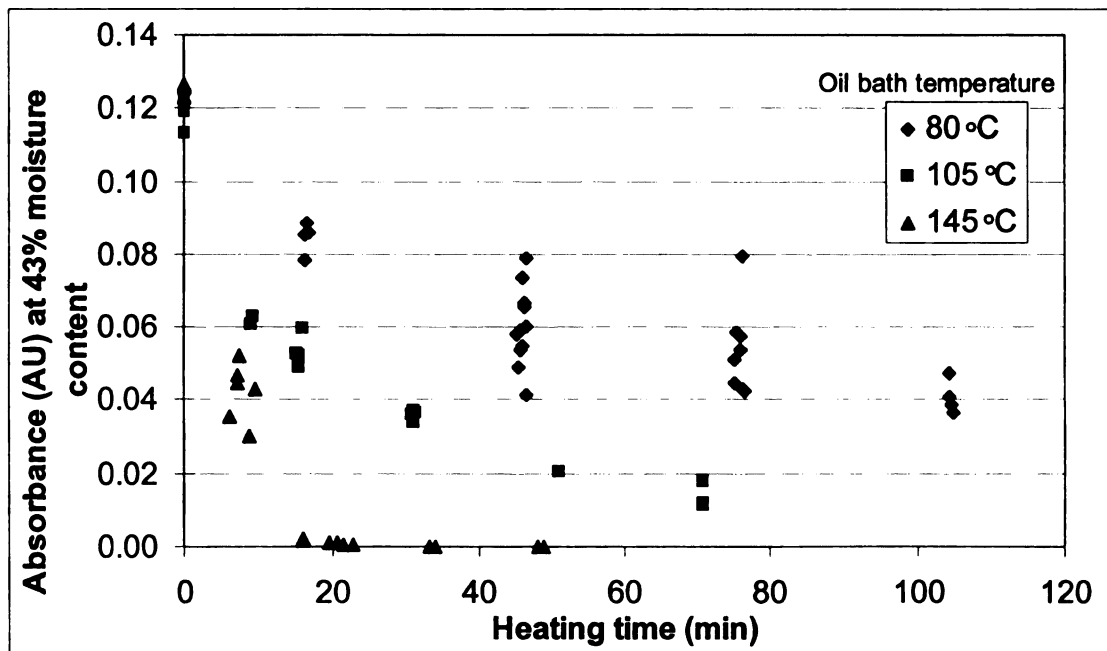
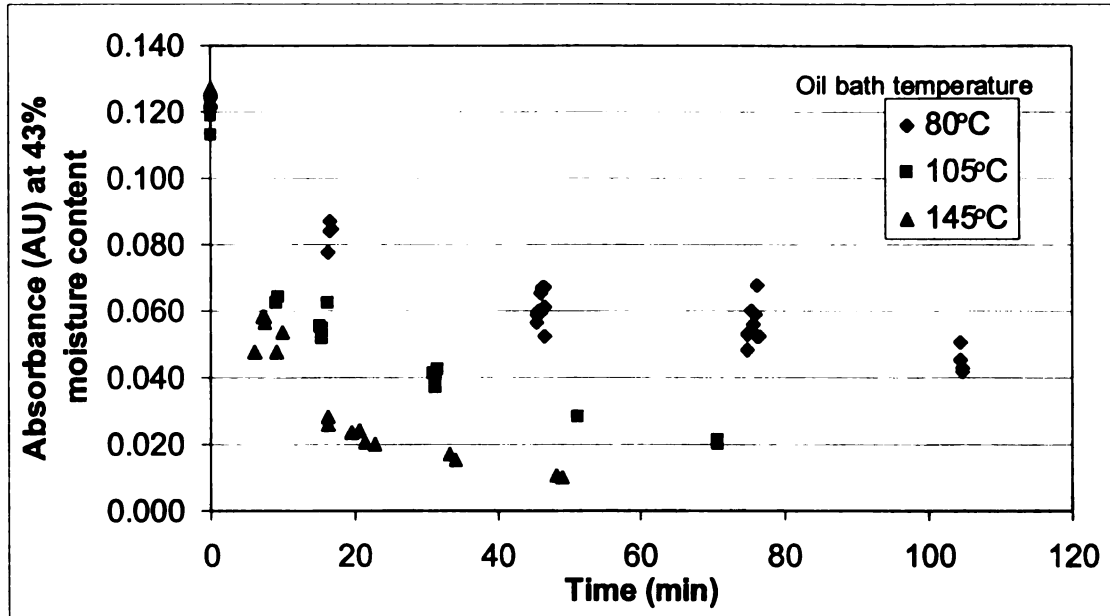


Figure 4.1.7 – Moisture content over time for samples heated isothermally at 80°C and nonisothermally at 105°C and 145°C.



a)



b)

Figure 4.1.8 - Absorbance of samples in Figure 4.1.1 versus time corrected to reference 43% moisture content for a) 1st-order and b) *n*th-order reaction.

4.1.4 Estimation of parameters and confidence intervals

First-order reaction

The reference conditions for this thermal study were: $T_r = 353.15^\circ\text{K}$ (80°C) and $MC_r = 43\%$ (db). The starting value of reaction rate was obtained by taking the slope of $\ln(C/C_o)$ against time data from 43% moisture content samples heated isothermally at $T_r = 80^\circ\text{C}$ (Figure 4.1.3) to yield $k_r = 0.00750 \text{ min}^{-1} = 0.000125 \text{ s}^{-1}$. The starting values of k_r and $C_o = 0.122 \text{ AU}$, along with initial guesses of $\Delta E = 5,000; 50,000; 500,000 \text{ J/g-mol}$ were used in the Solver function to minimize SS_E of Eq. (37) for 68 data points and 3 parameters (degrees of freedom = $68 - 3 = 65$). A wide range of ΔE starting values were selected to verify the convergence to the minimum SS_E (Van Boekel 1996).

Table 4.1.1 shows the parameter estimates found using both least-squares and weighted least-squares regression. Estimates for k_r and ΔE from both LS and WLS regression were similar. However, $C_o = 0.119 \pm 0.0002$ AU from WLS was closer to the experimental average $C_o = 0.122 \pm 0.004$ AU than $C_o = 0.110$ from LS. Except for $\rho_{k,r}$, the correlation coefficients between parameters (Table 4.1.1) were well below 0.99 (critical value), meaning the parameter estimates had little influence on each other. Figure 4.1.9a and b show the best-fit nonlinear regression line for 1st-order reaction using LS and WLS regression.

Table 4.1.1 - Nonlinear estimation results of parameters using reference temperature $T_r = 353.15\text{K}$ (80 °C) in Eq. (37) or (39)

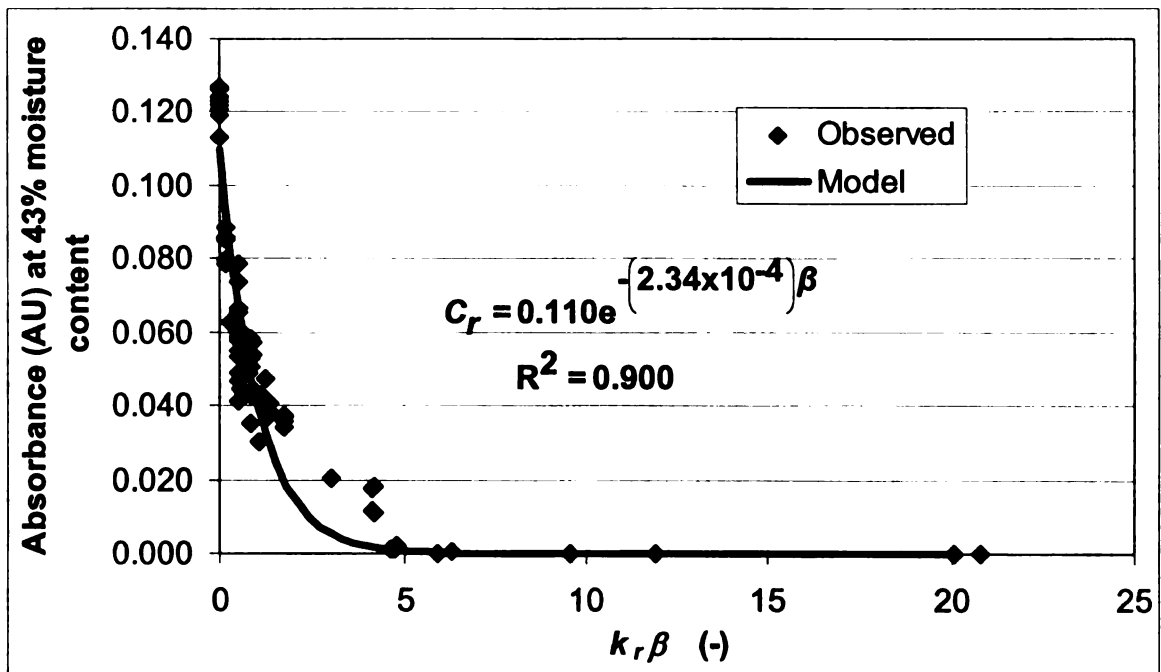
n	Weight	R^2	SS	Parameter	Estimate	Standard Error	95% CI ^a	Correlation coefficient, ρ
1	-	0.900	0.0084	k_r (s ⁻¹)	2.34×10^{-4}	$\pm 9.9 \times 10^{-7}$	$\pm 19.9 \times 10^{-7}$	$\rho_{k_r, \Delta E} = -0.489$
				ΔE (J/g-mol)	76,073	± 215	± 429	$\rho_{\Delta E, C_0} = -0.118$
				C_0 (AU)	0.110	± 0.0002	± 0.0004	$\rho_{k_r, C_0} = 0.616$
1	C^2	0.962	0.000028	k_r (s ⁻¹)	2.81×10^{-4}	$\pm 1.1 \times 10^{-6}$	$\pm 2.1 \times 10^{-6}$	$\rho_{k_r, \Delta E} = -0.467$
				ΔE (J/g-mol)	75,273	± 197	± 394	$\rho_{\Delta E, C_0} = -0.101$
				C_0 (AU)	0.119	± 0.0002	± 0.0004	$\rho_{k_r, C_0} = 0.592$
3.66	-	0.973	0.0017	k_r [C] ¹⁻ⁿ s ⁻¹	0.254	± 0.138	± 0.275	$\rho_{k_r, \Delta E} = 0.590$
				ΔE (J/g-mol)	80,116	± 3682	± 7357	$\rho_{\Delta E, C_0} = 0.004$
				C_0 (AU)	0.121	0.002	± 0.003	$\rho_{k_r, C_0} = 0.111$
				n (-)	3.66	0.209	± 0.417	$\rho_{n, k_r} = 0.996$
								$\rho_{n, C_0} = 0.096$

^a The 95% confidence intervals are approximate.

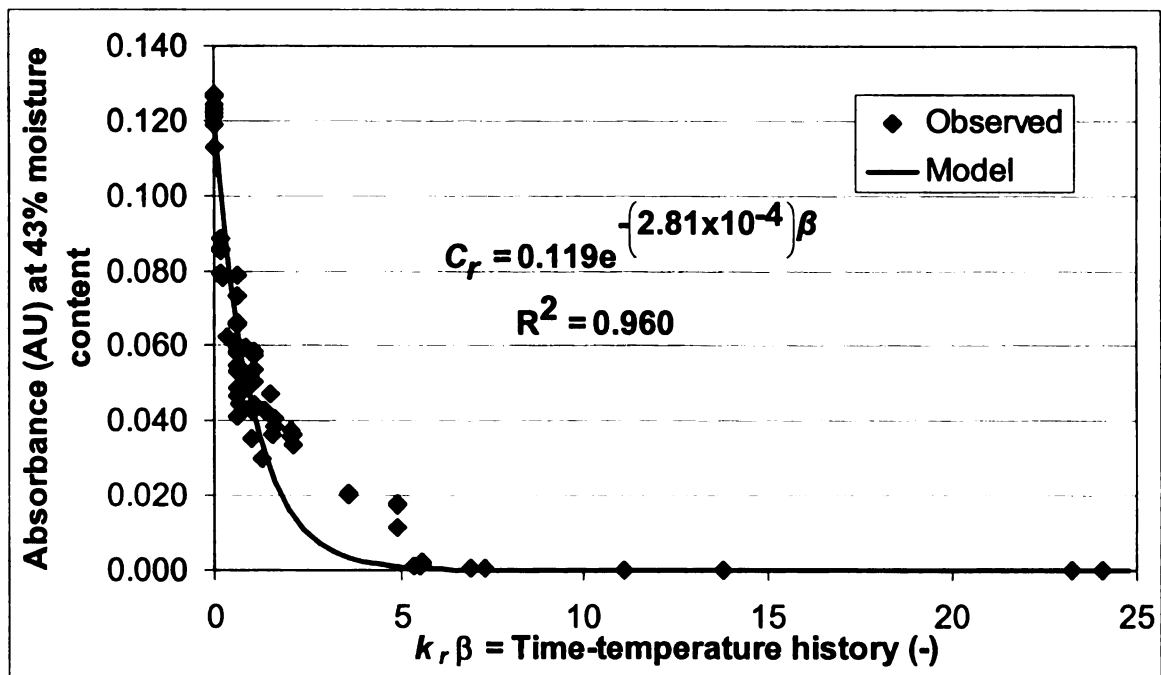
1
2
3
4
5
6
7
8
9
10
11
12
13
14
15
16
17
18
19
20
21
22
23
24
25
26
27
28
29
30
31
32
33
34
35
36
37
38
39
40
41
42
43
44
45
46
47
48
49
50
51
52
53
54
55
56
57
58
59
60
61
62
63
64
65
66
67
68
69
70
71
72
73
74
75
76
77
78
79
80
81
82
83
84
85
86
87
88
89
90
91
92
93
94
95
96
97
98
99
100

a

b
c
d



a)



b)

Figure 4.1.9 – Best-fit nonlinear regression line for absorbance versus time- temperature history for 1st-order reaction using a) least-squares and b) weighted least-squares regression.

Table 4.1.2 compares the kinetic parameters from this study to published work on thermal degradation of anthocyanins. To date, no published work was found using solid media, such as a grape pomace-flour mixture, in a thermal study. Published activation energy values, found using anthocyanins in model systems, ranging from ~67 – 123 kJ/g-mol (Tanchev and Yoncheva 1974, Cemeroglu and others 1994) were comparable with this study. Reference reaction rate constant, k_r , was converted to k_o using the equation:

$$k_o = k_r \exp\left(\frac{\Delta E}{RT_r}\right) \text{ to yield } k_o = 2.24 \times 10^9 \text{ min}^{-1} \text{ for comparison with published}$$

values. Our k_o values were smaller by 2 – 11 orders of magnitude, consistent with our finding that increasing moisture increases rate of degradation. Highest moisture was juice and buffer (Tanchev and Yoncheva study), then juice concentrate (Cemeroglu and others study), and grape pomace-flour mixture from our study.

Table 4.1.2 - Published kinetic parameters from thermal study of anthocyanin degradation using 1st-order reaction.

Media	Heating Temperatures (°C)	Parameters	Sources
Sour cherry juice concentrate 15°Brix	50, 60, 70, 80	$\Delta E = 68.5 \text{ kJ/g-mol}$ $k_0 = 5.62 \times 10^{10} \text{ min}^{-1}$	Cemeroglu and others (1994)
45°Brix	50, 60, 70, 80	$\Delta E = 75.9 \text{ kJ/g-mol}$ $k_0 = 4.80 \times 10^{11} \text{ min}^{-1}$	
71°Brix	50, 60, 70, 80	$\Delta E = 80.1 \text{ kJ/g-mol}$ $k_0 = 1.38 \times 10^{12} \text{ min}^{-1}$	
Malvidin-3-glucoside in juice pH 2.5	78, 88, 98, 108	$\Delta E = 99.3 \text{ kJ/g-mol}$ $k_0 = 1.48 \times 10^{22} \text{ min}^{-1}$	Tanchev and Yoncheva (1974)
pH 3.5		$\Delta E = 92.8 \text{ kJ/g-mol}$ $k_0 = 1.70 \times 10^{21} \text{ min}^{-1}$	
pH 4.5		$\Delta E = 87.3 \text{ kJ/g-mol}$ $k_0 = 2.65 \times 10^{20} \text{ min}^{-1}$	

Table 4.1.2 (continue) - Published kinetic parameters from thermal study of anthocyanin degradation using 1st-order reaction.

Media	Heating Temperatures (°C)	Parameters	Sources
Malvidin-3-glucoside in buffer pH 2.5	78, 88, 98, 108	$\Delta E = 123 \text{ kJ/g-mol}$ $k_0 = 3.64 \times 10^{25} \text{ min}^{-1}$	Tanchev and Yoncheva (1974)
pH 3.5		$\Delta E = 113 \text{ kJ/g-mol}$ $k_0 = 1.06 \times 10^{24} \text{ min}^{-1}$	
pH 4.5		$\Delta E = 114 \text{ kJ/g-mol}$ $k_0 = 1.48 \times 10^{24} \text{ min}^{-1}$	
Delphinidin-3-rutinoside in juice pH 2.5	78, 88, 98, 108	$\Delta E = 98.2 \text{ kJ/g-mol}$ $k_0 = 2.16 \times 10^{22} \text{ min}^{-1}$	Tanchev and Yoncheva (1974)
pH 3.5		$\Delta E = 79.8 \text{ kJ/g-mol}$ $k_0 = 1.03 \times 10^{20} \text{ min}^{-1}$	
pH 4.5		$\Delta E = 84.4 \text{ kJ/g-mol}$ $k_0 = 2.45 \times 10^{20} \text{ min}^{-1}$	

Table 4.1.2 (continue) - Published kinetic parameters from thermal study of anthocyanin degradation using 1st-order reaction.

Media	Heating Temperatures (°C)	Parameters	Sources
Delphinidin-3-rutinoside in buffer pH 2.5	78, 88, 98, 108	$\Delta E = 83.0 \text{ kJ/g-mol}$ $k_0 = 1.06 \times 10^{20} \text{ min}^{-1}$	Tanchev and Yoncheva (1974)
pH 3.5		$\Delta E = 83.6 \text{ kJ/g-mol}$ $k_0 = 1.73 \times 10^{20} \text{ min}^{-1}$	
pH 4.5		$\Delta E = 86.0 \text{ kJ/g-mol}$ $k_0 = 3.02 \times 10^{20} \text{ min}^{-1}$	
Grape pomace-flour mixture	~37 – 140	$\Delta E = 75.2 \text{ kJ/mol}$ $k_0 = 2.24 \times 10^9 \text{ min}^{-1}$	Current study

nth-order reaction

The reaction rate was found to be $n = 3.66$ from iteration on Eq. (39) performed to solve for moisture constant b (Section 4.1.2) and the parameters estimates at this n were: $k_r = 0.254 \pm 0.138 [C]^{1-n} s^{-1}$, $\Delta E = 80,116 \text{ J/g-mol} \pm 3,682$, $C_o = 0.121 \pm 0.002 \text{ AU}$. The estimates of ΔE and C_o are comparable to 1st-order reaction. However, the value of k_r is much higher for $n = 3.66$ which is expected since k_r is highly dependent on n (Eqn. (12)). This is evident from a large correlation coefficient: $\rho_{k,n} = 0.996$ (Table 4.1.1). Other correlation coefficients between parameters were all below the critical value of 0.99. Figure 4.1.10 shows the best-fit nonlinear regression line for n^{th} -order reaction plotted with observed values.

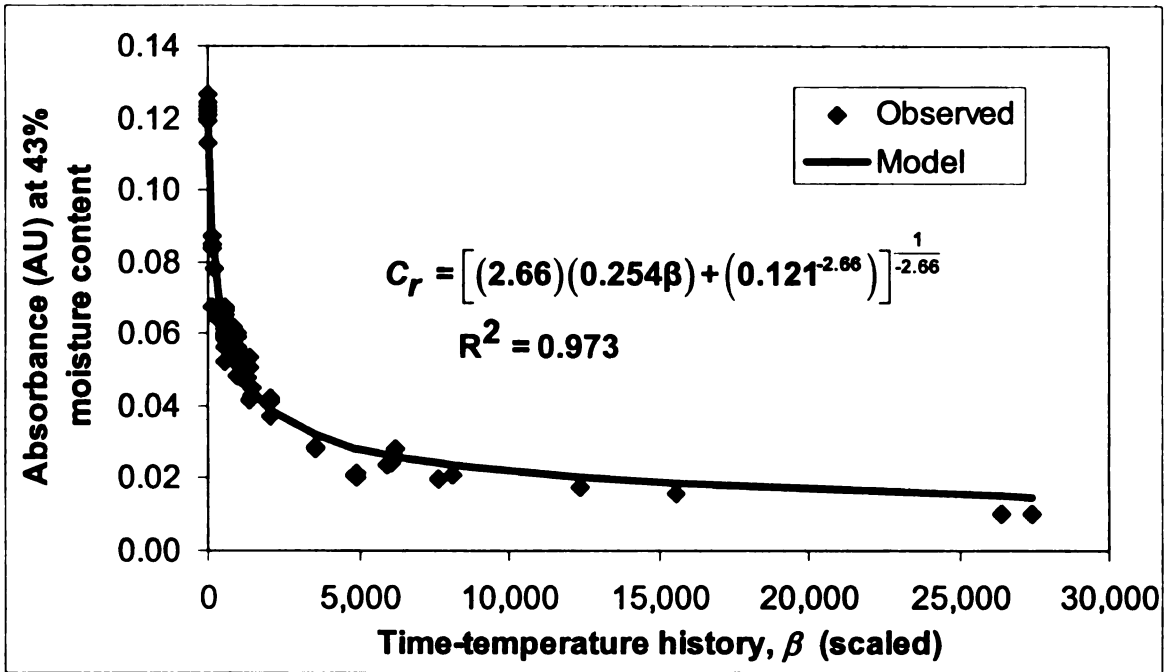


Figure 4.1.10 – Best-fit nonlinear regression line for absorbance versus time-temperature history for n^{th} -order reaction.

Comparing 1st- and n^{th} -order reaction

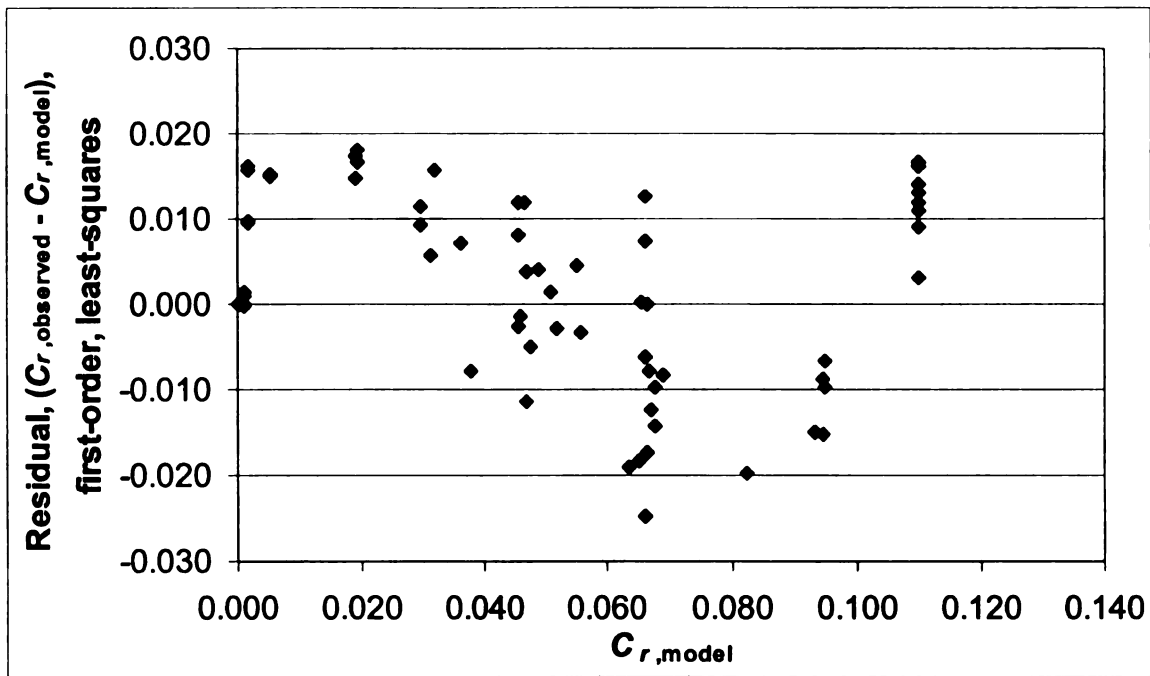
Asymptotic standard errors were used to approximate standard deviations and confidence intervals so the values in Table 4.1.1 may be an underestimation (Johnson and Fault 1992). Comparing 1st- and n^{th} -order reaction results, the standard deviations and 95% confidence intervals from n^{th} -order results are higher percentage of the estimates values. This is especially significant in the standard deviation for the estimate of ΔE , where $\Delta E = 75,206 \pm 197$ J/g-mol ($n = 1$) while $\Delta E = 80,116 \pm 3,682$ J/g-mol ($n = 3.66$). For nonlinear models, the estimation of confidence intervals are not straightforward, bias, and asymmetric; the extent of asymmetry depends on the nonlinearity of the function and number of data points (Van Boekel 1996). Since the parameters were estimated in regression algorithms by linear approximations, the validity of the estimate and confidence intervals also depends on the linear approximation. Therefore,

potentially higher asymmetry for n^{th} -order results may lead to larger confidence intervals when compared to 1st-order values.

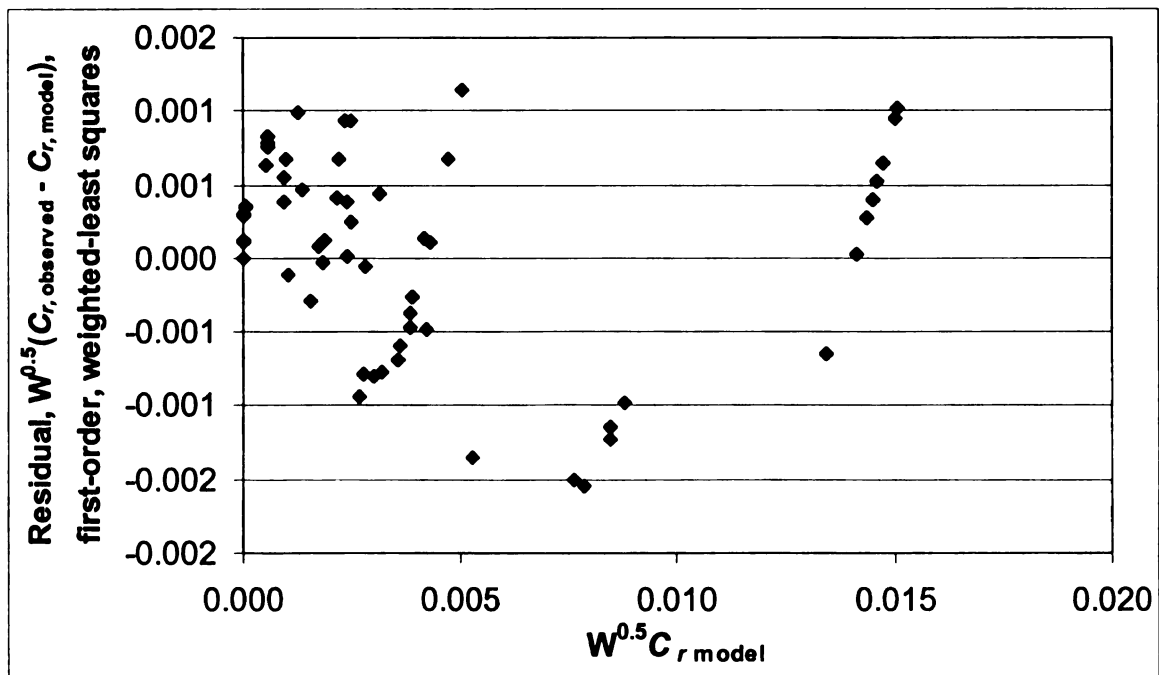
Residuals plotted against model values from 1st-order LS & WLS regression and n^{th} -order reaction results are shown in Figure 4.1.11a, b, and c, respectively. In all cases, the residuals did not exhibit any systematic pattern, which shows the 'goodness' of fit between observed values and fitted line. Comparing Figure 4.1.11a and b, it shows that WLS regression (Figure 4.1.11b) had a better prediction of C_o with smaller variance when compared to LS regression. Residuals for n^{th} -order reaction were smaller. Parameter estimate of C_o from WLS 1st-order ($C_o = 0.119 \pm 0.0002$) and n^{th} -order ($C_o = 0.122 \pm 0.002$) very closely predicted the measured value of $C_o = 0.121$. The model in order of overall best fit (R^2 and SS_E) was WLS 1st-order, n^{th} -order, and unweighted LS 1st-order.

Because the n^{th} -order fit was only slightly better than 1st-order WLS model, thermal degradation of anthocyanins was modeled using a 1st-order reaction (analyzed using WLS regression), in agreement with other published work using isothermal heating of liquids and linear regression (Daravingas and Cain 1968, Adams 1973, Tanchev and Yoncheva 1974, Cemeroglu and others 1994). Despite some skewness, the normal probability plot of residuals for WLS 1st-order reaction (Appendix 7, Figure A.7.1) is fairly linear which verifies the assumption of normality (for using least-squares regression, Van Boekel 1996) is appropriate. The values of parameters $k_r = 2.81 \times 10^{-4} \text{ s}^{-1}$ and $\Delta E = 75,206 \text{ J/g-mol}$ (which

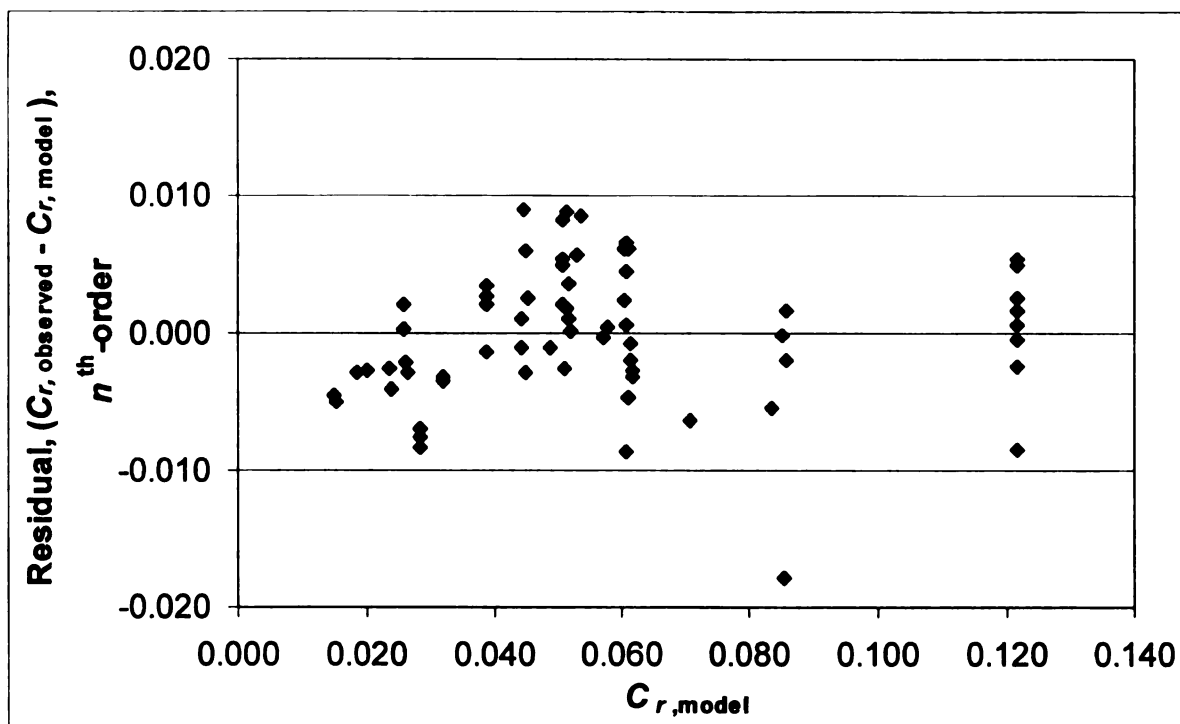
covered the temperature range of 37 – 140°C) were used to solve for degradation of anthocyanin due to thermal effects from extrusion.



a)



b)



c)

Figure 4.1.11 – Residuals versus model values for a) 1st-order, least-squares; b) 1st-order, weighted least-squares; and c) n^{th} -order reaction.

4.2 Extrusion of grape-pomace flour mixture

The color of the extrudates was brownish-purple, possibly because the pH was nearly neutral. Due to limitations of the available equipment, acidic solvents could not be employed during extrusion to improve extrudate color. Because of high % torque and heat dissipation from the screws, extrusion at ambient temperature could not be achieved. Extrudates exited at 70°C even when cooling of the barrel was used. Therefore, the following results apply only to low and high temperature extrusion.

4.2.1 Mean residence time

Figure 4.2.1 and 4.2.2 show a representative RTD curve for low and high temperature extrusion at 30% (43% db) moisture content, respectively, from one

replication. At higher screw speeds, there is more feed input and positive conveyance so near plug flow can be achieved as evident by the sharp RTD curve at 400 rpm. During lower screw speeds, more mixing occurs, so the RTD curve is spread out (more axial mixing), as shown at 50 rpm.

Table 4.2.1 shows the mean residence time values from replicate runs at high and low temperature profile. On the replicate run using the low temperature profile at 50 rpm, the feed rate had to be decreased due to product back up. However, the mean residence time was twice as long as the first replicate, which we suspect may be erroneous. Therefore, the second replicate run at 50 rpm using low-temperature profile was deleted. As expected, at increasing screw speeds the extrudate particle traverse faster in the extruder and had a shorter mean residence time. There was not a strong influence between high and low barrel temperature profile on mean residence time, in agreement with the findings of Altomare and Ghossi (1986).

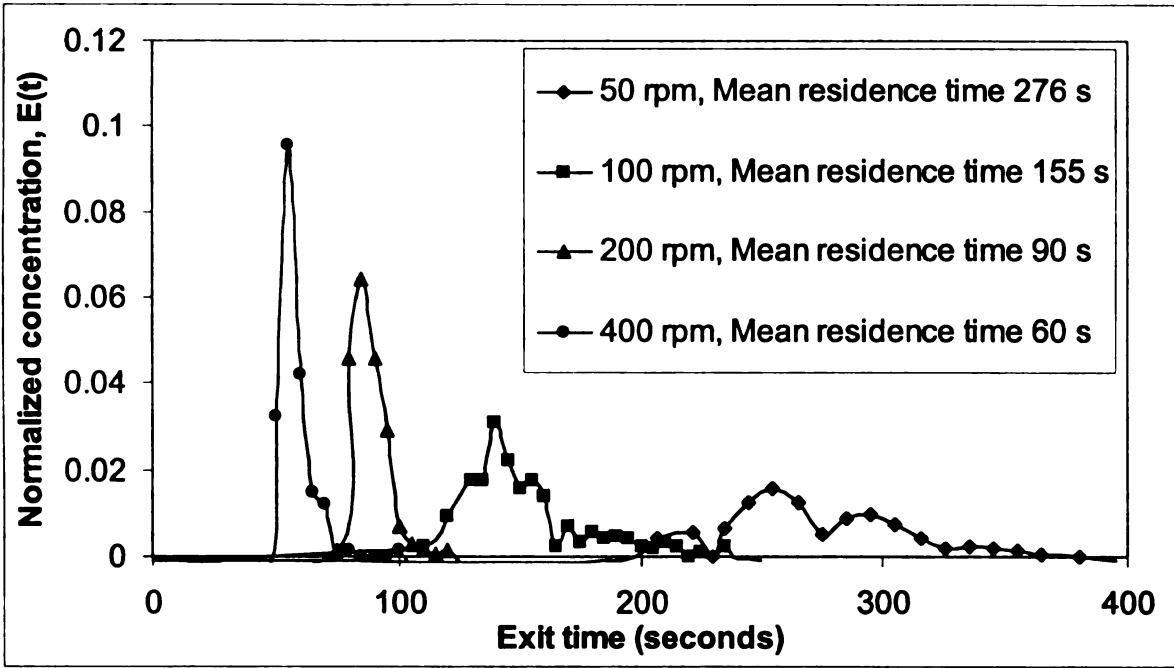


Figure 4.2.1 – RTD curves for low temperature extrusion at 50, 100, 200, and 400 rpm at 43% moisture.

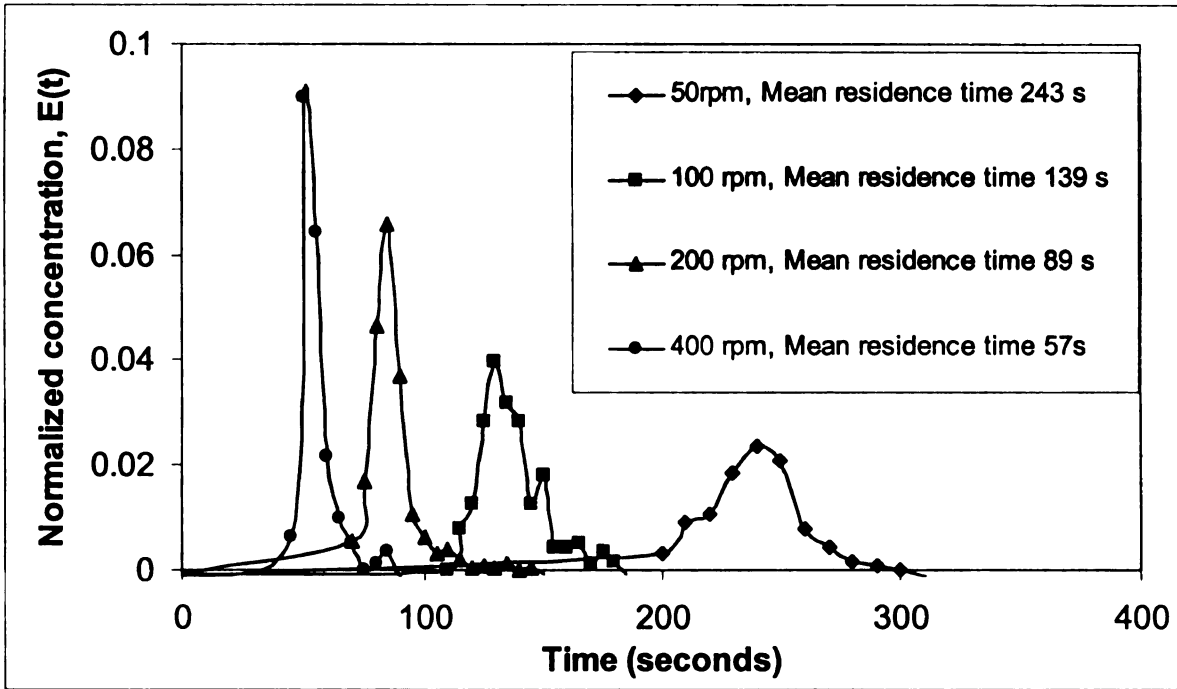


Figure 4.2.2 – RTD curves for high temperature extrusion at 50, 100, 200, and 400 rpm at 43% moisture.

Table 4.2.1 – Mean residence times from extrusion under high and low temperature profiles at screw speeds 50, 100, 200, and 400 rpm

Temperature profile	Screw speed (rpm)	Mean residence time ^a (seconds)
High	50	248.7 (± 7.2)
High	100	141.30 (± 3.0)
High	200	111.00 (± 30.5)
High	400	66.30 (± 12.3)
Low	50	276.6 ^b
Low	100	170.70 (± 22.5)
Low	200	106.50 (± 22.5)
Low	400	74.40 (± 18.7)

^a Average between replicate samples. Standard deviation given in parentheses.

^b Mean residence time from one extrusion run.

4.2.2 Color versus concentration calibration curve

Figure 4.2.3 displays the data points for concentration versus Hunter color values for samples extruded under high temperature at 50, 200, and 300 rpm. At higher concentrations, there was more deviation in the color readings. No specific trend was observed of color values from samples extruded at different screw speeds as shown in Figure 4.2.3 for concentrations of 0.014 and 0.110 g color/g mixture. Therefore, the calibration curve was applied to all screw speeds. The data points were fitted to the equation displayed in Figure 4.2.4. This equation form was used because higher polynomials did not fit the data well. The calibration curve was used to convert all Hunter a* color values to color concentration in the mean residence time study.

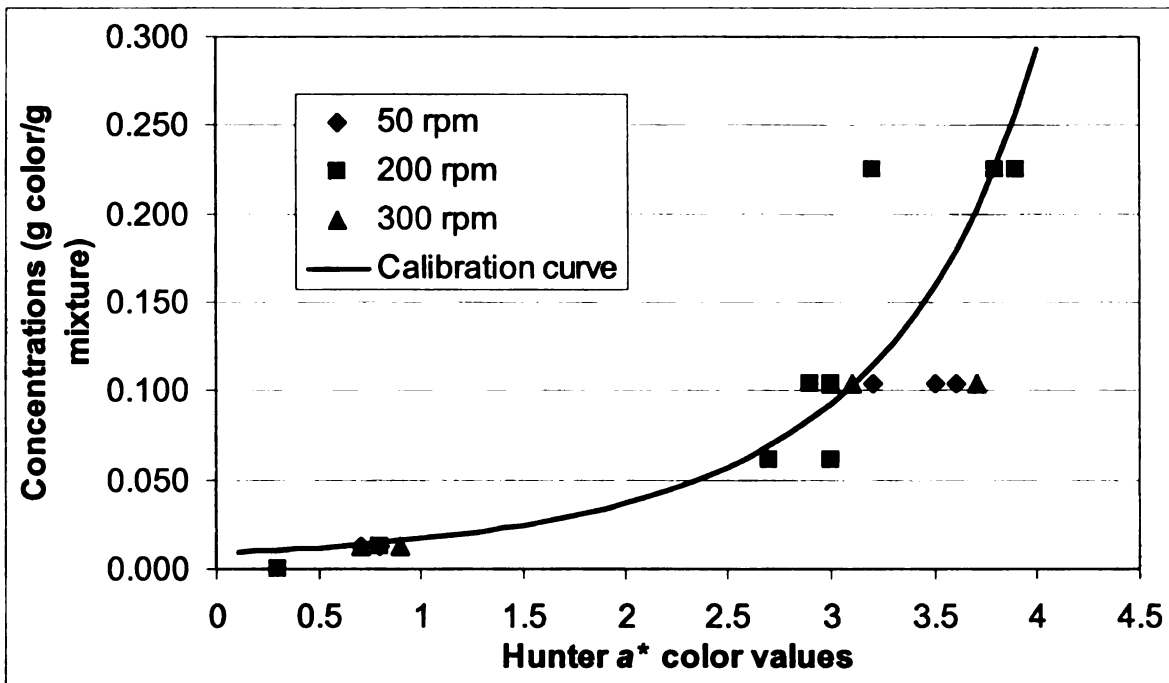


Figure 4.2.3 – Calibration curve for color concentration versus Hunter color values (a^*) extruded under high temperature profile at screw speeds of 50, 200, and 300 rpm.

4.2.3 Extruder degree of fill

Figure 4.2.4 displays the percent fill calculated from samples extruder under high temperature profile at 50, 200, and 400 rpm. The measured dough density was 1.1 g/cm^3 . Extruder void volume was obtained from Suparno and others (2002) as 120 ml. There was not an overlap of percent fill at the three tested screw speeds, so feed rates were estimated by keeping the percent fill at approximately 35%.

Figure 4.2.5 is a pictorial view of the extruder degree of fill opened after dead-stop at 200 rpm. As expected, the paddles and single-lead screws were roughly 100% filled. The mass of the dough in each barrel section (m_i), averaged from replicate measurements, is listed in Table 4.2.2 and was used in Eq. (42) to

estimate the element residence time for the calculation of thermal retention of anthocyanins from extrusion.

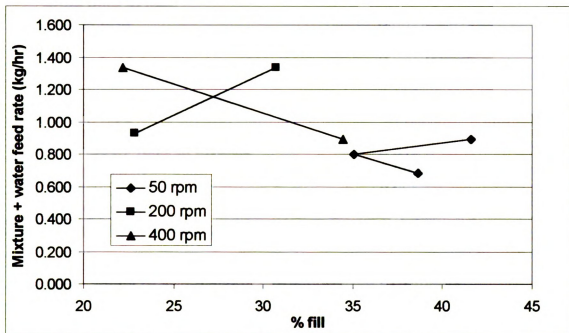


Figure 4.2.4 – Percent fill calculated from samples extruded under high temperature at 50, 200, and 400 rpm.

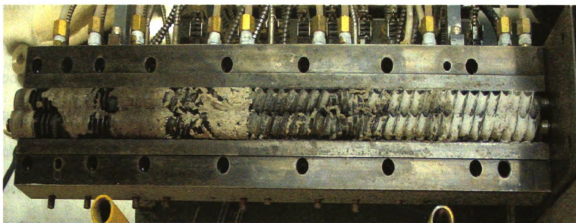


Figure 4.2.5 – Pictorial view of extruder degree of fill opened after dead-stop at 200 rpm.

Table 4.2.2 - Mass of dough from designated extruder sections taken from extrusion run at high temperature, screw speed 200 rpm

<i>Extruder section (from inlet to die)</i>	<i>Dough weight (kg)¹</i>
8D twin-lead	0.0027
7x30° forward paddles	0.0024
4D twin-lead	0.0046
4x60° forward paddles & 4x30° reverse paddles	0.0050
2D twin-lead	0.0012
6x60° forward paddles & 4x30° reverse paddles	0.012
1D single-lead	0.0022
7x90° paddles	0.0058
2D single-lead	0.0079

¹Dough weight taken as average of two measurements.

4.2.4 Study of anthocyanin extraction from extrudates

The absorbance versus extruded samples containing 5, 15, and 25% grape pomace (wb) processed under high temperature at 400 rpm and 43% moisture is shown in Figure 4.2.6 (raw data in Appendix 8, Table A.8.1). Result shows that after extrusion, anthocyanins from extrudates were still extractable, as shown by the expected increasing absorbance versus higher % grape pomace (anthocyanin source). Therefore, we can compare the results between non-extruded (raw material) and extruded samples despite their different product characteristics. Camire and others (2002) also evaluated anthocyanin content before and after extrusion, however, they did not perform a study on the extractability of anthocyanins.

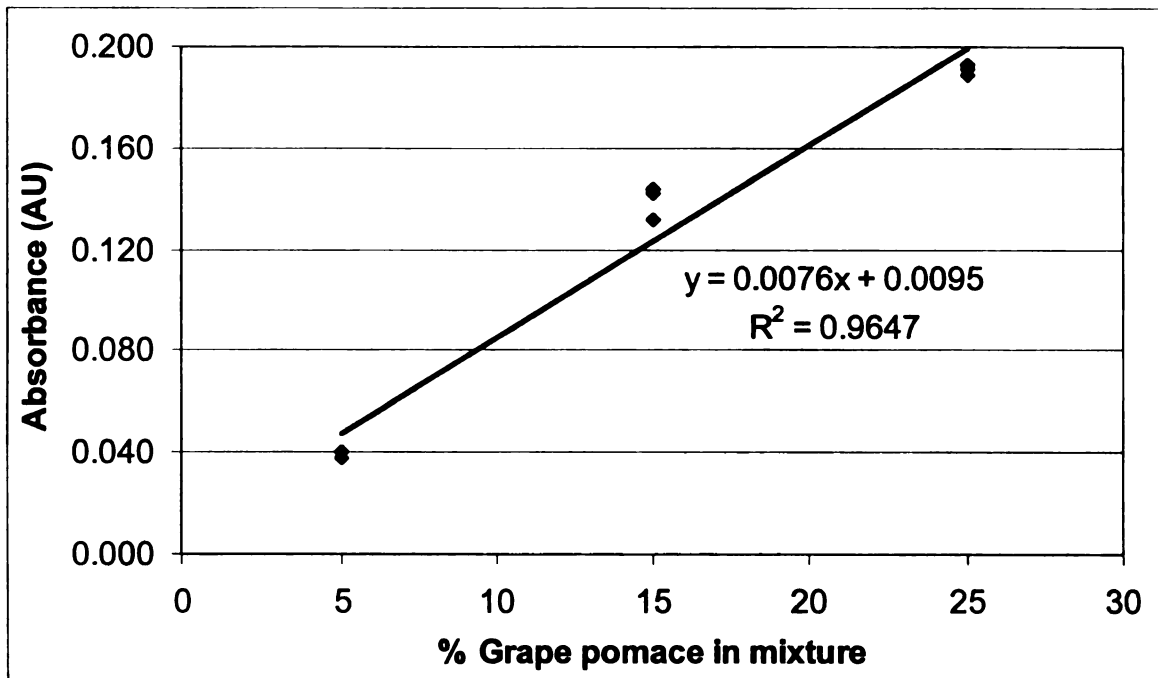


Figure 4.2.6 – Absorbance versus % grape pomace in mixture from samples extruded under high temperature at screw speed of 400 rpm and 30% moisture.

4.2.5 Effects of dough moisture content on anthocyanins

Figure 4.2.7 shows the results from samples extruded using the high temperature profile and 400 rpm at 30, 35, and 40% dough moisture content (wb, raw data in Appendix 8, Table A.8.2). Due to raw material properties and extrusion conditions, this was the range of dough moisture content obtainable. The slope was not well-defined (low R-square value) in this range of moisture content, so moisture rate constant in the extruder, b , could not be calculated from this study. Guzman-Tello and Cheftel (1987) investigated the influence of dough moisture content on thiamin destruction during extrusion and found the rate of thiamin degradation decreased markedly with increasing moisture ($b < 0$).

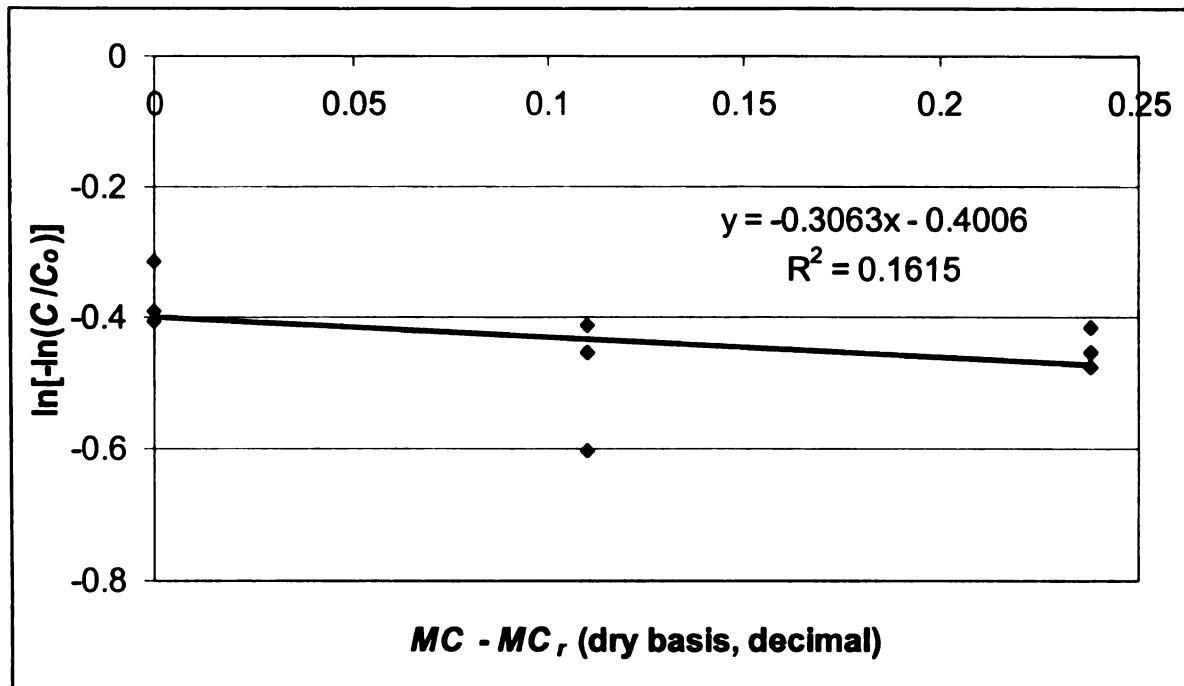


Figure 4.2.7 – Constant heating time method to estimate the moisture rate constant, b , from samples extruded under high temperature, screw speed 400 rpm, at 30, 35, and 40% moisture content (wb).

4.2.6 Thermal and mechanical effects on anthocyanins in extruded wheat flour

Thermal effects

Figure 4.2.8 shows an example of the product temperature measured by thermocouples versus barrel distance fitted with a best-fit line. At barrel location $x \leq 0.272$ m, temperatures were best expressed linearly, whereas a 2nd-order polynomial was used to fit temperatures at $x > 0.272$ m. The equations were used to calculate temperature at any barrel location, $T(x)$, for calculating time-temperature history in Eq. (43) to obtain thermal retention. It was especially important to ensure a close fit of $T(x)$ near the die, because the majority of thermal degradation occurred at the higher temperatures.

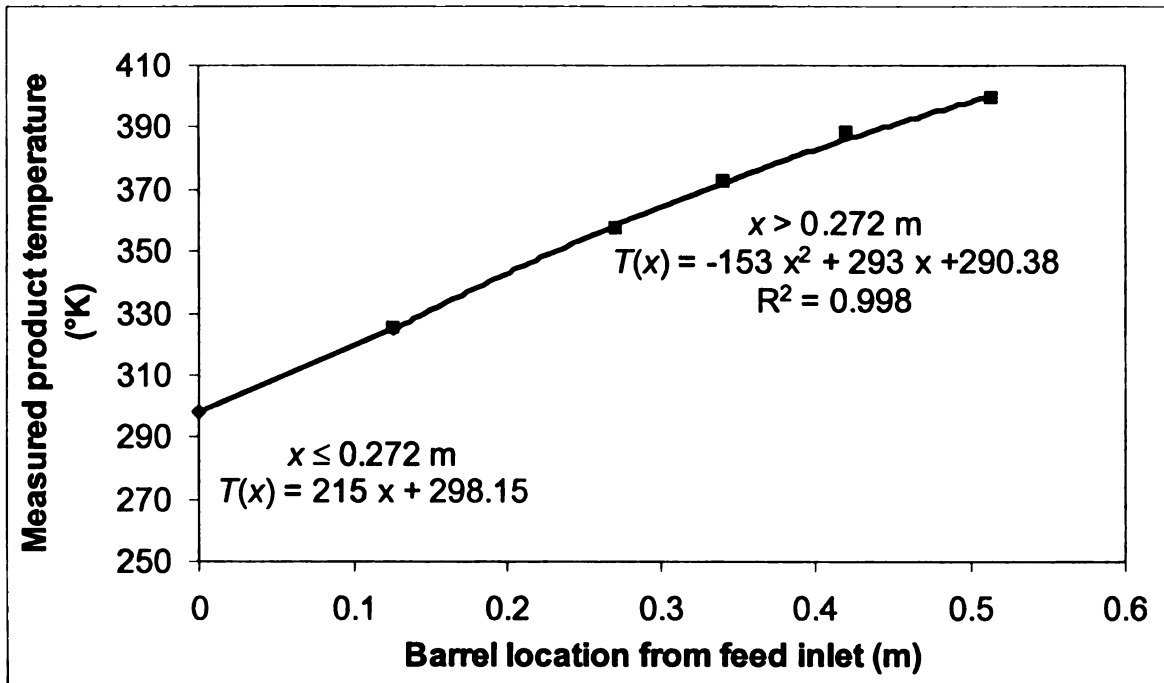


Figure 4.2.8 – Product temperature versus thermocouple distance from feed inlet end of the extruder barrel (from high temperature profile, 50 rpm).

The total retention (measured absorbance from extrudates), retention due to thermal effects (calculated from kinetic parameters), and retention due to mechanical effects (calculated using Eq. (8)) are tabulated in Appendix 9, Table A.9.1 (raw data in Appendix 8, Table A.8.3). For samples from extrusion at 50 rpm at the high temperature profile, average mechanical retention was calculated as 102%, which is physically impossible (Appendix 6, Table A.6.1). This result is probably due to thermal effects having much more influence on degradation than mechanical effects at low screw speeds. Therefore, these R_p values were set to 100% for the remainder of data analysis. Retention values were converted to anthocyanin total loss (Eq. (47)), thermal loss (Eq. (49)), and mechanical loss (Eq. (51), Appendix 9, Table A.9.2) and displayed in Figures 4.2.9 and 4.2.10 for high and low temperature, respectively.

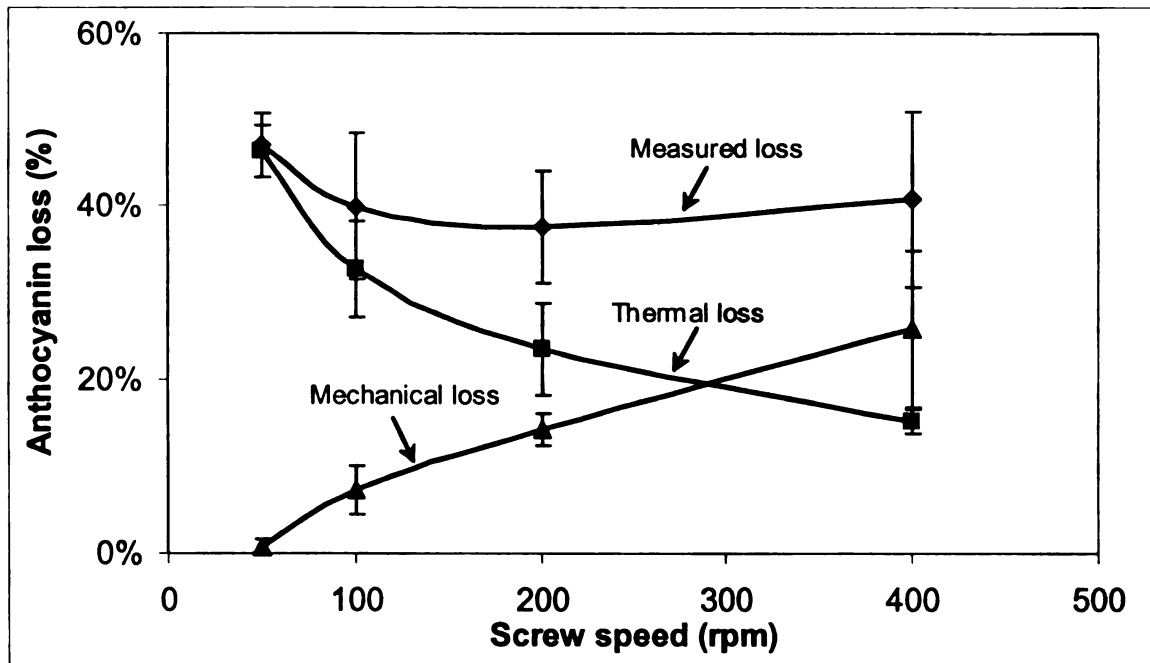


Figure 4.2.9 – Measured, thermal, and mechanical loss of anthocyanins versus screw speed for samples extruded under high temperature. Data are from two replications, each on different days.

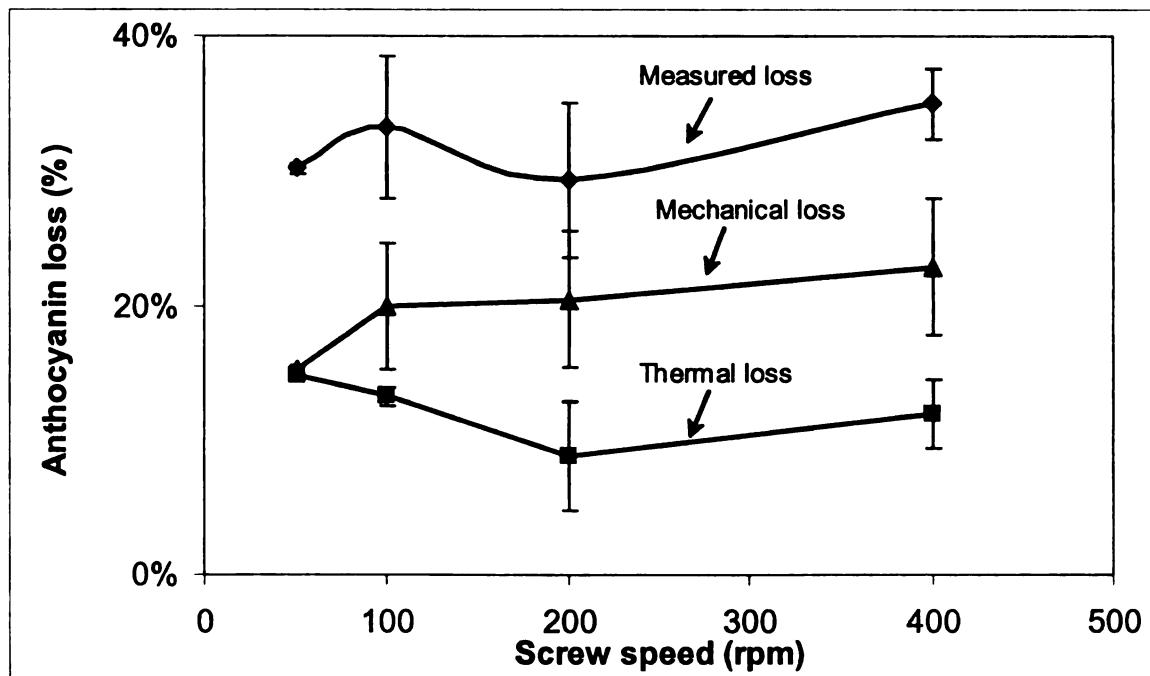


Figure 4.2.10 – Total, thermal, and mechanical loss of anthocyanins versus screw speed for samples extruded under low temperature. Data are from two replications, each on different days.

For high temperature extrusion, total measured loss ranged from ~37 – 47%. Thermal effects accounted for nearly 100% of total loss at 50 rpm but accounted for only 37% of total loss at 400 rpm (Table 4.2.3). Lower thermal loss at higher screw speeds are expected, because at higher screw speeds, mean residence time decreased and the extrudate particle exposure time to heat was shorter. Similarly, mechanical effects on total loss increased (from ~1 to 63%) with increasing screw speed due to higher levels of shear (Table 4.2.3).

Table 4.2.3 – Total anthocyanin loss and % of total loss due to thermal & mechanical effects from extrusion at high-temperature at 50, 100, 200, 400 rpm

Screw speed (rpm)	Total loss (%)	% of total loss due to thermal effects	% of total loss due to mechanical effects
50	47	99	1
100	40	82	18
200	38	62	38
400	41	37	63

For low temperature extrusion, total loss ranged from ~29 – 35% (Appendix 9, Table A.9.2). At 50 rpm, total loss was almost equally divided between thermal and mechanical loss (Table 4.2.4). From 50 – 200 rpm, mechanical loss increased with screw speed. For extrusion at 400 rpm, despite using cooling water, temperature at the die increased to ~115°C compared to ~105°C at other screw speeds (Appendix 10, Table A.10.1), which explains why thermal loss increased slightly at 400 rpm (Figure 4.2.10).

Table 4.2.4 – Total anthocyanin loss and % of total loss due to thermal & mechanical effects from extrusion at low-temperature at 50, 100, 200, 400 rpm

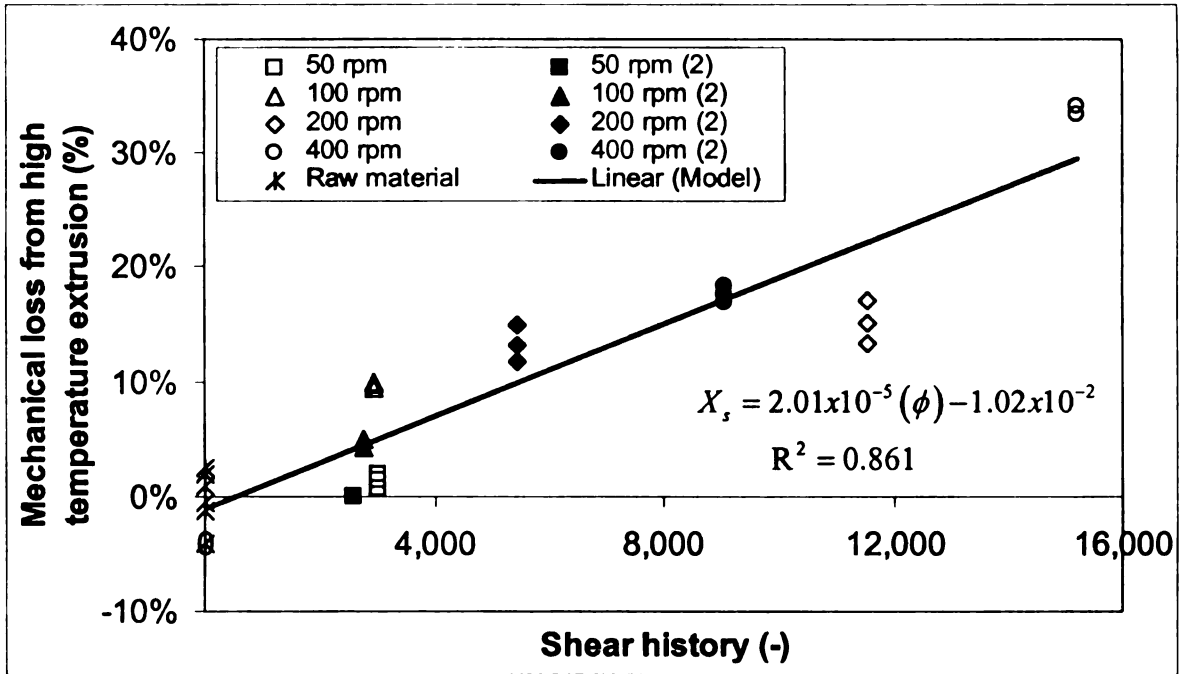
Screw speed (rpm)	Total loss (%)	% of total loss due to thermal effects	% of total loss due to mechanical effects
50	30	49	51
100	33	40	60
200	29	30	70
400	35	34	66

4.3 Mechanical effects

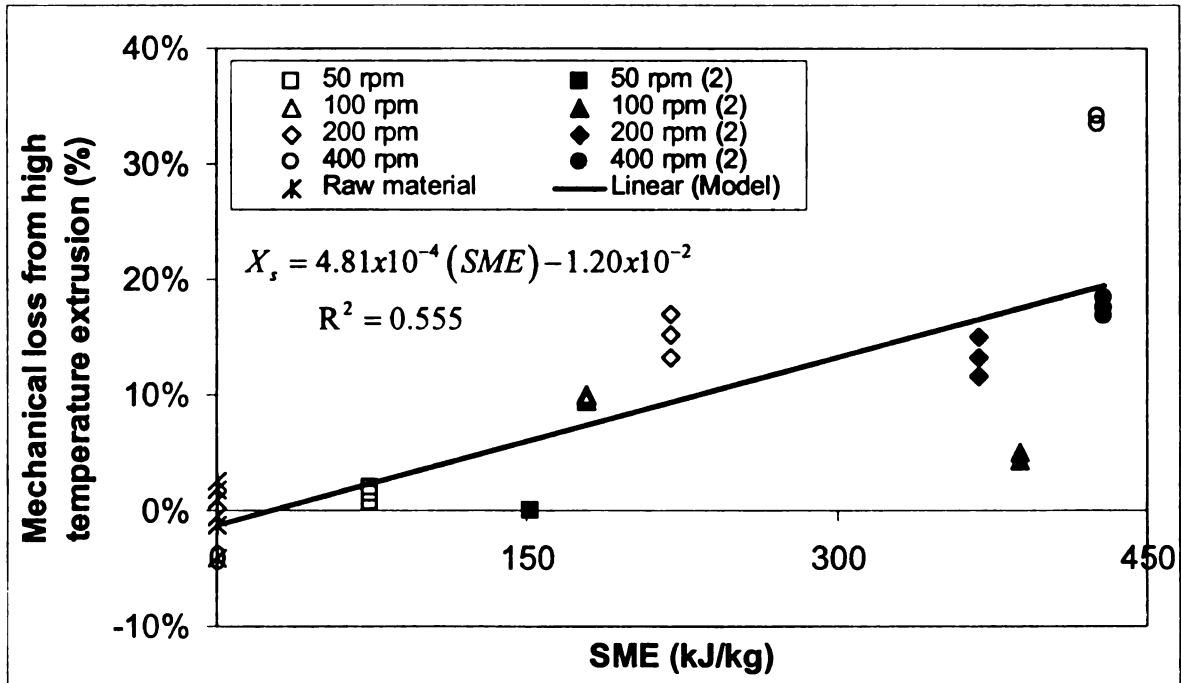
4.3.1 High-temperature extrusion

Figure 4.3.1a, b, and c display mechanical loss (X_s) versus screw speed, shear history, and *SME* for high temperature extrusion. The % loss was relatively linear, ranging from ~0 – 34% with increasing screw speed; therefore data points were fitted with a linear trendline ($X_s = c_1(S) + c_2$). The linear fit was generally good for X_s versus screw speed and shear history, however, there was more scatter for X_s versus *SME* (Figure 4.3.1c, $R^2 = 0.555$). Since the grape pomace-flour mixture was less homogeneous compared to typical extrusion raw material, like cornstarch or flour, the % torque and die pressure were not as reproducible between runs (Appendix, Table A.10.1), thus yielding quite different *SME* values. Although it would be easier to model X_s versus *SME*, because processors can obtain *SME* in real-time during extrusion, the data from this study does not exhibit a sufficiently clear trend.

X_s versus shear history (Figure 4.3.1b, $R^2=0.861$) was a better fit than X_s versus screw speed (Figure 4.3.1a, $R^2=0.835$). Shear history accounts for screw speed, the degree of fill, and mean residence time. The latter two may not be



b)



c)

Figure 4.3.1 – % mechanical loss from high temperature extrusion versus a) screw speed, b) shear history, and c) SME.

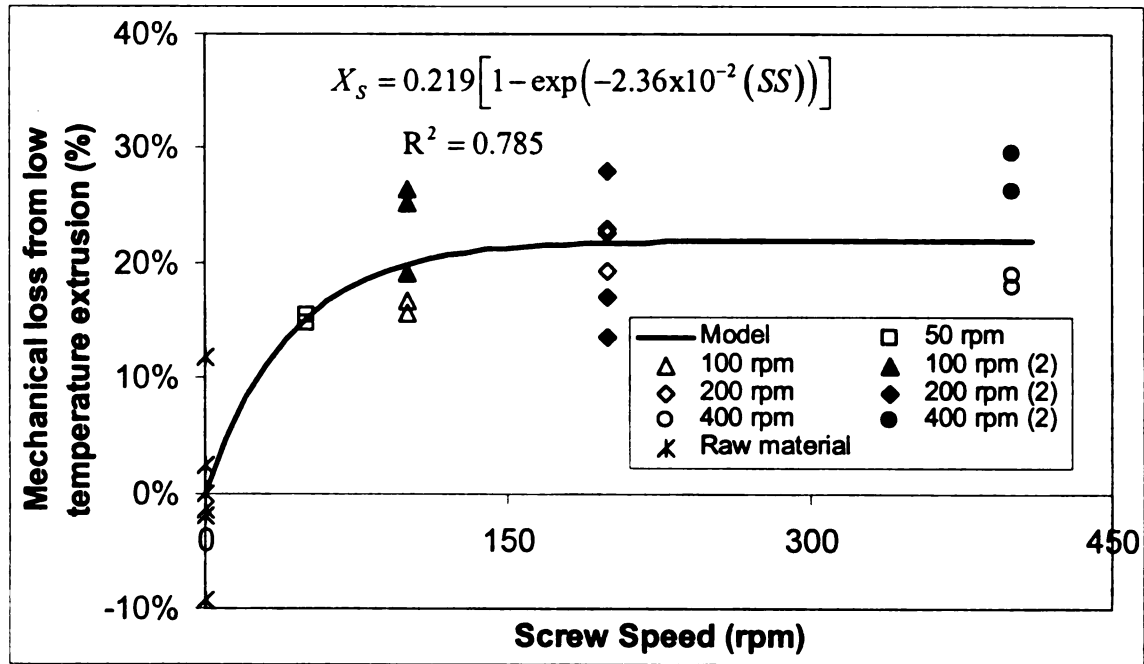
4.3.2 Low-temperature extrusion

Figure 4.3.2a, b, and c display X_s versus screw speed, shear history, and *SME* for low-temperature extrusion. Generally, there was more scatter in the low-temperature compared to the high-temperature results. Since X_s values were obtained after correcting for temperature, the trend of X_s versus screw speed, shear history, or *SME* for both high- and low-temperature conditions was expected to be the same. But the trend of X_s from low temperature extrusion was different from that for high-temperature, exhibiting more of an exponential increase (rather than linear increase in high temperature results), with X_s of ~15 – 23% as screw speed increased. An exponential model of the form:

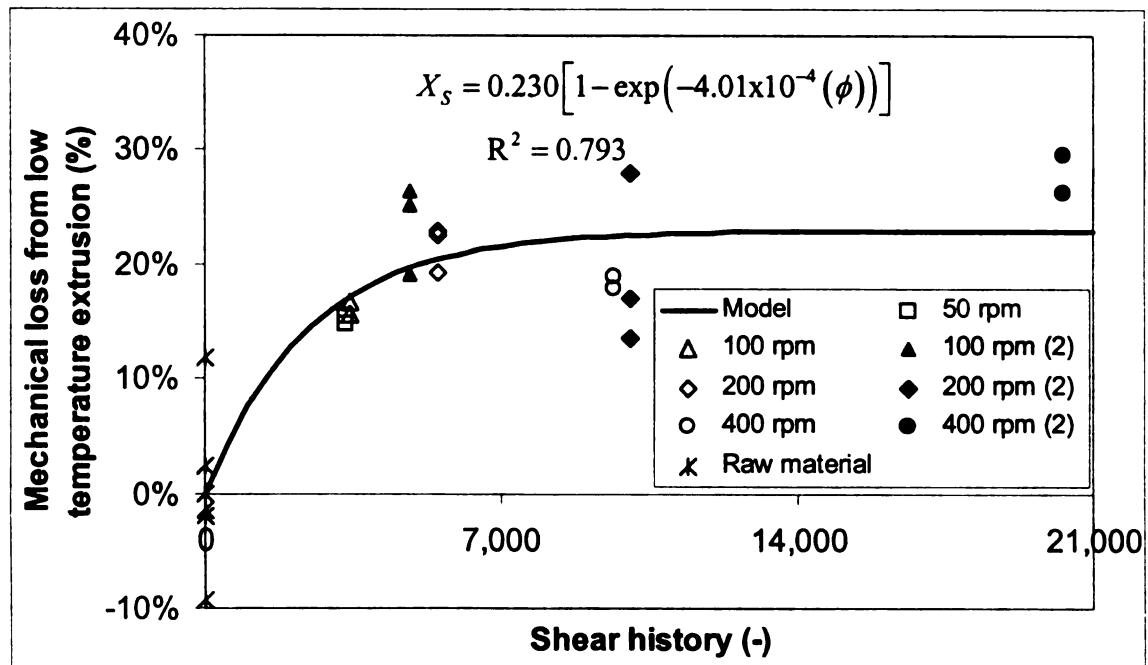
$X_s = c_1 [1 - \exp(-c_2 \cdot S)]$ was used to fit X_s against screw speed, shear history, and *SME*.

Modeling X_s versus shear history and *SME* produced a better fit than versus screw speed. A small improvement of the R^2 value when screw speed was replaced with shear history can be seen by noting that the mechanical loss values at 100 rpm, 200 rpm, and 400 rpm (first replicate) samples (Figure 4.3.2a) were shifted closer to the trendline when graphed against shear history (Figure 4.3.2b). Samples with longer shear history exhibit higher mechanical loss at 100 and 400 rpm (although *SME* were also higher in these cases). No trend was found at 200 rpm. *SME* values from the replicate run were all greater than the first run (Figure 4.3.2c). The replicate run was performed nearly three months after the first run (due to equipment maintenance), so there may have been some changes in the raw material that could have yield such different *SME* results.

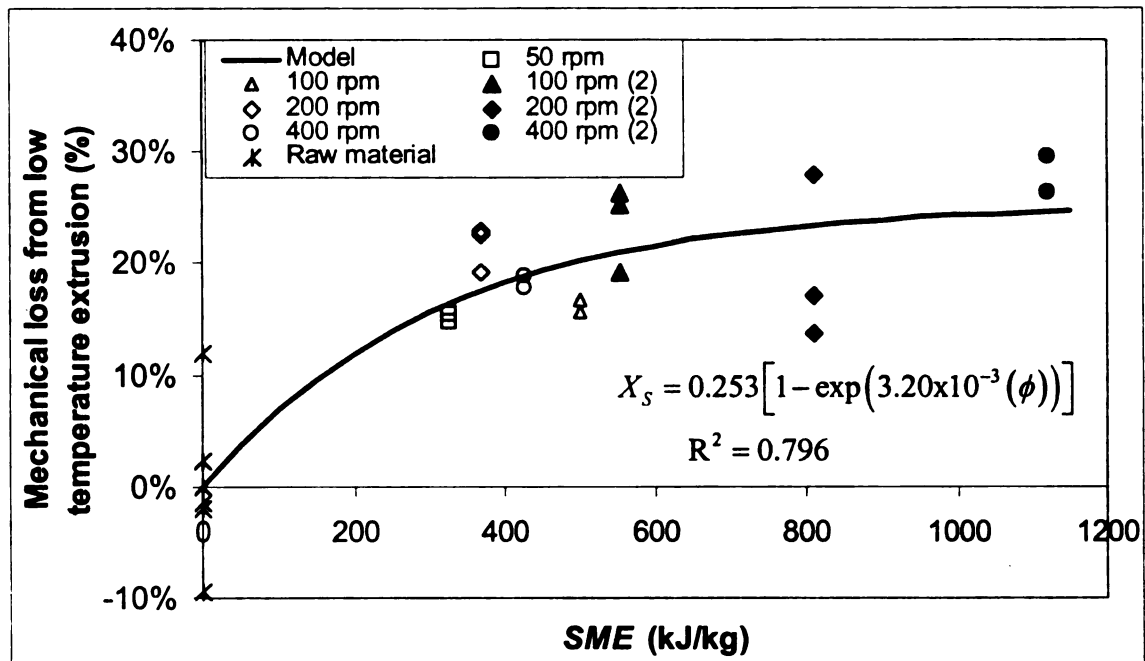
The fit of the trendline for mechanical loss versus shear history and *SME* were comparable.



a)



b)



c)
Figure 4.3.2 – % mechanical loss from low temperature extrusion versus a) screw speed, b) shear history, and c) SME.

By observation, the two trends of X_s at high- and low-temperature are different, demonstrating an interaction between product temperature and mechanical loss. However, to prove this statistically, trendlines using the same model must be compared. First, we assumed both lines were nonlinear and described it using $X_s = c_1 [1 - \exp(-c_2 \cdot S)]$. The parameters c_1 and c_2 were predicted using 'proc nlin' function from SAS; however, for high-temperature extrusion data, values for the parameters did not converge because the data points followed a linear trend.

Therefore, we fit the data from both temperatures using the linear model, $X_s = c_1(S) + c_2$, and compared the slope of the trendlines using the 'proc reg' function from SAS at 95% confidence level where null hypothesis was 'no

difference between slopes'. The p-values are listed in Table 4.2.5. The trendlines between high- and low-temperature conditions for mechanical loss versus screw speed and shear history were significantly different ($p < 0.0001$) which was expected. However, that was not the case for X_s versus SME ($p = 0.1545$), although it is apparent there is a difference in trend. The SME data between the two temperatures did not overlap much, because high-temperature SME values were generally all lower than those from low temperature.

Table 4.2.5 – p-values for comparing the slope between high and low-temperature extrusion linear trendlines for mechanical loss versus screw speed, shear history, and SME

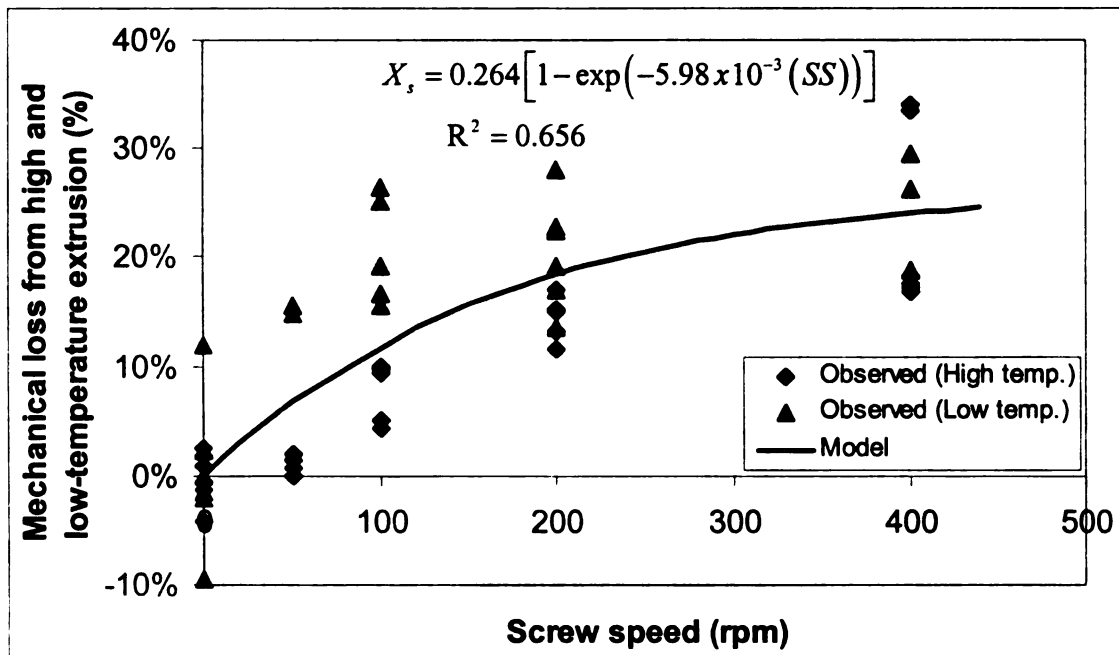
<i>Shear term</i>	<i>p-value</i>
Screw speed	$<0.0001^a$
Shear history	$<0.0001^a$
SME	0.1545

^aSlopes were significantly different at 95% confidence level.

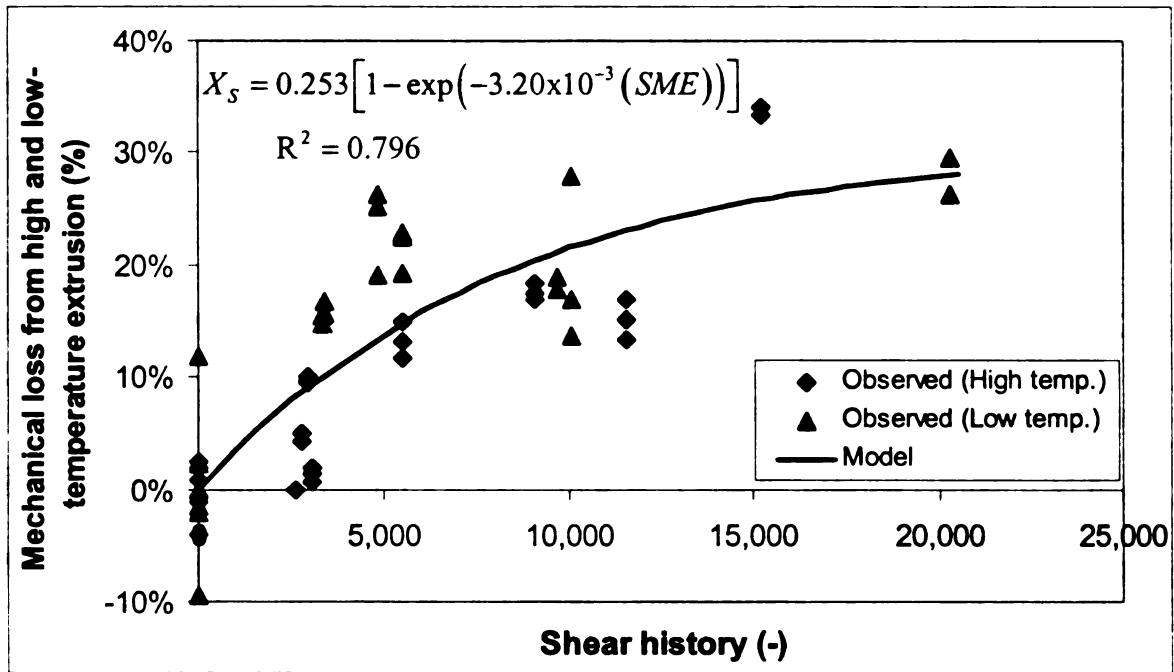
4.3.3 Combining mechanical loss from high and low-temperature extrusion

Mechanical loss versus screw speed, shear history, and SME from both high- and low-temperature profiles data was combined to observe any overall pattern (Figure 4.3.3a, b, and c). Despite a difference in the trend between high- and low-temperature data, there appears to be an overall exponential increase in mechanical loss (Figure 4.3.3a,b, and c). This is especially evident for mechanical loss versus SME (Figure 4.3.3c) where the low-temperature data extend the high-temperature data at larger SME values. Mechanical loss versus shear history had the best-fit (Figure 4.3.3b, $R^2 = 0.694$), while the fit for mechanical loss versus SME was comparable (Figure 4.3.3c, $R^2 = 0.656$).

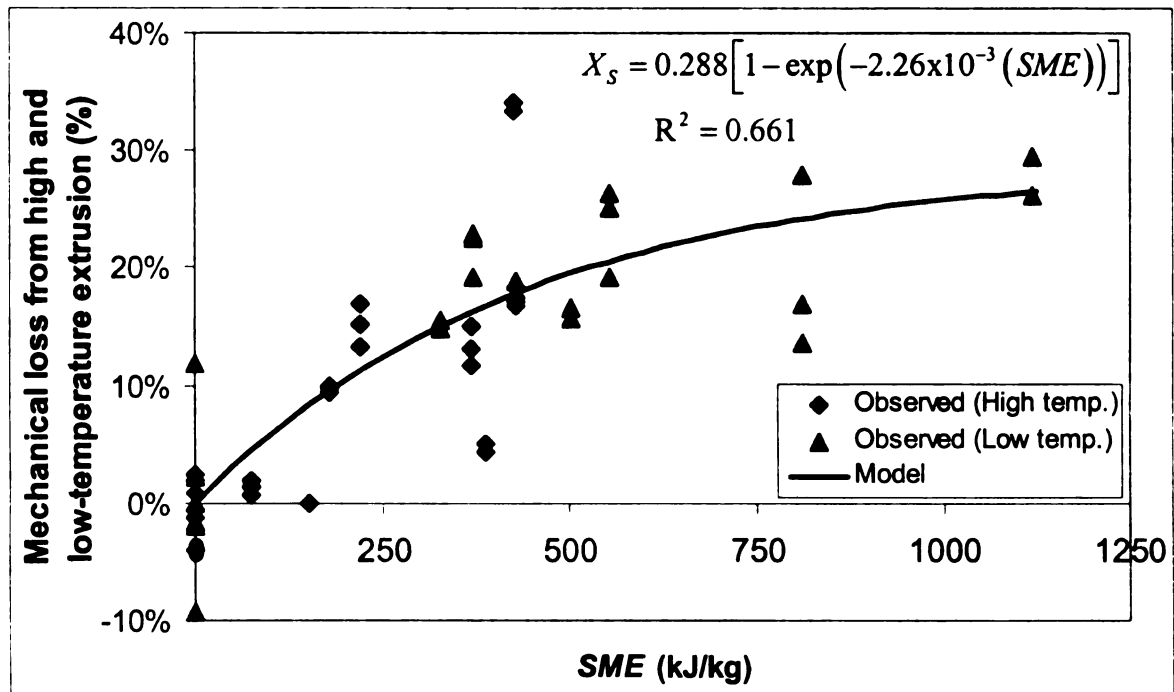
The advantage to modeling mechanical loss in terms of *SME* is that *SME* is easier to calculate than shear history. Also, since barrel temperature affects dough viscosity, which in turn affects the extruder torque reading used to calculate *SME*, *SME* should compensate for different temperature profiles. However, the effects of temperature did appear, since the trendlines for X_s versus *SME* were different between low- and high-temperature extrusion (Figure



a)



b)



c)

Figure 4.3.3 - % mechanical loss from high and low temperature extrusion versus a) screw speed, b) shear history, and c) SME.

4.3.1c and 4.3.2c). Thus, it is not possible to explain the difference between X_s versus *SME* results from low- and high-temperature extrusion as purely a temperature effects.

On the other hand, temperature is not directly involved in the shear history calculation ($\phi = \dot{\gamma}_a \bar{t} \propto k' N \bar{t} \propto (\% \text{ fill}) N \bar{t}$; temperature has only a small effect on \bar{t} and % fill). Therefore, using shear history to predict X_s for both low- and high-temperature extrusion seems appropriate, and any difference between X_s from low- and high-temperature can be attributed to temperature effects. Also, using shear history (which includes the mean residence time) as a predictor of mechanical loss is important because results have shown that in addition to the level of shear (screw speed), the length of time (mean residence time) the compound was sheared is also important.

As a result, mechanical loss was modeled versus shear history for high and low-temperature extrusion. Since only two barrel temperature profiles were investigated in this study, more extrusion experiments at other temperature profiles would be needed to describe mechanical effects as a function of temperature. The resulting model equation for total anthocyanin loss in a 1:3 grape-pomace/wheat flour extruded product at 30% moisture (wb) is

- For die temperature ~ 95°C

$$X_T = \left[1 - \int_0^{\infty} \exp(-2.81 \times 10^{-4} \beta) E(t) dt \right] + \left[0.230 \left(1 - \exp(-4.01 \times 10^{-4} \phi) \right) \right] \quad (82)$$

- For die temperature ~ 125°C

$$X_T = \left[1 - \int_0^{\infty} \exp(-2.81 \times 10^{-4} \beta) E(t) dt \right] + \left[2.01 \times 10^{-5} (\phi) - 0.0102 \right] \quad (83)$$

- For die temperature ~95°C and 125°C

$$X_T = \left[1 - \int_0^{\infty} \exp(-2.81 \times 10^{-4} \beta) E(t) dt \right] + 0.303 \left[1 - \exp(-1.21 \times 10^{-4} (\phi)) \right] \quad (84)$$

$$\beta = \int_0^t \exp \left[\frac{-75.27}{R} \left(\frac{1}{T(t)} - \frac{1}{353.15} \right) \right] dt$$

where dt is in seconds and ϕ is dimensionless. This model is applicable for extrusion using the high-shear screw configuration employed in this study.

4.4 Model validation

Since the predictive model for 1st-order reaction thermal loss (X_β) had a high correlation (R-squared value) of 0.960, model validation was not performed on those results. The *PRESS* and *SSE* values calculated for mechanical loss in terms of shear history are tabulated in Table 4.2.6. Error values were lowest for results from extrusion at 95°C die temperature and highest for the model combining extrusion at both 95°C and 125°C die temperature. The fairly close agreement between *PRESS* and *SSE* values suggests the model developed in this study is a good candidate for predicting mechanical loss as a function of shear history for extrusion at the temperature profiles employed in this work.

Table 4.2.6 – *PRESS* values for the model validation of mechanical loss in terms of shear history at various extrusion temperature conditions.

Temperature profile	<i>PRESS</i> value	<i>SSE</i> value
95°C die temperature	0.067	0.059
125°C die temperature	0.198	0.181
95°C and 125°C die temperature	0.325	0.302

5. Conclusions and Recommendations

5.1 Summary and conclusions

A model equation was developed to predict total anthocyanin loss from extrusion processing. It was assumed that thermal and mechanical shear effects from extrusion were the two primary causes of degradation of anthocyanins. Total anthocyanin retention was modeled as the product of thermal retention and mechanical retention.

The raw material was made up of grape pomace (anthocyanin source) mixed with wheat pastry flour at 1:3 w/w (db). It was extruded using two different temperature profiles (95°C and 125°C die temperature) at 50, 100, 200, and 400 rpm. Total anthocyanin retention was measured from extrudates. To calculate thermal retention, thermal kinetic parameters were estimated from separate isothermal (80°C) and nonisothermal (105°C and 145°C) oil bath studies. Nonlinear regression was used to establish the degradation of total anthocyanin as pseudo first-order. Reference reaction rate constant was estimated as $k_{80\text{ }^\circ\text{C}} = 2.81 \times 10^{-4} \pm 1.1 \times 10^{-6} \text{ s}^{-1}$ (standard error) and activation energy as $\Delta E = 75,273 \pm 197 \text{ J/g-mol}$.

Mean thermal retention in extrudates was calculated by integrating first-order thermal retention over the element residence time distribution. Mechanical retention was solved for by mathematically removing thermal effects from measured total retention. All retention values were converted to loss. For extrusion high temperature at 50 – 400 rpm, total anthocyanin loss ranged from 38 – 47%, of which mechanical effects were responsible for 1% at 50 rpm to 63%

at 400 rpm. For low-temperature extrusion, total anthocyanin loss ranged from 29 – 35%, of which mechanical loss accounted for 51% at 50 rpm to 66% at 400 rpm.

An empirical equation was developed to model mechanical loss versus shear history. For high-temperature extrusion, ϕ was the best predictor ($R^2 = 0.861$); and for low-temperature extrusion, SME was the best predictor ($R^2 = 0.796$). Combining both temperature profiles, shear history was the best predictor ($R^2 = 0.694$).

The trendlines fit to mechanical loss against shear history data were statistically different between high and low temperature extrusion, indicating an interaction between temperature profile and mechanical shear. The final model equations for 30% moisture content grape pomace-flour mixture, in terms of loss, were:

- For die temperature ~ 95°C

$$X_T = \left[1 - \int_0^{\infty} \exp(-2.81 \times 10^{-4} \beta) E(t) dt \right] + \left[0.230 (1 - \exp(-4.01 \times 10^{-4} \phi)) \right]$$

- For die temperature ~ 125°C

$$X_T = \left[1 - \int_0^{\infty} \exp(-2.81 \times 10^{-4} \beta) E(t) dt \right] + \left[2.01 \times 10^{-5} (\phi) - 0.0102 \right]$$

- For die temperature ~95°C and 125°C

$$X_T = \left[1 - \int_0^{\infty} \exp(-2.81 \times 10^{-4} \beta) E(t) dt \right] + 0.303 \left[1 - \exp(-1.21 \times 10^{-4} (\phi)) \right]$$

where $\beta = \int_0^t \exp \left[\frac{-75.27}{R} \left(\frac{1}{T(t)} - \frac{1}{353.15} \right) \right] dt$.

Model validation using the $PRESS_p$ criterion confirmed the reliability of the model equations developed in this study.

5.2 Recommendations for future research

The following topics are recommended for future research:

1. Extrude grape pomace-flour mixture (1:3 w/w dry basis) at 2 to 3 more temperature profiles to obtain mechanical loss as a function of temperature.
2. Run the isothermal oil bath experiments in Table 3.1.2 at 80 °C and varying % moisture content for at least 5 heating times to investigate whether reaction order, n , is a function of moisture content. Include a moisture content term in the final model.
3. Investigate effect of other raw materials (e.g. maize grits, soy) on anthocyanin loss.
4. Employ acidic solvents during extrusion to improve extrudate color.

Appendix 1

Appendix 1 – Anthocyanin analysis

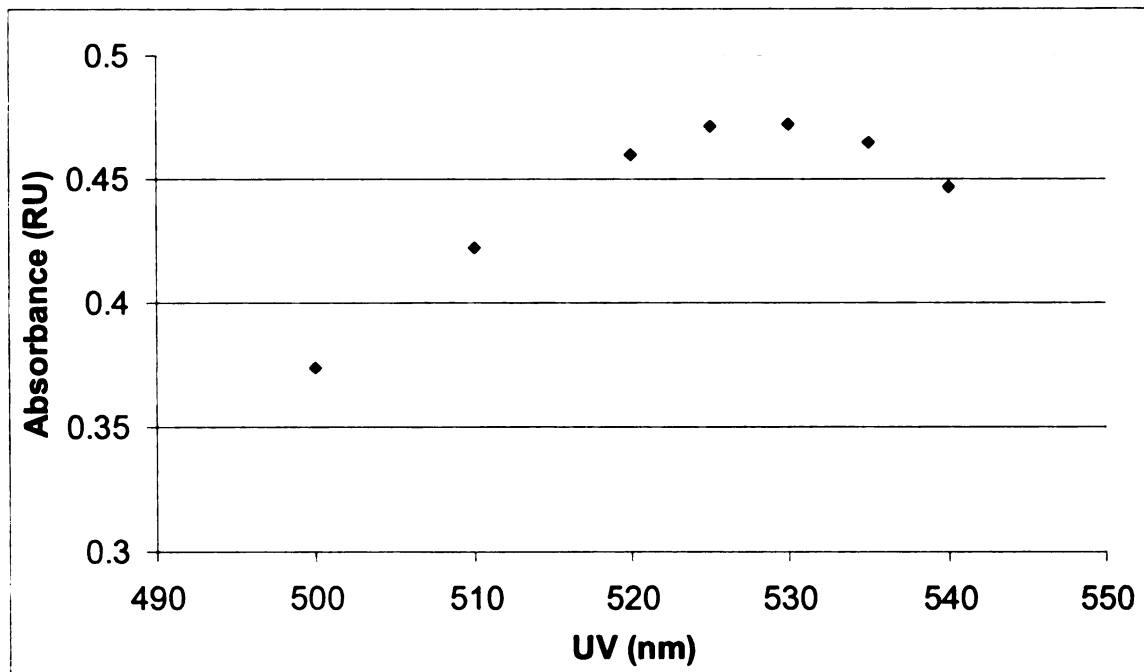


Figure A.1.1 – Finding the maximum absorbance using extracts diluted at dilution factor = 3 with pH 1.0 buffer.

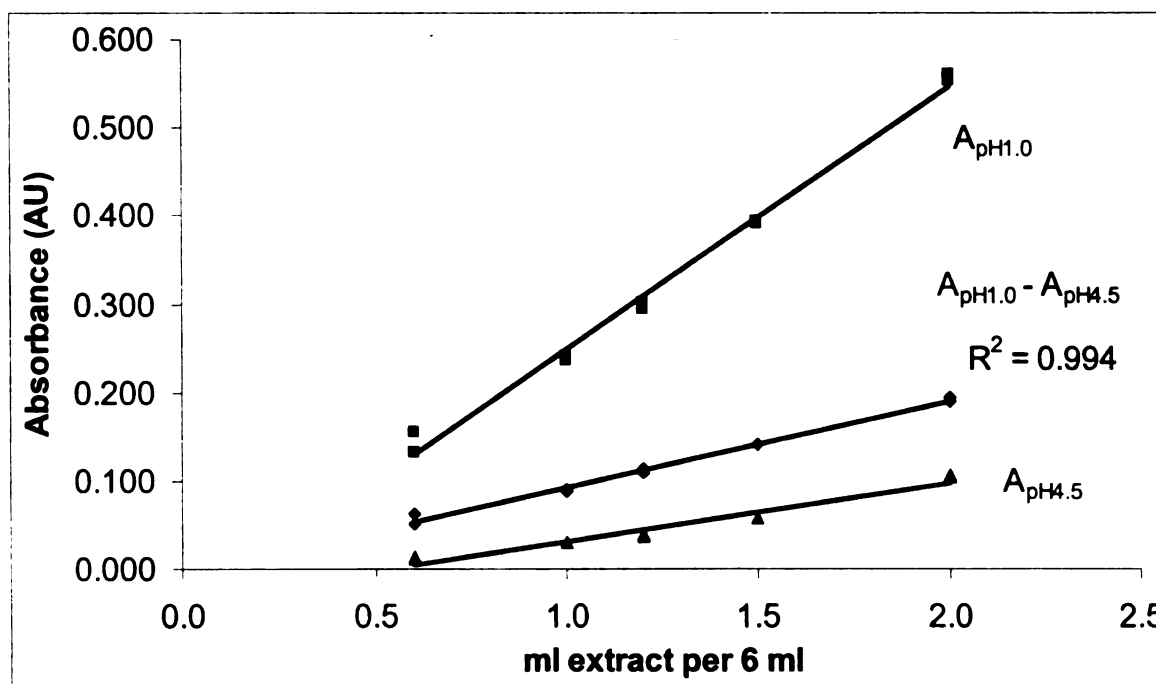


Figure A.1.2 – Linear range of absorbance versus anthocyanin concentration using extracts diluted with pH 1.0 and 4.5 buffer.

Appendix 2

Appendix 2 – Sample approximate confidence intervals calculations

Approximate confidence intervals were calculated for the estimates k_r , ΔE , and C_o . This is the example for thermal kinetic parameters from WLS 1st-order reaction model. The procedures were the same for n^{th} -order reaction model with the addition of the parameter n .

Sensitivity coefficients (Eq. (67) – (69)) was used to calculate the sensitivity matrix \mathbf{X} (Eq. (63), 68 x 3 Jacobian matrix):

$$\mathbf{X} = \begin{pmatrix} 0.00 & -4.74 \times 10^{-5} & 3.51 \times 10^{-11} \\ \vdots & \ddots & \vdots \\ -155 & 9.06 \times 10^{-8} & 0.344 \end{pmatrix}$$

The Hessian matrix (3x3) was calculated as the inverse of the sensitivity matrix multiplied by its transpose:

$$\text{Hessian} = [\mathbf{X}^T \mathbf{X}]^{-1} = \begin{pmatrix} 2.61 \times 10^{-6} & -228 & 2.76 \times 10^{-4} \\ -228 & 9.17 \times 10^{10} & -8911 \\ 2.78 \times 10^{-4} & -8911 & 0.0844 \end{pmatrix}$$

The symmetric parameter variance-covariance matrix ($\text{cov}(\mathbf{a})$, Eq. (63)) was calculated by multiplying the Hessian matrix by mean square error ($MSE = SS_E \div (m-p) = 4.24 \times 10^{-7}$):

$$\text{cov}(\mathbf{a}) = \begin{pmatrix} 1.11 \times 10^{-12} & -9.68 \times 10^{-5} & 1.18 \times 10^{-10} \\ -9.68 \times 10^{-5} & 38,879 & -3.78 \times 10^{-3} \\ 1.18 \times 10^{-10} & -3.78 \times 10^{-3} & 3.58 \times 10^{-8} \end{pmatrix}$$

where the asymmetric standard errors are square root of the corresponding diagonal term:

$$\begin{aligned} k_r &= \sqrt{1.11 \times 10^{-12}} = 1.11 \times 10^{-6} \\ \Delta E &= \sqrt{38,879} = 197 \\ C_o &= \sqrt{3.58 \times 10^{-8}} = 0.0002 \end{aligned}$$

The confidence intervals were found by multiplying the asymmetric standard errors with 1.997 (t -statistic at 95% confidence and degrees of freedom = 68 data points – 3 parameters = 65).

Appendix 3

Appendix 3 – Equations referenced in Results and Discussion section

(58) Mass-average sample temperature for each heating time

$$T_{\text{average}}^i = \left(\frac{T_c^i + T_w^i}{2} \right)$$

(21) Constant heating time method to estimate b for 1st-order reaction

$$\ln \left[-\ln \left(\frac{C}{C_o} \right) \right] = \ln(k_r t) + b(MC - MC_r)$$

(22) Constant heating time method to estimate b for n^{th} -order reaction

$$\ln \left(-\frac{C^{1-n} - C_o^{1-n}}{1-n} \right) = \ln(k_r t) + b(MC - MC_r)$$

(28) Moisture content correction factors for nonisothermal heating samples

$$CF_{NI} = \frac{\beta}{\beta_{T,MC}}$$

(35) Moisture content correction factors for isothermal heating samples

$$CF_i = \exp[-b(MC - MC_r)]$$

(37) First-order reaction model in terms of concentration

$$C_r = C_o \exp(-k_r \beta)$$

(39) n^{th} -order reaction model in terms of concentration

$$C_r = \left[(n-1)k_r \beta + C_o^{1-n} \right]^{\frac{1}{1-n}}$$

(12) n^{th} -order primary model describing rate of concentration degradation

$$\frac{C^{1-n}}{1-n} - \frac{C_o^{1-n}}{1-n} = - \int_0^t k dt$$

(42) Element residence time in extrusion

$$\Delta t_i = \frac{m_i}{\sum_i m_i} t$$

(43) Time-temperature history of each section i over the total number of barrel sections f

$$\beta(t) = \sum_{i=1}^f \exp \left[\frac{-\Delta E}{R} \left(\frac{1}{T(x_i)} - \frac{1}{T_r} \right) \right] \left(\frac{m_i}{\sum_j m_j} \right) t$$

(8) Total retention

$$R_T = R_\beta R_S$$

(47) Total loss

$$X_T = 1 - R_T = 1 - R_\beta R_S$$

(49) Thermal loss

$$X_\beta = 1 - \int_0^\infty \exp(-k_r \beta(t)) E(t) dt = 1 - R_\beta$$

(51) Mechanical loss

$$X_S = R_\beta (1 - R_S)$$

Appendix 4

Appendix 4 – Lumped heat-capacity analysis

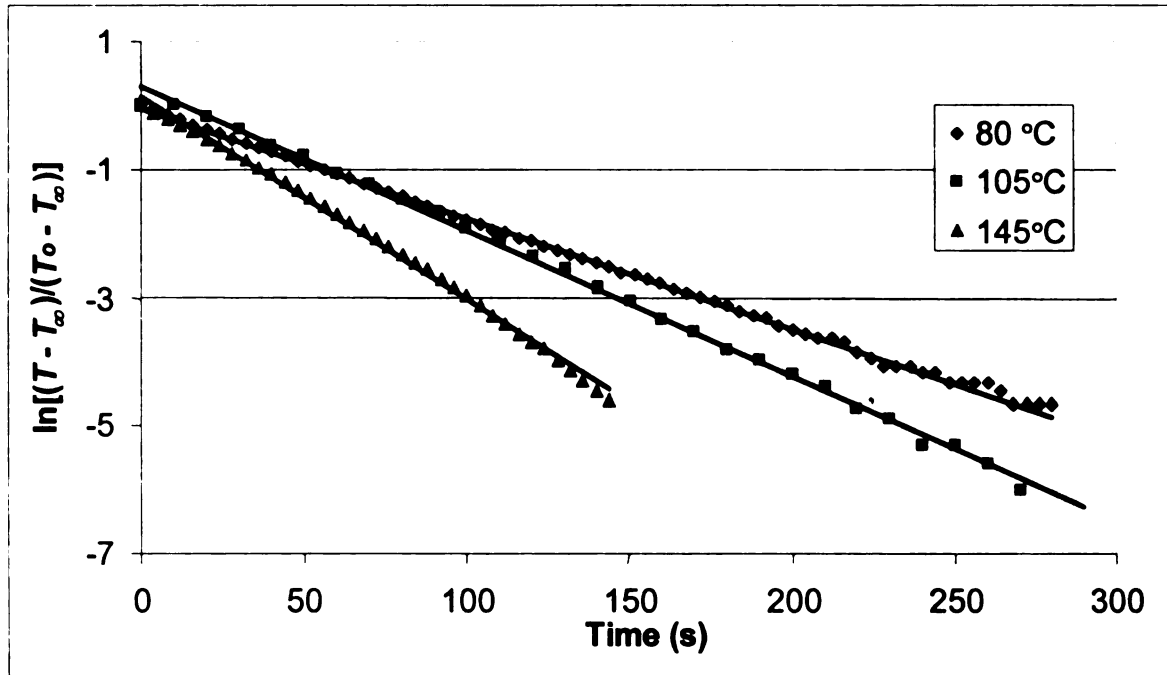


Figure A.4.1 – The log of temperature ratio versus time used in lumped heat capacity analysis to calculate heat transfer coefficient.

The slope of the trendline was averaged from duplicate runs and used in Eq. (62) to solve for the heat transfer coefficient at oil bath temperatures of 80, 105, and 145 °C. The heat transfer coefficients were calculated as:

- 80°C: $h = 122.8 \text{ w/m}^2 \text{ }^\circ\text{C}$
- 105°C: $h = 162.3 \text{ w/m}^2 \text{ }^\circ\text{C}$
- 145°C: $h = 238.8 \text{ w/m}^2 \text{ }^\circ\text{C}$

Appendix 5

Appendix 5 – Anthocyanin measurements from isothermal heating at 80°C and nonisothermal heating at 105 °C and 145 °C

Table A.5.1 – Absorbance values for 43% (db) samples heated isothermally at 80°C and nonisothermally at 105°C and 145°C for various times.

80°C		105°C		145°C	
Time (min)	Absorbance (AU)	Time (min)	Absorbance (AU)	Time (min)	Absorbance (AU)
0	0.123 ^a	0	0.113 ^a	0	0.121 ^a
0	0.127 ^a	0	0.119 ^a	0	0.124 ^a
0	0.126 ^a	0	0.123 ^a	0	0.122 ^a
6	0.055	9	0.064	16	0.080
7	0.068	9	0.066	16	0.087
7	0.066	15	0.057	17	0.089
7	0.064	15	0.054	17	0.087
9	0.060	15	0.057	46	0.063
10	0.061	16	0.064	46	0.070
16	0.047	31	0.044	46	0.071
16	0.044	31	0.039	46	0.064
19	0.041	31	0.043	75	0.052
20	0.041	31	0.045	75	0.056
21	0.038	51	0.031	75	0.063
23	0.036	51	0.031	76	0.060
33	0.032	71	0.023	104	0.055
34	0.029	71	0.024	104	0.049
48	0.020	71	0.022	105	0.046
49	0.020	71	0.022	105	0.046

^aAbsorbance of raw material before heating.

Table A.5.2 – Absorbance values for 10% (db) and 20% (db) samples heated isothermally at 80°C for various times.

80°C, 10% (db)		80°C, 20% (db)	
Time (min)	Absorbance (AU)	Time (min)	Absorbance (AU)
0	0.123 ^a	0	0.123 ^a
0	0.127 ^a	0	0.127 ^a
0	0.126 ^a	0	0.126 ^a
18	0.078	16	0.088
18	0.074	16	0.087
45	0.084	17	0.092
46	0.088	18	0.079
47	0.090	45	0.074
47	0.077	46	0.076
76	0.083	46	0.076
76	0.090	76	0.070
77	0.077		

^aAbsorbance of raw material before heating.

Appendix 6

Appendix 6. Moisture content correction factors

Table A.6.1 - Correction factors for 43% moisture content (db) heated nonisothermally at 105°C and 145°C for 1st-order ($n = 1$) and $n = 3.66$ reaction. $CF_{NI} = \beta/\beta_{T,MC}$, (Eq. (28)).

Temperature (°C)	Time ^a (min)	$n = 1$ Correction factor (-)	$n = 3.66$ Correction factor (-)
105	9.00	1.08	1.08
105	9.33	1.08	1.08
105	15.2	1.11	1.11
105	15.4	1.12	1.12
105	15.4	1.12	1.12
105	16.0	1.12	1.12
105	30.8	1.21	1.20
105	31.1	1.12	1.12
105	31.1	1.13	1.13
105	31.3	1.21	1.21
105	51.2	1.31	1.31
105	51.2	1.31	1.31
105	70.8	1.43	1.42
105	70.8	1.43	1.43
105	70.8	1.12	1.12
105	70.8	1.12	1.12
145	6.07	1.57	1.57
145	7.20	1.62	1.62
145	7.27	1.64	1.64
145	7.40	1.30	1.30
145	8.93	1.98	1.97
145	9.73	1.52	1.51
145	17.0	4.10	4.12
145	17.0	4.10	4.12
145	19.4	4.48	4.50
145	20.5	4.39	4.42
145	23.3	5.00	5.01
145	23.8	5.00	5.00
145	33.1	5.43	5.42
145	33.9	5.55	5.54
145	48.0	5.85	5.81
145	48.8	5.87	5.83

^aMoisture content versus time shown in Figure 4.1.7.

Table A.6.2 - Correction factors for 10, 20, and 43% moisture content (db) heated isothermally at 80 °C for 1st-order ($n = 1$) and $n = 3.66$ reaction. $CF_1 = \exp[-b(MC - MC_r)]$, (Eq. (35)).

Moisture content (%, db)	Time ^a (min)	$n = 1$ Correction factor (-)	$n = 3.66$ Correction factor (-)
10%	45.3	4.21	4.17
10%	46.0	4.12	4.08
10%	46.5	4.09	4.05
10%	46.5	4.08	4.04
10%	76.0	4.10	4.06
10%	76.3	4.13	4.09
10%	76.5	4.11	4.07
20%	45.4	2.74	2.72
20%	45.7	2.72	2.70
20%	46.0	2.56	2.54
20%	76.3	2.69	2.67
43%	16.2	1.14	1.14
43%	16.3	1.20	1.20
43%	16.5	1.14	1.14
43%	16.8	1.11	1.11
43%	45.7	1.19	1.19
43%	46.2	1.26	1.25
43%	46.2	1.23	1.23
43%	46.4	1.18	1.18
43%	75.0	1.27	1.26
43%	75.0	1.20	1.19
43%	75.3	1.20	1.20
43%	75.8	1.25	1.25
43%	104.3	1.28	1.28
43%	104.3	1.28	1.28
43%	104.6	1.25	1.25
43%	104.7	1.32	1.31

Appendix 7

Appendix 7 – Normal probability plot of residuals

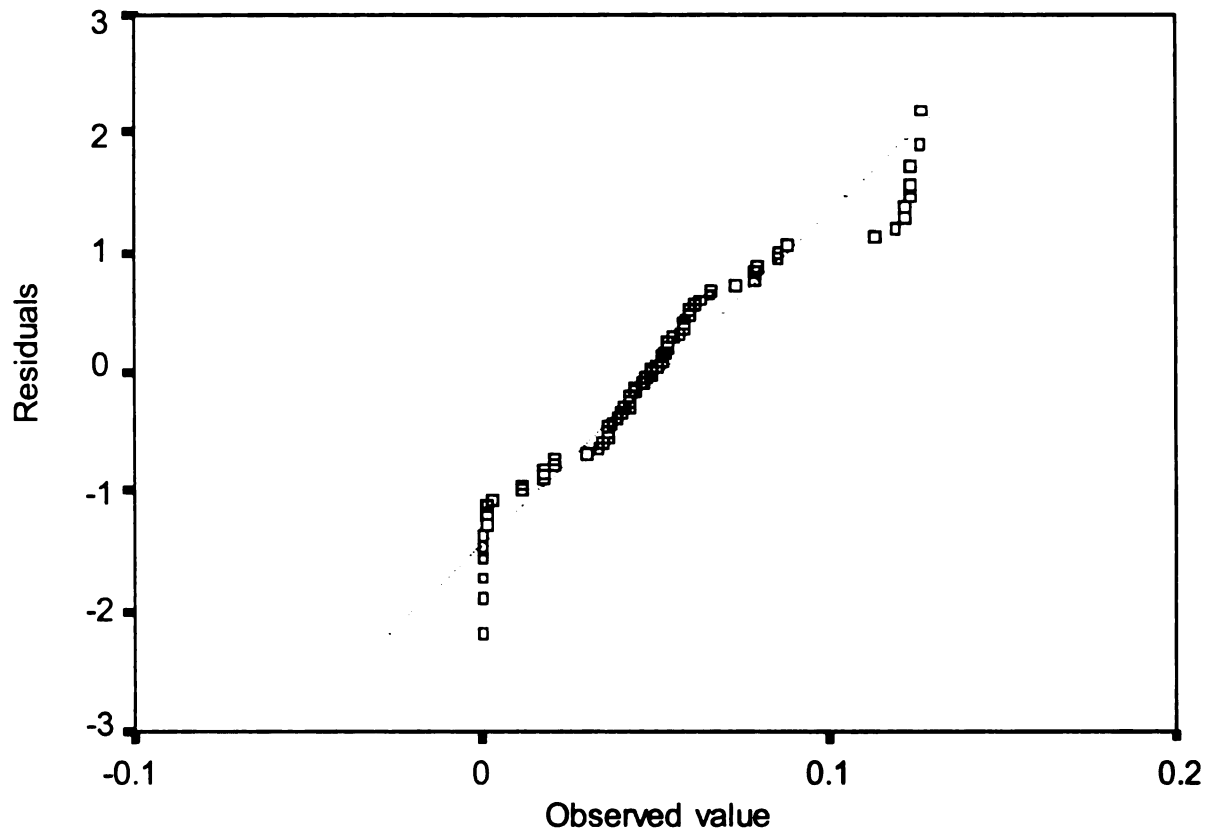


Figure A.7.1 – Normal probability plot of residuals for WLS 1st-order reaction.

Appendix 8

Appendix 8 – Anthocyanin measurements from extrusion

Table A.8.1 – Averages and standard deviation for anthocyanin content (absorbance, dry weight basis) in raw material and extruded products at high-temperature and 400 rpm containing 5, 15, and 25% grape pomace (wb)

% Grape pomace in extrudate (wb)	Average absorbance in raw material (dry wt.)	Average absorbance in extruded products^a (dry wt.)
5	0.113 ± (0.002)	0.039 ± (0.001)
15	0.310 ± (0.012)	0.139 ± (0.006)
25	0.276 ± (0.009)	0.191 ± (0.002)

^aAverage based on three measurements. Standard deviation given in parentheses.

Table A.8.2 – Averages and standard deviation for anthocyanin content (absorbance, dry weight basis) in raw material and extruded products at high-temperature and 400 rpm at 30, 35, and 40% dough moisture content (wb)

% dough moisture content (wb)	Average absorbance in raw material (dry wt.)	Average absorbance in extruded products^a (dry wt.)
30	0.271 ± (0.007)	0.138 ± (0.007)
35	0.271 ± (0.007)	0.156 ± (0.004)
40	0.271 ± (0.007)	0.152 ± (0.004)

^aAverage based on three measurements. Standard deviation given in parentheses.

Table A.8.3 - Averages and standard deviation for anthocyanin content (absorbance, dry weight basis) in raw material and extruded products

Temperature profile	Screw speed (rpm)	Average absorbance in raw material (dry wt.)	Average absorbance in extruded products^a (dry wt.)
High	50	0.201 ± (0.005)	0.081 ± (0.001)
High	50	0.121 ± (0.004)	0.073 ± (0.005)
High	100	0.201 ± (0.005)	0.106 ± (0.000)
High	100	0.121 ± (0.004)	0.082 ± (0.001)
High	200	0.201 ± (0.005)	0.092 ± (0.003)
High	200	0.121 ± (0.004)	0.083 ± (0.002)
High	400	0.201 ± (0.005)	0.100 ± (0.001)
High	400	0.121 ± (0.004)	0.083 ± (0.001)
Low	50	0.130 ± (0.003)	0.091 ± (0.001)
Low	50	0.245 ± (0.027)	0.162 ± (0.002)
Low	100	0.130 ± (0.003)	0.092 ± (0.001)
Low	100	0.245 ± (0.027)	0.166 ± (0.018)
Low	200	0.130 ± (0.003)	0.095 ± (0.003)
Low	200	0.245 ± (0.027)	0.154 ± (0.005)
Low	400	0.130 ± (0.003)	0.087 ± (0.001)
Low	400	0.245 ± (0.027)	0.153 ± (0.010)

^aAverage based on three measurements. Standard deviation given in parentheses.

Appendix 9

Appendix 9 – Anthocyanin retention values from extrusion

Table A.9.1 - Values for total, thermal, and mechanical retention from samples extruded under high and low temperature at 50, 100, 200, and 400 rpm

Temp. profile	Screw speed (rpm)	Total retention ^a (%)	Percent of total retention due to thermal effects ^b	Percent of total retention due to mechanical effects ^b
High	50	55 ± (6.5)	54 ± (3.0)	102 ± (7.0)
High	100	60 ± (8.4)	67 ± (5.6)	89 ± (5.0)
High	200	62 ± (6.5)	77 ± (5.3)	81 ± (3.4)
High	400	59 ± (10)	85 ± (1.3)	70 ± (11)
Low	50	68 ± (2.0)	80 ± (6.0)	86 ± (4.1)
Low	100	67 ± (5.3)	87 ± (0.7)	77 ± (5.6)
Low	200	71 ± (5.7)	91 ± (4.0)	78 ± (5.6)
Low	400	65 ± (2.6)	88 ± (2.5)	74 ± (4.9)

^aAverage based on 6 measurements from 2 extrusion runs. Standard deviation given in parentheses.

^bAverage based on calculations from 2 extrusion runs. Standard deviation given in parentheses.

Table A.9.2 - Values for total, thermal, and mechanical loss from samples extruded under high and low temperature at 50, 100, 200, and 400 rpm

Temp. profile	Screw speed (rpm)	Total loss ^a (%)	Loss due to thermal effects ^b (%)	Loss due to mechanical effects ^b (%)
High	50	47 ± (3.8) ^c	46 ± (3.0) ^c	1 ± (0.9) ^c
High	100	40 ± (8.4)	33 ± (5.6)	7 ± (2.8)
High	200	37 ± (6.5)	23 ± (5.3)	14 ± (1.9)
High	400	41 ± (10)	15 ± (1.3)	26 ± (9.0)
Low	50	30 ± (0.4) ^d	15 ± (0.0) ^d	15 ± (0.4) ^d
Low	100	33 ± (5.3)	13 ± (0.7)	20 ± (4.7)
Low	200	29 ± (5.7)	9 ± (4.0)	21 ± (5.1)
Low	400	35 ± (2.6)	12 ± (2.5)	23 ± (5.0)

^aAverage based on 6 measurements from 2 extrusion runs. Standard deviation given in parentheses.

^bAverage based on calculations from 2 extrusion runs. Standard deviation given in parentheses.

^cLoss values calculated after correcting retention values to 100%.

^dCalculated using measurements from 1 extrusion run

Appendix 10

Appendix 10. Extrusion Data

Table A.10.1 - Processing data for extrusion under high and low temperature

Temperature Profile	Screw speed (rpm)	Melt temp. (°C)^a	Product temp. at die (°C)	% base torque	% torque^b	Die pressure (psi)
High	50	52/84/99/115	126	19	7.3	75
High	50	43/85/99/114	124	26	14.1	190
High	100	52/89/108/ -	128	22.5	9.6	250
High	100	43/85/104/114	124	33.5	20.7	425
High	200	54/88/100/112	126	24	9.9	115
High	200	43/86/101/112	124	30.5	16.6	335
High	400	52/89/108/ -	128	28.5	13.5	300
High	400	43/96/101/112	125	28.5	13.5	330
Low	50	42/67/78/ -	101	11.8	29.3	295
Low	50	42/66/78/88	102	12	18.4	162
Low	100	42/69/81/ -	107	39.5	26.7	510
Low	100	42/70/79/81	103	41.5	28.6	195
Low	200	41/69/82/ -	102	30	16.2	320
Low	200	43/71/86/84	105	50	35.8	270
Low	400	41/71/96/ -	110	28	13	380
Low	400	41/65/99/93	117	50	34.6	250

^aTemperature from zone 1-4. Thermocouple at zone 5 did not give stable readings. Slash mark (-) means thermocouple in that zone not working on that day.

^bValue after base torque (at 0 rpm) has been subtracted.

Table A.10.2 – Data used to calculate SME and shear history

Screw speed (rpm)	Temperature profile	Total feed rate (kg/s)	Degree of fill (%)	Average shear rate (1/rev)	Mean residence time (s)
50	High	0.000216	41	11.9	253.8
50	High	0.000203	37	10.6	243.6
100	High	0.000233	25	20.4	143.4
100	High	0.000233	24	19.8	139.2
200	High	0.000394	38	87.3	132.6
200	High	0.000394	26	61.1	89.4
400	High	0.000554	31	202.8	75.0
400	High	0.000549	23.5	157.8	57.6
50	Low	0.000196	41	11.8	276.6
50 ^a	Low	0.000107	43	12.5	532.2
100	Low	0.000233	27	21.9	154.8
100	Low	0.000227	32	25.9	186.6
200	Low	0.000383	26	60.4	906.
200	Low	0.000388	36	82.1	122.4
400	Low	0.000532	24	160.9	61.2
400	Low	0.000543	36	231.4	87.6

^aThis set was excluded from data analysis.

References

AACC. 1982. Association of Cereal Chemists Approved Methods, 10th ed., St. Paul, MN.

Adams, JB. 1973. Thermal degradation of anthocyanins with particular reference to the 3-glycosides of cyanidin. I. In acidified aqueous solution at 100 °C. *J. Sci. Food Agric.* 24: 747-762.

Akdogan, H and McHugh, TH. 1999. Twin screw extrusion of peach puree: rheological properties and product characteristics. *J. Food Processing Preservation.* 23: 285-305.

Altomare, RE and Ghossi, P. 1986. An analysis of residence time distribution patterns in a twin screw cooking extruder. *Biotech Progress* 2(3): 157-163.

Anonymous. 1998. *Grape Statistics*. Concord Grape Association.

Anonymous. 2002. *Statistics of fruits, tree nuts, and horticultural specialties*. USDA-NASS.

Bates, DM and Watts, DG. 1988. *Nonlinear regression analysis and its applications*. New York: J Wiley & Sons.

Bhattacharya, S and Choudhury, GS. 1994. Twin-screw extrusion of rice flour: effect of extruder length-to-diameter ratio and barrel temperature on extrusion parameters and product characteristics. *J. Food Proc. Pres.* 18(5): 389-406.

Bridle, P and Timberlake, CF. 1997. Anthocyanins as natural food colours – selected aspects. *Food Chem.* 58(1-2):103-109.

Brouillard, R and Delaporte, B. 1977. Chemistry of anthocyanin pigments. 2. Kinetic and thermodynamic study of proton transfer, hydration, and tautomeric reactions of malvidin 3-glucoside. *J. Am. Chem. Soc.* 99(26): 8461-8468.

Brouillard, R. 1982. Chemical structure of anthocyanins. In *Anthocyanins as Food Colors*, Markakis, P., Ed., Academic Press, New York, 1982, 1.

Cai, W and Diosady, LL. 1993. Model for gelatinization of wheat starch in a twin-screw extruder. *J. Food Sci.* 58(4): 872-875.

Calvi, JP and Francis, FJ. 1978. Stability of Concord grapes (*V. labrusca*) anthocyanins in model systems. *J. Food Sci.* 43(5): 1448-1456.

Camire, ME, Camire, A, Krumbar K. 1990. Chemical and nutritional changes in foods during extrusion. *Crit. Rev. Food Sci. Nutr.* 29(1): 35-37.

- Camire, ME, Chaovanalikit, A, Dougherty, MP and Briggs, J. 2002. Blueberry and grape anthocyanins as breakfast cereal colorants. *J. Food Sci.* 67(1): 438-441.
- Cha JY, Dolan KD, and Ng, PKW. 2001. Modeling thermal and mechanical effects on retention of thiamin in extruded foods. Abstract 289. Amer. Assoc. Cereal Chemists Annual Meeting 10/14-17.
- Cemeroglu, B, Velioglu, S, and Isik, S. 1994. Degradation kinetics of anthocyanins in sour cherry juice and concentrate. *J. Food Sci.* 59(6): 1216-1218.
- Clifford, MN. 2000. Anthocyanins – nature, occurrence and dietary burden. *J. Sci. Food Agric.* 80:1063-1072.
- Clydesdale, FM, Main, JH, Francis, FJ, and Damon, RA. 1978. Concord grape pigments as colorants for beverages and gelatin desserts. *J. Food Sci.* 43:1687-1697.
- Daravingas, G and Cain, RF. 1968. Thermal degradation of black raspberry anthocyanin pigments in model system. *J. Food Sci.* 33: 138-142.
- Davidson, VJ, Paton, D, Diosady, LL, and Rubin, LJ. 1984. A model for mechanical degradation of wheat starch in a single-screw extruder. *J. Food Sci.* 49:1154-1157.
- Dolan KD. 2003. Estimation of kinetic parameters for nonisothermal food processes. In press. *J. Food Sci.* 68(3):728-741
- Fichtali, J and van de Voort, FR. 1989. Fundamental and practical aspects of twin screw extrusion. *Cereal Food World.* 34(11):921-929.
- Francis, FJ. 1989. Food colorants: anthocyanins. *Crit. Rev. Food Sci. Nutr.* 28(4): 273-314.
- Fuleki, T and Francis, FJ. 1968a. Quantitative methods for anthocyanins. 1.Extraction and determination of total anthocyanin in cranberries. *J. Food Sci.* 33: 72-77.
- Fuleki, T and Francis, FJ. 1968b. Quantitative methods for anthocyanins. 2. Determination of total anthocyanin and degradation index for cranberry juice. *J. Food Sci.* 33: 78-83.
- Giusti, MM and Wrolstad, RE. 2001. Characterization and measurement of anthocyanins by UV-visible spectroscopy. *Current Protocols in Food Analytical Chemistry.* John Wiley & Sons, Inc.

- Greaves, J. 2002. Colorants for cereal and snack foods. *Cereals Food World*. 47(8):374-377.
- Guzman-Tello, R and Cheftel, JC. 1987. Thiamine destruction during extrusion cooking as an indicator of the intensity of thermal processing. *Inter. J. Food Sci and Tech*. 22:549-562.
- Hang, YD and Woodams, EE. 1985. Grape pomace: a novel substrate for microbial production of citric acid. *Biotech Letters*. 7(4): 253-254.
- Hang, YD. 1988. Recovery of food ingredients from grape pomace. *Proc Biochem*. 2-4.
- Harper, JM. 1978. Extrusion processing of foods. *Food Tech*. 67-72.
- Harper, JM. 1981. *Extrusion of Foods.*, CRC Press, Inc.
- Holman, JP. 1976. *Heat transfer. 8th Edition*. McGraw-Hill, Inc.
- Hrazdina, G. 1975. Anthocyanin composition of Concord grapes. *Lebensmitt.-Wiss u Technol*. 8:111.
- Johnson, ML and Fault, LM. 1992. Parameter estimation by least-squares methods. *Methods Enzymol*. 210: 1-37.
- Joseph, JA and others. 1999. Reversals of age-related declines in neuronal signal transduction, cognitive, and motor behavioral deficits with blueberry, spinach, or strawberry dietary supplementation. *J Neuroscience*. 19(18): 8114-8121.
- Ingalsbe, DW, Neubert, AM, and Carter, GH. 1963. Concord grape pigments. *J. Ag. Food Chem*. 11: 263.
- Komolprasert, V and Ofoli, R. 1990. Effect of shear on thermostable α -amylase activity. *Lebensm.-Wiss. U.-Technol*. 23: 412-417.
- Kvålseth, TO. 1985. Cautionary note about R^2 . *The Amer. Statistician*. 39(4) pt. 1: 279-285.
- Labuza, TP and Riboh, D. 1982. Theory and application of Arrhenius kinetics to the prediction of nutrient losses in foods. *Food Tech*. 66-74.
- Levenspiel, O. 1999. *Chemical reaction engineering. 3rd Edition*, John Wiley and Sons.

- Mackey, KL, Morgan, RG, and Steffe, JS. 1987. Effects of shear-thinning behavior on mixer viscometry techniques. *J. Texture Stud.* 18:231-240.
- Markakis, P, Livingston, GE, Fellers, CR. 1957. Quantitative aspects of strawberry pigment degradation. *Food Res.* 22: 117-130.
- Mazza, G. 1995. Anthocyanins in grape and grape products. *Crit Rev Food Sci Nutr.* 35(4):341-371.
- Mazza, G and Brouillard, R. 1987. Recent developments in the stabilization of anthocyanins in food products. *Food Chem.* 25: 207-225.
- Metzner, AB and Otto, RE. 1957. Agitation of non-Newtonian fluids. *J. Am. Inst. Chem. Eng.* 3:3-10.
- McLellan, MR and Cash, JN. 1979. Application of anthocyanins as colorants for maraschino-type cherries. *J. Food Sci.* 44(2): 483-487.
- Mohamed, IO, Ofoli, RY, and Morgan, RG. 1990. Modeling the average shear rate in a co-rotating twin screw extruder. *J. Food Process Engineering* 12:227-246.
- Neter, J, Kutner, MH, Nachtsheim, CJ, and Wasserman, W. 1996. *Applied Linear Statistical Models. 4th Edition.* Times Mirror Higher Education Group, Inc.
- Niketic, GK and Hrazdina, G. 1972. Quantitative analysis of the anthocyanin content in grape juices and wine. *Lebensm. Wiss. U. Technol.* 5:163.
- Peng, J, Huff, HE, and Hsieh, F. 1994. An RTD determination method for extrusion cooking. *J. Food Processing and Preservation* 18: 263-277.
- Prior, RL and others. 1998. Antioxidant capacity as influenced by total phenolic and anthocyanin content, maturity, and variety of *Vaccinium* species. *J. Agric. Food Chem.* 46(7): 2686-2693.
- Rao, MA, and Rizvi, SSH. 1986. *Engineering Properties of Foods.* New York, NY: Marcel Dekker, Inc. 398 pp.
- Rhim, JW, Nunes, RV, Jones, VA, and Swartzel, KR. 1989. Determination of kinetic parameters using linearly increasing temperature. *J. Food Sci.* 54(2): 446-450.
- Robinson, WB, Wiers, LD, Bertina, JJ and Mattick, LR. 1966. The relation of anthocyanin composition to color stability of New York State wines. *Amer. J. Enol. Viticult.* 17:178.

- Rossen, JL and Miller, RC. 1973. Food extrusion. *Food Tech.* 47-52.
- Sastry, LVL and Tischer, RG. 1952. Behavior of the anthocyanin pigments in Concord grapes during heat processing and storage. *Food Tech.* 82-86.
- Scharrer, A and Ober, M. 1981. 1981. Anthocyanosides in the treatment of retinopathies. *Klin. Monatsbl. Augenheikd.* 178(5):386-389.
- Shewfelt, RL and Ahmed, EM. 1966. The nature of the anthocyanin pigments in South Carolina Concord grapes. *S. Carolina Agric. Expt. Sta. Tech. Bull.*, 1025.
- Sondheimer, E and Kertesz, Z. 1948b. Anthocyanin pigments. Colorimetric determination in strawberries and strawberry products. *Anal. Chem.* 20: 245-248.
- Stout, GM. 2002. Exploring colorants from natural sources. *Cereal Foods World.* 47(7):314-318.
- Suparno M, Dolan KD, Cha JY, Ng PKW. 2002. Modeling extruder average shear rate as a function of flow behavior index and degree of fill. Abstract #349. Amer Assoc Cereal Chem Annual Meeting 10/13-17.
- Tanchev, St.S and Yoncheva, N. 1974. Kinetics of thermal degradation of the anthocyanins in delphinidin-3-rutinoside and malvidin-3-glucoside. *Die Nahrung.* 18(8): 747-752.
- Timberlake, CF. 1980. Anthocyanins – occurrence, extraction and chemistry. *Food Chem.* 5:69-80.
- Timberlake, CF and Henry, BS. 1988. Anthocyanins as natural food colorants. *Prog. Clin. Biol. Res.* 280:107-121.
- Thompson, DR, Wolf, JC, and Reineccius, GA. 1976. Lysine retention in food during extrusion-like processing. *Transactions of the ASAE.* 989-992.
- Valiente, C, Arrigoni, E, Esteban, RM and Amado, R. 1995. Grape pomace as a potential food fiber. *J. Food Sci.* 60(4): 818-820.
- Van Buren, JP, Bertino, JJ, Einset, J, Renaily, GW, and Robinson, WB. 1970. A comparative study of the anthocyanin pigment composition in wines derives from hybrid grapes. *Amer. J. Enol. Viticult.* 21:1117.
- Van Boekel, MAJS. 1996. Statistical aspects of kinetic modeling for food science problems. *J. Food Sci.* 61(3): 477-489.

Wang, H, Cao, G, and Prior, RL. 1997. Oxygen radical absorbing capacity of anthocyanins. *J. Agric. Food Chem.* 45(2): 304-309.

Wang, H, Nair, MG, Strasburg, GM, Chang, YC, Booren, AM, Gray, JI, and DeWitt DL. 1999. Antioxidant and anti-inflammatory activities of anthocyanins and their aglycon, cyaniding, from tart cherries. *J. Natural Prod.* 62(2): 294-296.

MICHIGAN STATE UNIVERSITY LIBRARIES



3 1293 02504 9598